Characterization of anti-β_1-adrenoceptor antibodies with Förster resonance energy transfer microscopy

Charakterisierung von anti-β_1-Adrenozeptor Antikörpern mittels Förster Resonanz Energie Transfer Mikroskopie

Doctoral thesis for a doctoral degree
at the Graduate School of Life Sciences,
Julius-Maximilians-Universitaet Würzburg,
Section Biomedicine

submitted by

Angela Schlipp

from

Grünstadt, Germany

Würzburg, 2011

Submitted on: **28.07.2011**

Members of the *Promotionskomitee*:

Chairperson: **Prof. Thomas Huenig**

Primary Supervisor: **Prof. Roland Jahns**

Supervisor (Second): **Prof. Martin J. Lohse**

Supervisor (Third): **Prof. Thomas Mueller**

Date of Public Defence: ……..……

Date of Receipt of Certificates: …….

Affidavit

I hereby confirm that my thesis entitled “Characterization of anti-β_1-adrenoceptor antibodies with Förster resonance energy transfer microscopy” is the result of my own work. I did not receive any help or support from commercial consultants. All sources and/or materials applied are listed and specified in the thesis.
Furthermore, I confirm that this thesis has not yet been submitted as part of another examination process neither in identical nor in similar form.

Würzburg 28.07.2011 Angela Schlipp

Date Signature

Eidesstattliche Erklärung

Hiermit erkläre ich an Eides statt, die Dissertation „Charakterisierung von anti-β_1-Adrenozeptor Antikörpern mittels Förster Resonanz Energie Transfer Mikroskopie“ eigenständig, d.h. insbesondere selbstständig und ohne Hilfe eines kommerziellen Promotionsberaters, angefertigt und keine anderen als die von mir angegebenen Quellen und Hilfsmittel verwendet zu haben.
Ich erkläre außerdem, dass die Dissertation weder in gleicher noch in ähnlicher Form bereits in einem anderen Prüfungsverfahren vorgelegen hat.

Würzburg 28.07.2011 Angela Schlipp

Datum Unterschrift

Contents

Abbreviations

ASP	ammonium sulfate precipitation
AA(s)	amino acid(s)
(a)ab(s)	(auto-) antibodie(s)
AC	adenylyl cyclase
ACEI	angiotensin-converting enzyme inhibitor
ACh	acetylcholine
ADP	adenosine diphosphate
ANP	atrial natriuretic peptide
APS	ammonium peroxo sulphate
AT1	angiotensin II type 1 receptor
AR	adrenoceptor
ARVC/M	arrhythmogenic right ventricular cardiomyopathy
AT_1	angiotensin receptor type 1
ATPase	adenosine-triphosphate hydrolase
β_1EC_{II}	second extracellular loop of the β_1-adrenoceptor
BDM	2,3-butanedione monoxime
BES	N,N-Bis(2-hydroxyethyl)-2-aminoethanesulfonic acid
Biso	bisoprolol
BNP	B-type natriuretic peptide
BSA	bovine serum albumin
BW	body weight
CA	caprylic acid precipitation
CAG	combination of the cytomegalovirus early enhancer element and chicken beta-actin promoter
cAMP	cyclic adenosine monophosphate
CAP	caprylic acid precipitation
CD	cluster of differentiation
CFP	cyan fluorescent protein
CGP 20712	1-[2-((3-Carbamoyl-4-hydroxy)phenoxy)ethylamino]-3-[4-(1-methyl-4-trifluoromethyl-2-imidazolyl)phenoxy]-2-propanol dihydrochloride
CHO	Chinese hamster ovary cell line
CHW	Chinese hamster fibroblast cell line
CP	cyclic peptide
cpm	counts per minute
DAG	diacyl glycerol
DCM	dilated cardiomyopathy
DMEM	Dulbecco's modified Eagle's medium
DMF	dimethylformamide
DMSO	dimethyl sulfoxide
DNA	desoxyribonucleic acid
DPBS	Dulbecco's phosphate buffered saline
E	energy transfer
EC_I	first extracellular loop

EC_{II}	second extracellular loop
EC_{50}	half maximal effective concentration
EDTA	ethylenediaminetetraacetic acid
ELISA	enzyme-linked immunosorbent assay
Epac1	exchange protein directly acrivatd by cAMP-1
Fcγ	fragment crystalline γ
FCS	fetal calf serum
Fmoc	fluorenylmethyloxycarbonyl chloride
Fmoc-Glu(OH)-Odmab	N-[(9H-fluoren-9-ylmethoxy)carbonyl]-L-glutamic acid
Foxp3	forkhead box p3
FRET	Förster resonance energy transfer
$G_{12/13}$	GTPase-activating G protein
G418	geneticin
G_{α}	alpha subunit of G protein
$G_{\beta\gamma}$	beta and gamma subunit of G protein
GDP	guanosine-5'-diphosphate
GPCR(s)	G protein-coupled receptor(s)
GFP	green fluorescent protein
G protein(s)	heterotrimeric guanine nucleotide-binding protein(s)
$G_{i/o}$	inhibitory G protein
$G_{q/11}$	PLC-activating G protein
GRK(s)	GPCR kinase(s)
G_s	stimulatory G protein
GST	glutathion-S-transferase
GTP	guanosine-5'-triphosphate
GTPase	guanosine-5'-triphosphate hydrolase
$5\text{-}HT_4$	serotonin type 4 receptor
HC	Ig heavy chain
HCM	hypertrophic cardiomyopathy
HEPES	4-(2-hydroxyethyl)-1-piperazineethanesulfonic acid
HHD	hypertensive heart disease
HLA	human leucocyte antigen
$[I_{50}]$	concentration of antagonist inhibiting 50 % of specific binding
IC	intracellular loop
ICI	ICI-118551
ICM	ischemic cardiomyopathy
IF	immunofluorescence
Ig	immunoglobulin
IL	interleukin
i.p.	intraperitoneal
IP_3	inositol-1,4,5-trisphosphate
(-) iso	(-) isoproterenol
i.v.	intravenous
K_I	inhibitory equilibrium constant
K_L	equilibrium constant for ligand binding
[L]	ligand concentration
LB	Luria broth
LC	Ig light chain

LTCC	L-type calcium channel
LV	left ventricular
LVEF	left ventricular ejection fraction
M	muscarinic acetylcholine receptor
MAB	monoclonal antibody
MALDI	matrix-assisted laser desorption/ionization
MAPK(s)	mitogen-activated protein kinase(s)
MHCs	major hisocompatibility complex molecules
MW	molecular weight
MWCO	molecular weight cut-off
NMR	nuclear magnetic resonance
NYHA	New York Heart Association
OPD	o-phenylenediamine
PAB	polyclonal antibody
PBS	phosphate buffered saline
PDL	poly-D-lysin
PEG	polyethylene glycol
PLB	phospholamban
PLC	phospholipase C
PKA	protein kinase A
PKC	protein kinase C
POD	peroxidase
r	distance between donor and acceptor FRET molecule
R^2	coefficient of determination
R_o	Förster distance
RAAS	renin angiotensin aldosterone system
RIA	radioimmunoassay
RNA	ribonucleic acid
RNase	ribonuclein acid hydrolase
rpm	rotations per minute
RyR	ryanodine receptor
RT	room temperature
SCID	severe combined immune deficient
scr	scrambled
SD	standard deviation
SDS	sodium dodecyl sulfate
SDS-PAGE	SDS-polyacrylamide gel electrophoresis
SEM	standard error of mean
SERCA	SR calcium-ATPase
SR	sarcoplasmatic reticulum
TAA	thiophilic agarose adsorption
TEMED	tetramethylethylenediamine
TGFβ	transforming growth factor β
T_H1	helper T lymphocyte 1
T_H2	helper T lymphocyte 2
TNFα	tumor necrosis factor α
T_{reg}	regulatory T-lymphocytes
Tris	tris(hydroxymethyl)aminomethane

TSH	thyroid stimulating hormone
U	unit
YFP	yellow fluorescent protein

1 Introduction

Dilated cardiomyopathy (DCM) has long been used as a synonym for idiopathic heart disease because the etiology of most cases remained elusive. Today a multitude of different causes has been acknowledged for this disease complex, including an autoimmune attack of cardiac β_1-adrenoceptors (AR) by functionally active autoantibodies (aabs). These aabs bind to the second extracellular loop (EC_{II}) of the β_1-AR in its native conformation; however, their key binding epitope has not been identified, yet. Despite these previous reports and findings diagnostic procedures for the detection of such aabs in blood samples of DCM-patients are not standardized and suffer from poor reproducibility. A specific treatment option addressing the autoimmune nature of this disease has not yet been developed for clinical application. The present work aims to identify and characterize the epitope recognized and bound by conformational β_1-AR abs and, thereby, to pave the way for novel specifically aab-directed diagnostic and therapeutic strategies.

1.1 The β_1-AR as a member of the G protein-coupled receptors

G protein-coupled receptors (GPCRs) represent a protein superfamily of more than 1000 members and comprise about 3 % of the genes of the human genome. They are key mediators of the olfactory and the (photo-)visual system as well as important in neuronal and endocrine signaling.[1, 2] Their wide range of physiological functions and pathophysiological impact make GPCRs a major drug target for diseases as diverse as heart failure,[3] asthma,[4] cancer,[5-7] metabolic diseases,[8, 9] psychological disorders,[10-12] and neurodegeneration.[13] 50 to 60 % of the drugs currently on the pharmaceutic market target GPCRs.[14]

GPCRs consist of seven transmembrane α-helical regions that span the plasma membrane. The amino-terminal domain of the protein is localized extracellular, whereas the carboxy-terminal part is localized in the cytosol. The transmembrane parts of the protein are connected by six less structured extra- and intracellular loops. In 2000 the first three-dimensional structure of a GPCR, namely the photoreceptor rhodopsin, was published.[15-19] Since this publication more GPCR structures have been solved, including the human A_{2A} adenosine receptor,[20] human β_2-AR,[21] a modified turkey β_1-AR (Fig. 1),[22] the CXCR4 chemokine receptor,[23] and most recently the human histamine H_1-receptor.[24] These

structures reveal considerable variability in the lengths of transmembrane helices and the composition of the intra- and extracellular loops, although the overall architecture of the class A GPCRs, to which rhodopsin, β_1-, β_2-, and β_3-AR belong, is quite similar.[25]

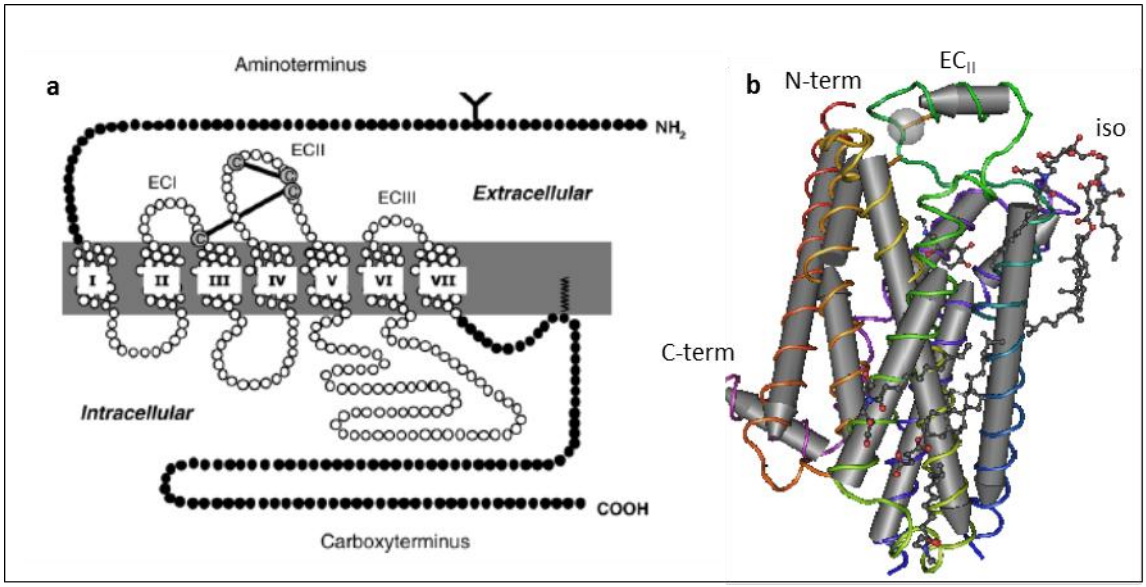

Fig. 1: Structure of the β_1-AR a) *Schematic representation of the β_1-AR (taken from Jahns* et al.*[26] based upon data by Frielle* et al.*[27]) ECI-III = first-third extracellular loop* **b)** *3D-crystal structure of the turkey β_1-AR with the bound agonist isoprenaline (based on Warne* et al.*[22], PDB ID 2Y03, designed using Cn3D 4.3. (NCBI, http://www.ncbi.nlm.nih.gov))*

GPCRs facilitate communication between cells by transmitting extracellular signals to the cytoplasm and nucleus which are mediated via small molecules or peptide ligands binding to the respective membrane receptors. Upon ligand binding the conformational structure of the receptor is altered and thereby its binding properties for intracellularly interacting proteins may be changed. The outcome of this conformational reorganization is determined by the nature of the ligand. Agonistic ligands possess high affinity and intrinsic activity resulting in receptor activation, whereas pure antagonists block the receptor by competition with agonistic ligands and have no intrinsic activity. The activation by an agonist or the inactivation by an antagonist may be submaximal, classifying these compounds as partial agonists or antagonists. Inverse agonists inhibit a constitutively signaling receptor and allosteric modulators modify the response of the receptor to other ligands.[28]

Upon binding of an agonist the receptor transmits this information to intracellular heterotrimeric guanine nucleotide-binding proteins (G proteins) bound to the membrane.[29] Unstimulated G proteins possess a $G_{\beta\gamma}$- and a guanosine-5'-diphosphate (GDP)-binding G_α-subunit. After stimulation of the G protein by an activated GPCR, GDP is exchanged for

guanosine-5'-triphosphate (GTP) and the G_{α}-subunit dissociates from the membrane-bound remainder of the complex into the cytosol where it contacts further downstream effectors of the signaling cascade. Due to its innate GTP hydrolase (GTPase) function the α-subunit converts GTP to GDP and regains its affinity for the $G_{\beta\gamma}$-subunit and translocates back to the membrane. There are four different sets of G_{α}-subunits that interact with different subsets of GPCRs and transmit information to diverse effector molecules. It is still under debate whether G proteins are precoupled to inactive receptors or are engaged only upon receptor activation in a collision coupling model.[30, 31] G_s is stimulatory and activates adenylate cyclase (AC) resulting in the production of cyclic adenosine monophosphate (cAMP); $G_{i/o}$ has an inhibitory effect on cAMP production; $G_{q/11}$ activates phospholipase C (PLC) β which in turn forms inositol-1,4,5-trisphosphate (IP_3) causing calcium release from intracellular stores and diacyl glycerol (DAG) activating protein kinase C (PKC); $G_{12/13}$ mediates GTPase signaling, and even the $G_{\beta\gamma}$-subunit alone can feature signaling properties and interact with L-type calcium channels (LTCC).[32]

Activated GPCRs are phosphorylated by GPCR kinases (GRKs) leading to the recruitment of β-arrestin to the GPCR complex.[33] β-arrestin silences G protein signaling and decreases downstream effects resulting in desensitization of the cell to further signals.[34, 35] In addition, β-arrestin also leads to an internalization of the receptor via clathrin-coated pits into the endosomes where the receptor is either degraded or recycled back to the membrane.[36] Besides its silencing effects, β-arrestin can also switch on alternative signaling pathways downstream of GPCR-activation involving mitogen-activated protein kinases (MAPKs).[37]

It was a long-standing concept in GPCR-research that GPCRs, in contrast to many other classes of transmembrane receptors, function as monomeric entities. This principle has been challenged in recent years by the discovery that many GPCRs – among those also the β_1- and β_2-AR[38] – form transient or stable homo- or heteromeric complexes.[38] These multimeric GPCR-interactions influence and modulate the cell's responses to external stimuli.

Adrenergic receptors (AR) represent a particular subfamily of GPCRs, which are pharmacologically distinguishable as α_1-, α_2- and β-ARs.[39-41] Within the β-ARs three types are recognized as β_1-, β_2, and β_3-ARs.[42] ARs react to the catecholamines epinephrine and norepinephrine, which are released locally by the sympathetic nervous system as well as systemically by the adrenal glands and mediate the fight-or-flight reaction in mammals. α_1-AR of the subtypes A, B, and D are $G_{q/11}$-coupled and activate PLC upon stimulation and thereby increase intracellular calcium levels, α_2-ARs of the subtypes A, B, or C are $G_{i/o}$-coupled and inhibit adenylate cyclase, leading to decreased intracellular cAMP-

levels,[43] increased opening probability of membrane potassium channels and decreased opening of calcium channels. In contrast, β-ARs mediate their effects via G_s-coupled signaling and subsequent increase of intracellular cyclic adenosine monophosphate (cAMP) concentrations.[44] Stimulation of the β_1-AR acts mainly on the heart, whereas β_2-ARs mediate the relaxation of smooth muscles[45] and the β_3-subtype increases lipolysis. How can these conflicting responses to a unified stimulus then lead to an orchestrated reaction of the organism? This phenomenon is achieved by the differential tissue-distribution of receptor subtypes. The main AR in the lungs and peripheral vessels is the β_2 type, whereas the β_3-AR is found predominantly in brown adipose tissue.[46] There is also evidence that the β-ARs engage in $G\alpha_{i/o}$ coupling and exert differential effects upon different ligands.[47, 48]

In the human heart 75-80 % of the β-ARs are of the β_1 type, the remainder are of the β_2 type, with the β_3 type being almost negligible in cardiac tissue.[49, 50] This distribution pattern explains why the β_1-AR is the key mediator of the sympathetic system in the heart. During fight-or-flight reactions the body releases epinephrine and norepinephrine from the adrenal glands into the bloodstream. Norepinephrine, and to a lesser extent epinephrine, bind to and activate β_1-ARs on the cell membrane of cardiomyocytes. The ligand binding pocket for the aforementioned endogenous ligands (and equally for synthetic agonists and antagonists) of the β_1-AR is buried within the receptor's transmembrane helices III, V and VI and is thought to be stabilized by the second extracellular receptor loop (EC_{II}).[22, 51] Activation of the β_1-AR via endogenous or synthetic ligands leads to the activation of a signaling cascade, which amplifies the initial signal and induces a multitude of molecular events in cardiac myocytes (Fig. 2). The ultimate effect of an activation of β_1-AR is the elevation of the cytosolic calcium concentration in the cardiomyocyte, resulting in increased contraction force (positive inotropy) and beating frequency (positive chronotropy). In addition, the heart becomes more sensitive to stimulation (positive bathmotropy), the steepness of the activation potential current is increased (positive dromotropy) and the relaxation of the heart muscle is accelerated (positive lusitropy).[52] This short-term enhancement of cardiac functions assures enough blood supply to organ systems required for physical activity on demand (e.g. during fight-or-flight reactions).

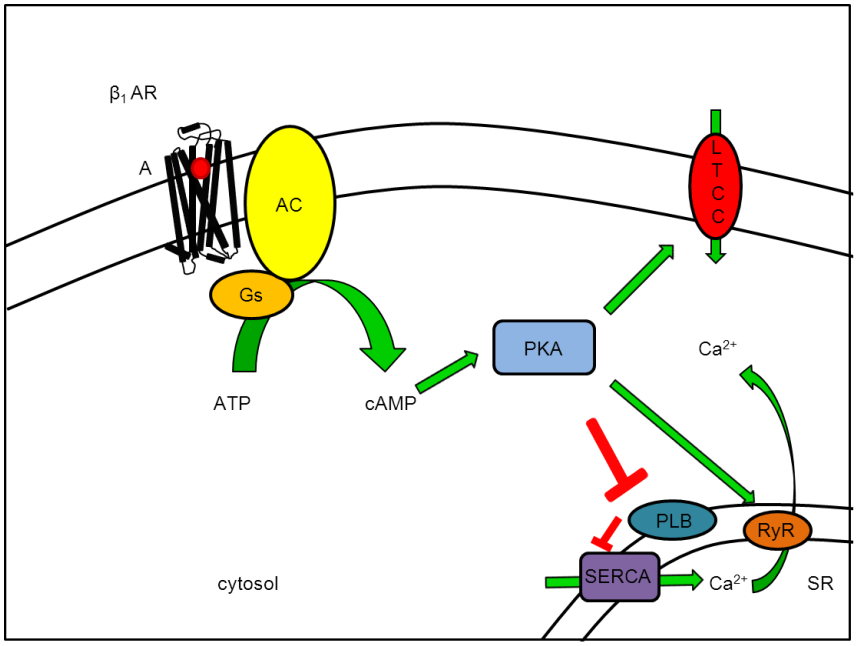

Fig. 2: The β_1-AR signaling cascade (Jahns, R.; Schlipp, A.; Boivin, V.; Lohse, M.J.: Targeting Receptor Antibodies in Immune Cardiomyopathy, Semin Thromb Hemost 2010; 36: 212-218, reprinted with permission)[53]. *Agonist (A) binding to the β_1-AR activates G_s and induces production of cAMP by activated AC. cAMP, in turn, activates protein kinase A (PKA) a key mediator of the pathway. PKA phosphorylates membrane LTCC and initiates calcium influx into the cytosol of the cardiac myocyte.[54] In addition the PKA-mediated phosphorylation of the ryanodine receptor (RyR) enhances calcium-induced calcium release from the sarcoplasmatic reticulum (SR) into the cytosol. Moreover, phospholamban (PLB), which inhibits the SR calcium-ATP hydrolase (SERCA) - serving to transport calcium back into the SR during diastole - is inactivated by PKA.*

1.2 The role of the β_1-AR in cardiac disease

If the sympathetic tone is chronically elevated at the heart muscle, as a maladaptive response this can result in severe cardiac pump failure and remodeling of the heart. To protect the heart, the heart muscle cells may adapt to some extent to adrenergic stimuli involving both short- and long-term adaptation. One short-term measure is the desensitization of β_1-AR, which results in uncoupling of the receptor from its corresponding G protein. This kind of response is either mediated by GRKs and β-arrestin, or initiated through PKA stimulation.[55] In addition, receptors can also be removed from the cell surface by a sequestration process involving clathrin-coated pits. The membrane-bound receptor is invaginated in vesicles and can either be degraded in lysosomes or be dephosphorylated and recycled back to the membrane (a process termed re-sensitization). A long-term measure to protect the heart from persistent sympathetic exposure is a reduction in receptor gene expression.[50, 56, 57] This mechanism affects β_1- more than β_2-ARs in overstimulated cardiac myocytes and therefore shifts the expression balance of the β-

adrenoceptors towards the β_2-AR subtype.[57] β_2-AR – in addition to coupling to G_s – also signals via G_i and thus mediates anti-apoptotic effects distinct from (and sometimes counter-acting) β_1-AR signaling.[58-60]

Despite these rescue mechanisms, chronic overstimulation of the heart has toxic long-term effects finally resulting in insufficient pump function and heart failure. In order to supply organs with enough oxygenated blood the heart rate is increased at the expense of diastole duration and, thus, the heart muscle itself suffers from a lack of oxygen. Renal malperfusion leads to activation of the renin angiotensin aldosterone system (RAAS),[61] resulting in an increase of plasma volume due to an increase in water and salt reabsorption in the kidneys. Blood pressure is also augmented by vasoconstriction mediated through vasopressin and endothelin. The increase of pre- and afterload further burdens the damaged heart muscle. Normally this vicious circle would be interrupted by the action of atrial and B-type natriuretic peptides (ANP and BNP) which lower RAAS and sympathetic activity,[62] However, in heart failure, these regulation mechanisms cease to work.

Loss of β_1-AR from the cardiomyocyte surface leads to a lack of adequate responses to genuine fight-or-flight reactions. One therapeutic principle applicable in this situation is to pharmacologically reduce β_1-AR activity by beta-blockers, which are β-AR antagonists.[63-65] In patients with chronic heart failure this therapeutic concept restores β_1-AR density on cardiomyocytes and in the long run results in improved cardiac function.[66] Regarding the potential benefit brought about by β_2-mediated signaling in the heart and its crucial role in airway dilatation,[67] the use of outmost β_1-AR selective antagonists like metoprolol and bisoprolol is warranted in the failing heart.

1.3 Autoimmune diseases

Autoimmunity – or as it has been coined by Paul Ehrlich *horror autotoxicus* – is the malfunction of adaptive immune responses.[68] Autoimmune disorders pose a major health problem on developing and industrialized countries with an estimated 20 % of the population suffering from autoimmune related diseases in the US, according to the latest information from the American Autoimmune Related Diseases Association (www.aarda.org). More than 60 autoimmune diseases are currently known and autoimmune components are continuously identified in the pathogenesis of known health disorders.[69] Since most autoimmune disorders are of chronic nature, require long-term treatment, and importantly influence the wellbeing of individual patients, they inflict a substantial burden on economics.

Under normal conditions, autoimmunity is prevented by several mechanisms. Selection processes take place in primary lymphoid organs (thymus and bone marrow) or in the periphery - therefore termed central and peripheral tolerance, respectively. Tolerance mechanisms keep the potentially harmful immune responses in a delicate balance; in case of tolerance failure the immune system may attack endogenous (self-)structures and lead to a specific kind of autoimmune disease.[70] The balance between an efficient immune protection against pathogens and the prevention of autoimmunity is critical and the difference between self-proteins and antigens can be minute.[71]

In healthy individuals the immune system is able to distinguish between foreign malicious antigens (e.g. during a viral or bacterial infection) which it attacks, and self-motifs that are ignored due to tolerance mechanisms.[72] Self-proteins are present in the body in high and constant concentrations and are presented to developing T-cells in the thymus. In the absence of an activation of the innate immune system and/or costimulatory proteins the developing T-cells will learn to tolerate them.[73] However, auto-reactive T- and B-cells are commonly produced by the immune system.[74] This is a necessary mechanism in immunity because some mildly self-reactive lymphocytes might also fight pathogens and their elimination might put the body at risk for infections. T- and B-cells that exhibit strong recognition of self-peptides bound to self major histocompatibility complex molecules (MHCs) are eliminated via negative selection leading to their deletion,[71] anergy[75] or receptor editing.[76] However, if T- or B-cells show no recognition of self-peptide-self-MHCs at all, they cannot receive signals stimulating their survival and thus die due to positive selection. Some tissue-specific antigens are not expressed in the thymus or bone marrow and, consequently, not presented to developing T- or B-cells. Therefore, additional tolerance mechanisms in the periphery are necessary.

There are intrinsic and extrinsic factors that maintain T- and B-lymphocyte responses in a beneficial range.[77] Intrinsic processes act on the cell by autoregulatory mechanisms, e.g. if B-cells become self-reactive after somatic hypermutation in germinal centers, the high concentrations of the self-antigen encountered drives these cells into apoptosis. In infection scenarios the pathogen’s antigen is mostly present at much lower concentrations and the specific B-cells survive and proliferate. Another intrinsic failsafe mechanism of the immune response is the “activation-induced cell death” which applies to activated T- or B-cell clones and sensitizes them to Fas ligands, which ultimately results in their apoptotic self-destruction (with only resting memory cells remaining after an efficiently combated infection). In autoimmune diseases the causative self-antigen usually cannot be cleared from the body and the aforementioned mechanism of immune control does not occur. Extrinsic control of the immune system is secured via regulatory T-cells (T_{reg})[78], which cause dominant

regulatory tolerance by production of interleukin (IL)-10 and transforming growth factor (TGF) β quiescing self-reactive T-cells.

Autoimmune diseases can be grouped into predominantly T-cell- or B-cell-mediated disorders, but like in the normal immune response both immune effector functions are usually involved supporting each other.[79] In predominantly B-cell-mediated autoimmune diseases crossing of aabs over the placenta can potentially transfer the disease to the fetus whereas T-cells cannot cross the placenta. Another way to distinguish autoimmune diseases is via their effect on the body, namely into systemic or organ-specific diseases.[80] It is common to find certain diseases clustered within an individual or a family, e.g. several systemic diseases, whereas it is unusual to find a systemic and a concomitant organ-specific autoimmune disease within one and the same patient.

The etiology of autoimmune diseases is poorly understood. The initiating event that triggers disease can rarely be identified, but several scenarios are possible. Weakly self-recognizing lymphocytes normally stay ignorant and do not affect the body unless stimulated by a trigger such as unspecific inflammation, ischemia or a smoldering specific infection.[81] Certain drugs and toxins have also been reported to initiate autoimmunity.[82] Random events – for example the unfortunate and improbable encounter of a self-reactive lymphocyte with its autoantigen in combination with inadequately elicited co-stimulatory factors – might also lead to proliferation of that self-reactive clone and subsequent disease.[83] Genetic susceptibility to autoimmunity is also reported, but can only in few cases be attributed to a specific single gene, rather it appears that a conglomerate of different gene variants affecting co-stimulatory factors, apoptosis, cytokine expression, lymphocyte signaling, antigen presentation, and/or antigen clearance determines whether an individual is prone to autoimmune disease development or not.[84] This is also reflected by certain MHC haplotypes that are more common in patients with autoimmune diseases than would be expected from their distribution in the general population.[85] Certain autoimmune diseases show a much higher frequency in either sex, which infers an association with sex hormones in these cases.[86] It is also conceivable that tissue damage – as encountered in myocardial infarction or inflammation – releases intracellular antigens which could be detected by self-reactive lymphocytes.[87] In other autoimmune diseases molecular mimicry seems to represent a pathogenic principle.[88] This has been, for example, shown in the case of Chagas cardiomyopathy: the true antigenic targets of the immune system are the ribosomal P1 and P2 proteins of *Trypanosoma cruzei*. Abs raised against these foreign proteins were shown to cross-react with an acidic AESDE amino acid motif in the EC_{II} of β_1-AR leading to chronic heart disease and arrhythmia.[89]

In autoimmunity tissues can be damaged directly via immunoglobulin (Ig) G or IgM opsonization of the cell surface and subsequent interaction with fragment crystalline (Fc) gamma receptors leading to recruitment of monocytes, neutrophils, tissue basophils, and mast cells interacting with the opsonized cells. Opsonization also attracts complement to the tissue and leads to lysis and destruction of the cells.[90] Direct T-cell mediated cytotoxicity or insufficient clearance of immune-complexes, are other mechanisms of tissue alteration in autoimmune diseases.

The pathogenic potential of circulating aabs largely depends on the relevance and accessibility of their target structures.[54] As GPCRs are situated in cell membranes their amino-terminus and the three ECs are accessible for circulating abs. The physiologic relevance of GPCRs is also given, considering their pivotal role as the initial molecule in the sympathetic transmembrane signaling cascade. This concept is corroborated by the fact that a single receptor molecule can activate several G proteins which activate even more second messengers relaying a single signal to a multitude of effector proteins. Prominent examples of pathogenic aabs targeting membrane receptors are Grave's disease, in which agonistic aabs against the thyroid stimulating hormone (TSH) receptor cause thyroid overfunction[91] and Myasthenia gravis, in which blocking aabs targeting the postsynaptic acetylcholine (ACh) receptor at the neuromuscular junction cause periodical muscle weakness.[92]

In order to establish autoimmunity as the underlying pathogenic principle of a certain disease a modified version of Koch's postulates, the so called Witebsky's postulates, were introduced.[93, 94] These state that circumstantial evidence for autoimmunity is provided if (a) the disease is associated with other autoimmune diseases, (b) lymphatic infiltration in the target organ is present, (c) certain MHC haplotypes are more prone to disease development, (d) aberrant MHC class II antigen expression is obvious, or (e) the patient reacts positively to immunosuppressive therapy.[69]

Indirect proof of autoimmunity is given, if the self-antigen can be identified leading to the generation of an experimental animal model with a comparable immune response and the subsequent development of a disease similar to the human condition being investigated, can be established.[54, 95] Reproduction of the disease in genetic animal models or the isolation of T-cells or aabs and determination of their target specificity in *in vitro* systems could also contribute to indirect evidence for autoimmunity.[69]

Direct evidence for autoimmunity can be provided by transfer of aabs from patients to immuno-deficient animals, or in rare cases by the accidental transfer of maternal aabs over the placental barrier to the fetus, reproduces the disease. In T-cell mediated autoimmune diseases transfer of peripheral T-cells to severe combined immune deficient (SCID) mice, used to abrogate MHC-incompatibility, is alternatively applied to test for disease

reproduction.[94] Transfer experiments of homologous pathogenic aabs or T-cells within an experimental animal model can also prove autoimmunity directly.[95]

1.4 Autoimmune DCM

A heterologous group of myocardial diseases with mechanical and/or electrical dysfunction of the heart have been termed “cardiomyopathies”. The current classification of cardiomyopathies differentiates between *primary* cardiomyopathies predominantly confined to the heart muscle and *secondary* cardiomyopathies with myocardial involvement being part of a generalized (multiorgan) disease.[96] Among the primary cardiomyopathies a further subclassification depending on disease origin is useful though challenging. Cardiomyopathies with an underlying *genetic* cause are hypertrophic (HCM), arrhythomgenic right ventricular (ARVC/M), left ventricular non-compaction, or ion channelopathic cardiomyopathies. *Acquired* cardiomyopathies may be associated with myocarditis (inflammatory cardiomyopathy), stress (Tako-Tsubo cardiomyopathy), pregnancy (peri- or postpartum cardiomyopathy), tachycardia or excessive alcohol consumption. A third category comprizes *mixed* genetic and nongenetic causes of cardiomyopathy such as primary restrictive non-hypertrophic cardiomyopathy and dilated cardiomyopathy (DCM).

DCM is a disease of the heart muscle characterized by dilatation and dysfunction of the left or both ventricles without significant coronary heart disease. In the Western world the annual incidence of DCM amounts to 100 patients per 1 million and its prevalence to about 400 patients per million.[97] 25 % of heart failure cases can be attributed to DCM.[98] DCM is the most common cause of heart transplantation. Clinical symptoms of DCM like dyspnea during exercise or rest, leg edema and reduced exercise capacity often manifest only after several years of persistent left ventricular dilatation and malfunction. About one third of all DCM cases is of familial origin and can be traced back to mutations in genes encoding contractile sarcomeric, cytoskeletal or sarcolemmal, nuclear envelope, mitochondrial or transcription machinery proteins.[99, 100]

Besides genetic causes a large body of data gathered in the last two decades supports the notion that both humoral and cellular cardiac autoimmune events might synergistically lead to tissue damage and remodeling of the heart resulting in DCM. Circulating aabs against the cardiac myosin heavy chain protein,[101, 102] the sarcolemmal sodium potassium ATPase,[103, 104] troponin I,[105] tropomyosin,[106] mitochondrial ADP/ATP carriers,[107, 108] actin,[109] laminin,[109] desmin,[109] cardiodepressant aabs,[110] as well as functionally active aabs against the muscarinic type 2 receptor[111]

and the β_1-AR[112, 113] have been detected in DCM patients. Cytokine involvement (elevated soluble IL-1,[114] IL-1β,[115] IL-2,[116] IL-6,[117] IL-10,[117] IL-17,[118] IL-23,[118] tumor necrosis factor (TNF)-α[117] and decreased TGFβ-1,[119] IL-10,[119] Foxp3[119]), lymphocyte, monocytes[120] and/or an importance of macrophage[121] infiltration into heart tissue, a decrease in regulatory T-cells[122], human leucocyte antigen (HLA) class II (DR4,[123] DRB1,[124] DPA1,[124] DPB1,[124] DQA1,[125] DQB1[126]), and complement activation[127, 128] have also been described in DCM. In this regard, the presence of functional aabs against the β_1-AR was found to be associated with a number of clinically relevant parameters. Patients positive for β_1-AR aabs presented with significantly more compromised left ventricular (LV) function,[129] a higher New York Heart Association (NYHA) class,[130] more ventricular arrhythmias,[131] and a 3-fold increase in cardiovascular mortality risk in a 10 year follow up study[132].

1.5 Diagnostic strategies in autoimmune DCM

The tools and methods to diagnose ab-mediated autoimmune diseases are still limited. By enzyme-linked immunosorbent assays (ELISA)[133] the binding of an aab to a known linear epitope can be monitored. However, the target should be presented in a conformation that is recognized by the aab. ELISA experiments with sera of DCM patients yielded a high number of false positive results. Consequently, recognition of a linear β_1EC_{II} fragment in ELISA is not sufficient to detect conformational (pathophysiologically potentially relevant) aabs. In the case of patients with autoimmune DCM only aabs recognizing the β_1-AR in its native conformation on a cell membrane were able to elicit an increase in cAMP in a cell-based assay. The same aabs proved to be clinically relevant.[129, 134] Immunogenicity of the β_1EC_{II} has been established with overlapping peptides and immunization experiments in animal models.[129, 135-137] However, the single amino acid residues relevant for aab binding to this (conformational!) epitope have not yet been thoroughly investigated.

Immunofluorescence (IF) methods detect selective binding of aabs to specific cells or tissue samples. In an IF approach selective binding of anti-heart aabs to cardiac, but not skeletal muscle tissue, has been previously proposed to identify autoimmune heart disease.[138, 139] An advantage of this assay is that the exact target epitope of the respective aabs must not be known and abs against various structures can be monitored and attributed to specific cell compartments. However, the molecular targets of these abs cannot be identified and potentially harmless bystander abs without any pathophysiologic

relevance are claimed as “false positive”. Furthermore, using this approach the potential functional aspects of an aab are neglected.

In general, diagnostic approaches in autoimmunity diagnostics are challenged (a) by the paucity of disease-specific aabs in comparison with other circulating abs, (b) the fact that abs often only bind to targets in their native conformation, and (c) the lack of assays for the pathophysiological effects of functionally active aabs. Cell-based assays that allow for a monitoring of physiological responses are generally difficult to conduct, reproduce, standardize and adapt for large-scale screening. In addition, the methods used so far to diagnose autoimmune diseases are diverse and hardly comparable with each other. A three-level ELISA, IF, cAMP radioimmunoassay (RIA) screening algorithm judged only 26 % of DCM patients as positive for cardiostimulatory aabs[112], whereas a questionable diagnostic echocardiographic study performed on chicken embryos as a read-out for functional aabs yielded a 63 % prevalence of cardiodepressant aabs in DCM patients.[140] A standard procedure to diagnose autoimmune DCM is still missing.[129, 141, 142]

1.6 Förster resonance energy transfer as a diagnostic strategy

A diagnostic assay to monitor the functional effects of aabs from DCM patients requires the β_1-AR to be presented in its native conformation as well as a means to visualize downstream effector processes within its signaling pathway. One possibility to achieve this goal is the application of a sensor for cAMP. In this study we utilized the Epac1-cAMP sensor (Epac1-camps) consisting of a single cAMP-binding domain of the exchange protein directly activated by cAMP-1 (Epac1) framed by a cyan fluorescent protein (CFP) and a yellow fluorescent protein (YFP).[143-146]

CFP and YFP are derivatives of the green fluorescent protein (GFP) from the jellyfish *Aequorea victoria*, a β-barrel-shaped 238 AA residue protein which revolutionized life sciences (Fig. 3a).[147, 148] The AA residues Ser65, Tyr66, and Gly67 chemically react with each other and spontaneously form a chromophore without the need of cofactors. Excitation of GFP with light of the wavelength of 400 nm (or to a lesser extent with 470 nm) leads to fluorescence of the molecule and emission of light at 505 nm (and to a lesser extent at 540 nm).[147] Variations of the GFP AA sequence lead to a multitude of spectral variants with altered excitation and emission properties covering the whole visible spectrum.[149-151] This arsenal of fluorescent proteins, along with their ease of expression in mammalian cells and transgenic animals, has lead to widespread use of fluorescent proteins in order to

address gene expression,[152] protein folding, localization and trafficking as well as *in vitro* and *in vivo* imaging.[153, 154]

In close molecular proximity two GFP variants may act as an donor/acceptor pair and engage in Förster resonance energy transfer (FRET) – a radiation-free energy exchange process – given that the emission spectrum of the donor overlaps with the excitation spectrum of the acceptor.[155] This energy transfer (E) is dependent on the distance between the chromophores of the donor and the acceptor molecule (r), and the Förster distance at which the energy transfer efficiency between both fluorescent proteins reaches 50 % (R_0) (Fig. 3b).[156] R_0 itself depends on the spectral overlap integral, the orientation of the fluorophores, and the quantum yield of the donor in the absence of an acceptor. The energy transfer in FRET can be observed as a loss of emission intensity in the donor and stronger emission intensity in the acceptor channel upon donor excitation in filter equipped fluorescence microscopes.

The FRET pair CFP and YFP used in the monomolecular Epac1-cAMP sensor is a reliable and widely used donor/acceptor combination. However, the spectral configuration is not ideal, as excitation of the donor CFP with 436 nm also leads to a certain amount of direct YFP acceptor excitation and up to 80 % (depending on the microscopy setup employed) of the signal in the acceptor emission channel is actually donor emission light (Fig 3c). Therefore, correction factors are applied.[157]

In the absence of cAMP the fluorophores of Epac1-camps are in close proximity and excited CFP acts as a FRET donor for YFP. Upon cAMP binding to Epac1-camps the molecule changes its conformation and the specific distance between CFP and YFP augments, resulting in an increase in CFP and a decrease in YFP emission (Fig 3d).[143] This phenomenon can be used in live-cell imaging to assess changes in cytosolic cAMP concentration in the physiological range, e.g. after β_1-AR activation with small molecular agonists or by DCM-specific functional receptor aabs.

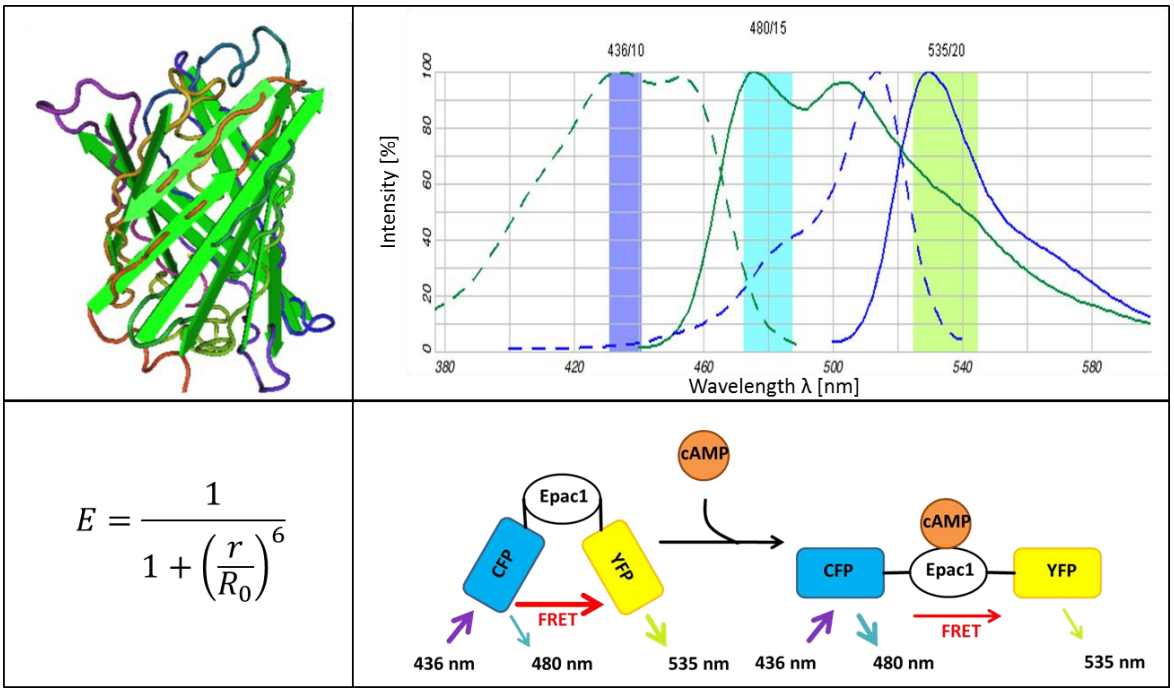

Fig. 3: Basis for FRET detection. a) *Ribbon representation of the eGFP molecule depicting the β-sheets of the barrel structure in green (based on Royant* et al*., 2011.[158], PDB ID 2Y0G, designed using Cn3D 4.3. (NCBI, http://www.ncbi.nlm.nih.gov)).* **b)** *Mathematical formula describing the FRET energy transfer efficiency (E) dependent on the chromophore distance (r) and the Förster distance (R_0) [159].* **c)** *Excitation (dashed line) and emission (solid line) spectra of CFP (green) and YFP (blue) and typical filters used in FRET microscopy (blue, cyan and green bars, designed using SpectrViewer (Invitrogen, Darmstadt).* ***d)*** *Epac1cAMP sensor in the unbound (left) and the cAMP bound conformation (right).*

1.7 Therapeutic options in autoimmune DCM

Autoimmune DCM often results in heart failure. Thus, the most recent guidelines for chronic and acute heart failure[160] should be applied recommending pharmacological therapy with angiotensin-converting enzyme inhibitors (ACEI) or AT_1-blockers. Beta-blockers are indicated in NYHA class II-IV, and diuretics are indicated as a symptomatic therapeutic approach in patients presenting with fluid retention. In case of a LVEF $\leq$ 40 % (NYHA III-IV) aldosterone antagonists should be added to beta-blocker- and ACEI- or AT_1-blocker treatment. Cardiac glycosides are recommended in patients with atrial fibrillation and from NYHA class II/III on can relieve heart failure symptoms in combination with ACEIs, but do not achieve a mortality benefit.

Treatment options for autoimmune diseases currently involve *anti-inflammatory* therapy with non-steroidal anti-inflammatory drugs or corticosteroids like prednisone[161]. Long-term treatment with high doses of prednisone is not recommended due to side-effects leading to Cushing's syndrome and osteoporosis. *Immunosuppressive treatment* with

cytotoxic drugs like azathioprine,[162] cyclophosphamide,[163] or mycophenolate[164] interferes with DNA synthesis in highly proliferative cells like activated lymphocytes. Severe side-effects of these drugs are common due to their unspecific action and, therefore, combination therapies of anti-inflammatory and immunosuppressive drugs are recommended to reduce their respective doses. More specific non-cytotoxic drugs like cyclopsporin A,[165] tacrolimus, or rapamycin[166] that interfere with T-cell signaling also have some drawbacks, because their dosage needs to be carefully balanced and their production is very expensive. A recent broadening of the spectrum of autoimmune therapy was gained by the introduction of therapeutic monoclonal antibodies (MABs) that either deplete lymphocytes or specifically target certain components of the immune system. Targets for these biological drugs are for example TNFα (infliximab[167] and etanercept[168]), IL-1 (anakinra),[169] α4-integrin (natalizumab),[170] cluster of different (CD) 52 (alemtuzumab),[171] CD20 (rituximab),[172] or the interaction between CD2 and CD58 (alefacept)[173]. MABs raised in mice frequently lead to adverse reactions in the human and, thus, mostly require humanization before they can be applied in a clinical setting. Cytokine modulation to switch immune reactions from harmful helper T lymphocytes (T_H) 1 to benign T_H2 responses[174] or to activate T_{reg} cells[175] is also possible in theory but difficult to control due to the complex expression pattern of cytokines. In some cases only a thorough elimination of the adaptive immune system followed by bone marrow transplantation is the ultimate option to treat autoimmune diseases with rapid progression[176].

In primarily B-cell-mediated autoimmunity experimental evidence indicates that removal of IgG by immunoadsorption might ameliorate the disease.[177-180] However, by immunoadsorption to protein A columns all IgGs are removed from the plasma and the aab producing B-cells themselves remain unaffected, potentially limiting the method to short-term intervention. The effect of this treatment might also be attributable to the *i.v.* Ig replacement generally following immunoadsorption: as previously shown, excess unspecific IgG effectively decreases Fc-receptor-mediated autoimmune responses.[181-183]

Another strategy to eliminate receptor-activating aabs would be their blockade by epitope-mimicking peptides. Such peptides are believed to specifically bind circulating aabs by competing with the native autoantigens.[184-186] This therapeutic approach is elegant, as it selectively targets the potentially causative aab while not depleting the patient of protective abs. It has been shown that functionally active aabs targeting GPCRs require a native receptor conformation for binding to – and subsequent activation of – the respective receptor. In our laboratory immunization of rats with β_1EC_{II}-glutathion S-transferase (GST)

fusion proteins induced the production of anti-β_1EC_{II} abs finally causing immune-DCM. In this model of intravenously injected cyclic peptides (CP) mimicking the β_1EC_{II} epitope we were able to prevent disease-development, and also – in manifest iDCM – we could revert the disease to some extent. Therefore, we propose that *i.v.* administration of these CPs might serve as a new therapeutic principle.[53, 145, 187-190] We suggest that cyclic – as compared to linear – peptides closer mimic the conformation in the native receptor loop and, additionally, degradation of the cyclic structure *in vivo* by endogenous peptidases is delayed.

Another advantage of CPs is that they can be easily modified and used in *in vitro* test systems to analyze their neutralizing efficiency of circulating (a)abs. This approach might not only lead to improve detection of DCM-related aabs, but also represent a tool to gain further insight in the molecular composition of potential antigenic epitopes.

1.8 Aims of the present work

The main goal of my work was to develop a reliable, reproducible screening assay for the detection of functionally active stimulating anti-β_1-AR abs (a) induced by immunization in animal models, (b) tailored monoclonal anti-β_1-AR abs, or (c) aabs isolated from DCM-patients.

We intended to adopt this assay for a large-scale screening of DCM-patients for functional aabs in a clinical routine setting.

In this aim we analyzed ab binding to various epitope-mimicking CPs and evaluated the ab-neutralizing efficiency of such (potentially therapeutically useful) CPs. In addition, the same epitope-mimicking CPs might prove helpful to gain more insight into the residues within the β_1EC_{II} targeted by aabs and thus, to identify relevant amino acid residues crucial for aab binding.

2 Material & Methods

2.1 Material

Chemicals, enzymes and buffers used in this study are listed in Appendix A-C.

2.2 Methods

2.2.1 Molecular biology and cells

2.2.1.1 Competent bacteria

Escherichia coli JM109 was pre-cultured in 5 ml of Luria broth (LB) medium over night at 37 °C under constant shaking at 200 rpm. This pre-culture was added to 250 ml LB medium and incubated under the above conditions until the optical density at λ = 600 nm reached 0.3 to 0.6. Bacterial cells were pelleted by centrifugation (5000 rotations per minute (rpm), 4 °C, 10 min). The supernatant was discarded and the pellet gently resuspended in 25 ml of ice-cold TBS buffer. The bacteria were incubated on ice for 8 h and aliquoted in 500 µl portions into sterile pre-cooled reagent tubes and immediately frozen in liquid nitrogen. Aliquots of competent *E. coli* bacteria were stored at -80 °C until further use. The transformation of *E. coli* was conducted by defrosting an aliquot of competent *E. coli* JM109 bacteria on ice. 10 pg of plasmid DNA in a volume of 10 µl was added to 20 µl of KCM buffer 5x and 70 µl of sterile deionized water. This transformation solution was pre-cooled on ice for 5 min. 100 µl of the bacteria suspension was added to the transformation solution, first incubated for 20 min on ice and then for 10 min at room temperature (RT). 1 ml of LB medium was added to the bacteria and the suspension further incubated at 37 °C under constant shaking for 1 h. Bacteria were pelleted by centrifugation (5000 rpm, RT, 5 min) and all but approximately 100 µl of the supernatant was discarded. The pellet was resuspended in the remaining supernatant and streaked on LB agar containing the appropriate selection antibiotic. As a control untransfected bacteria from the same frozen aliquot were streaked on another plate with selection LB agar. The plates were incubated at 37 °C for 16 h upside down and colonies were counted and picked for further use.

2.2.1.2 Nucleic acid preparation

For the isolation of plasmid desoxyribonucleic acid (DNA) from bacteria, alkaline lysis was applied.[191] Single colonies were incubated over night in LB medium with the appropriate selection antibiotic at 37 °C with constant shaking. 2 ml of the culture was centrifuged (14000 g, 4 °C, 30 sec). The supernatant was discarded and the pellet resuspended in 100 µl ice-cold L1 solution by vortexing. 200 µl of L2 solution was added and mixed by inverting the reaction tube. This leads to the lysis of the bacterial cell wall. 150 µl of L3 solution was added and mixed by inverting the reaction tube for pH neutralization. After incubation on ice for 5 min proteins, cell debris and genomic bacteria DNA was pelleted by centrifugation (14000 g, 4°C, 10 min). The supernatant was mixed with two volumes of ethanol in order to precipitate plasmid DNA, which was subsequently pelleted by centrifugation (14000 g, 4°C, 10 min). The supernatant containing the remaining ribonucleic acid (RNA) was discarded and the pellet washed with 500 µl of 70 % ethanol. After a last centrifugation step (14000 g, 4°C, 5 min) the supernatant was discarded and the pellet was dried for 15 min. The pellet was resuspended in 50 µl TE buffer I. For the preparation of plasmid DNA intended for sequencing a commercially available Plasmid Midi Kit was used according to manufacturer's instructions (Qiagen, Hilden, catalog no. 12143). For the preparation of endotoxin-free plasmid DNA intended for the transfection of mammalian cells the commercially available EndoFree Plasmid Maxi Kit was used according to manufacturer's instructions (Qiagen, Hilden, catalog no. 12362). The concentration of the prepared (plasmid) DNA was determined by spectrophotometry using the NanoDrop 2000c (Peqlab, Erlangen, catalog no. 91-ND-2000c). Nucleic acid restriction was carried out using restriction endonucleases according to manufacturer's instructions (New England Biolabs, Frankfurt am Main). Gel electrophoresis was performed using 0.8 % to 1.2 % agarose in TAE buffer with 1 $^{o}/_{ooo}$ ethidium bromide and loading buffer was added to the DNA. To assess fragment length and amount of DNA in the samples a 1 kb and a 100 bp DNA Ladder (New England Biolabs, Frankfurt am Main, catalog no. N3232L and N3231L) were run in parallel. The gels were run at 120 V in TAE buffer and analyzed under UV light at λ = 365 nm.

2.2.1.3 Primary cells

Primary adult murine cardiac myocytes were prepared according to the protocol PP00000125 by the Alliance for Cellular Signaling (available online at http://www.signaling-gateway.org/data/cgi-bin/ProtocolFile.cgi?PID=PP00000125) as previously published.[192]

In brief, stock perfusion buffer 10x, BDM solution, BSA solution, calcium chloride solutions I and II, trypsin solution, and liberase solution were prepared in advance, 1x perfusion buffer, digestion buffer, and stopping buffers I and II were prepared on the day of the experiment. The preparation of adult murine cardiac myocytes was carried out employing a custom-made apparatus consisting of two heatable water baths, an IDG tubing pump (IsmaTec, Glattbrugg, Switzerland), a tubing system for water heating and a blunted 23G hollow needle. 1x perfusion buffer, digestion buffer (without the enzymes), stopping buffer I and II, and the tubing system were pre-warmed to 37 °C. The tubing system was rinsed with 70 % ethanol, then water, and 1x perfusion buffer before the preparation. An adult transgenic CAG-Epac1-camps mouse[193] was treated with 100 µl heparin intraperitoneal (*i.p.*) for 10 min and killed by cervical dislocation. The heart was prepared and freed of fat and lung tissue. The aorta was cut to a length of approximately 3 mm, opened with the help of two fine pincers, put over the blunted needle, and fixed by means of thread and a crocodile clamp. The procedure from sacrificing the mouse until hanging the heart on the needle was completed in less than 10 min. The retrograde perfusion of the heart with 1x perfusion buffer was initialized immediately after the hanging process and continued for 5 min. The fluid flow was kept constant at 3.5 ml/min. In the meantime, liberase and trypsin aliquots were defrosted and added to 29.4 ml of the pre-warmed digestion buffer. 2.5 ml of the digestion buffer was set aside for later use, the rest was used to perfuse of the heart, which develops a pallid glassy appearance during the digestion process. After digestion the heart was taken off the apparatus, the atria were discarded and the ventricles were minced in 2.5 ml of digestion buffer with the help of a pair of fine scissors for 30 sec. 2.5 ml of stopping buffer I was added to the minced heart and the tissue pieces were further diminished by shearing in a 1 ml syringe for 3 min. The cell suspension was filtered through a piece of gauze and left at RT for 10 min. During this resting phase the cardiac myocytes settle on the bottom of the tube, the supernatant was removed and discarded and the cell pellet reconstituted in 10 ml of stopping buffer II. In order to resupplement the calcium stores, the cardiac myocytes were gradually addapted to a final calcium concentration of 1 mM. The cardiac myocytes were carefully pipetted on glass coverslips or 96-well-plates which were precoated with laminin solution for 30 min. The cells were incubated at 37 °C, 95 % humidity and 5 % CO_2 for one hour prior to their use in FRET experiments. Animal procedures were acknowledged by the local governmental regulatory authorities.

2.2.1.4 Cell lines

Human embryonic kidney cells (HEK293A, American Type Culture Collection, Manassas, USA, catalogue no. CRL-1573) with (HEKβ_1) or without (HEK) stably expressing 0.4 pmol/mg β_1-AR with (HEKβ_1E_1) or without (HEKβ_1) stable expression of Epac1-camps were grown in DMEM medium with 4.5 g/l glucose, 10% FCS, 2 mM L-glutamine, 100 units (U)/ml penicillin, 100 µg/ml streptomycin, 880 µg/ml geneticin, and 200 µg/ml hygromycin (only for HEKβ_1E_1-cells) at 37 °C, 95 % humidity and 7 % CO_2. Cells were plated on PDL-coated black 96-well-plates with optical bottom (IBIDI, Martinsried) for FRET experiments with the iMIC setup (TillPhotonics, Martinsried), the NOVOstar (BMG Labtech, Offenburg), or the Pathway 855 (BD Biosciences, Heidelberg) or on PDL-coated round 24 mm coverslips in 100 mm dishes for FRET experiments with the Zeiss Axiovert 200 setup. For all experiments cells were used 24 to 48 h after seeding. HEK293A cells were transiently transformed by calcium phosphate transfection. 440 µl sterile deionized water, 50 µl of calcium chloride solution III, 10 µg of plasmid DNA in 10 µl of volume and 500 µl of 2x BBS buffer were added under sterile conditions, vortexed for 5 sec and incubated at RT for 10 min. This solution was diluted 1:10 in the medium of the mammalian cells. The cells were incubated at 37 °C, 95 % humidity and 5 % CO_2 for 6 h. The medium was changed to normal culture conditions and the cells were incubated at 37 °C, 95 % humidity and 7 % CO_2 for 24 to 48 h before use. For stable transfection of mammalian cell lines the Effectene® Transfection Reagent Kit (Qiagen, Hilden, catalog no. 301425) was used according to manufacturer's instructions. Plasmids used for mammalian cell transfection include pcDNA3.1Epac1-camps (Dr. Viacheslav O. Nikolaev, Göttingen), pCEP4Epac1-camps (Dr. Viacheslav O. Nikolaev, Göttingen) and pBC-β_1 (Prof. Dr. Martin J. Lohse, Würzburg).

2.2.2 Ab generation

Polyclonal rat anti-β_1-abs (Tab. 1) were generated by immunization of male Lewis rats with a β_1EC_{II}-GST-fusion protein.[194] Polyclonal rabbit abs were raised against the same β_1EC_{II}-GST-fusion protein.[194] Monoclonal mouse anti-β_1EC_{II}-ab production was commissioned commercially to BioGenes (Berlin). MABs were generated by immunizing female BALB/c mice with the β_1EC_{II}-GST-fusion protein, fusion of the spleen cells of these mice with a SP2/0 hybridoma cell line and subcloning of the fusion cell lines. The subcloned cell lines were selected for anti-β_1-antibody production by ELISA. Supernatant from the cultured hybridoma cell lines was dialyzed against FRET buffer before use. Monoclonal rat anti-β_1EC_{II} abs and isotype control abs were generated by Dr. Vladimir Kocoski (Würzburg),

large-scale purified by InVivo BioTech Services (Hennigsdorf) and kindly provided for this work. Human IgG fractions were prepared from sera of both healthy controls and heart failure patients. Patients were recruited from the Cardiology Department of the University Hospital of Würzburg after obtaining informed consent. The study protocol has been approved by the Ethics Committee of the Medical Faculty of the University of Würzburg.

1° Antibodies	**Supplier**
Polyclonal rabbit anti-β_1EC_{II} IgG	Self-made[194]
ChromPure Rat IgG	Jackson ImmunoResearch Laboratories (West Grove, USA, catalog no. 012-000-003, lot no. 91788)
Monoclonal rat anti-β_1EC_{II} IgG 13F6	Dr. Vladimir Kocoski (Würzburg)
Monoclonal rat anti-β_1EC_{II} IgG 10E1	Dr. Vladimir Kocoski (Würzburg)
Monoclonal rat anti- β_1EC_{II} IgG 1D4	Dr. Vladimir Kocoski (Würzburg)
Monoclonal rat IgG isotype control	Dr. Vladimir Kocoski (Würzburg)
Monoclonal mouse anti-β_1EC_{II} IgG clone 23-6-7	BioGenes (Berlin)
2° Antibodies	**Supplier**
Biotin-SP-conjugated goat anti-rat IgG (H+L) $F(ab')_2$ fragment	Jackson ImmunoResearch Laboratories (West Grove, USA, catalog no. 112-066-003, lot no. 91930)
Biotin-SP-conjugated goat anti-mouse IgG, Fc_γ fragment specific	Jackson ImmunoResearch Laboratories (West Grove, USA, cataolg no. 115-065-008, lot no. 32715)

Tab. 1: Antibodies. *Primary and secondary mono- and polyclonal abs were purchased or custom-made for use in this study.*

2.2.3 Antibody purification

IgG from the sera were prepared by caprylic acid precipitation (CAP), a combination of ammonium sulfate precipitation (ASP) with CAP, or by thiophilic agarose affinity chromatography (TAA). Abs from cell culture supernatants were dialyzed against 1000-fold volume of FRET buffer for 16 h at 4 °C.

2.2.3.1 Caprylic acid precipitation

For CAP[195] of the sera, stripes of 14000 molecular weight cut-off (MWCO) dialysis hose (Visking by Carl Roth, Karlsruhe, catalog no. 0653.1) were cooked in 500 ml of dialysis hose buffer for 10 min, rinsed three times with PBS buffer and then stored in PBS at 4 °C for further use. Sodium acetate buffer was always freshly prepared and kept at RT before use. Serum was thawn and kept on ice until further use. One volume of serum was added to two volumes of sodium acetate buffer while stirring constantly. The volume of caprylic acid added to the serum was adapted according to species (human: 7 %, rat: 7.5 %, mouse: 4 %, rabbit: 7.5 %, and goat: 5.5 % of the serum volume, respectively). After stirring for 30 min at RT the solution turns cloudy as components precipitate. This suspension was centrifuged (5000 g, 4 °C, 15 min). If the supernatant remained cloudy the centrifugation step was repeated, if it still remains cloudy the supernatant was filtered through silicated glass wool. The cleared supernatant was carefully pipetted into pre-cooked dialysis hose, clamped at both ends and dialyzed against 1000-fold volume of pre-cooled FRET buffer for 16 h at 4 °C. After dialysis the samples were stored in non-protein-binding reaction tubes (Eppendorf, Hamburg, catalog no. 022431081) at -20 °C until further use.

2.2.3.2 Ammonium sulphate precipitation

Purity of the ab preparation is thought to be improved by combining the CAP method with an ASP step.[196] For the ASP serum was prepared by centrifuging (3000 g, 4 °C, 30 min). The supernatant was mixed with one volume of saturated ammonium sulphate solution (pH 7.34) and incubated at 4 °C for 6 h. Abs were pelleted by a centrifugation step (3000 g, 4 °C, 30 min). The pellet was resuspended in one volume of FRET-buffer and dialyzed against FRET-buffer over night as described above.

2.2.3.3 Thiophilic agarose adsorption

An alternative method for IgG preparation from sera is TAA, which can be either performed according to manufacturer's manual (Kem-en-tec, Taarstrup, DK), or as described by Boege *et al*.[197] The Kem-en-tec protocol consists of mixing 1 ml of serum with 2 ml ammonium sulphate solution I (0.75 M, pH 7.4) and incubating for 5 min before putting the mixture on a 1 ml column of thiophilic agarose. The column was incubated for 10 min, washed with 5 ml of the ammonium sulphate solution I and abs are eluted with 4 ml Tris buffer I. The eluted fraction was then immediately dialyzed against FRET buffer as

mentioned above. The Boege *et al*. protocol differs in using ammonium sulphate solution II (1 M, pH 7.4) and eluting abs with sodium chloride solution (0.5 M).

2.2.3.4 Protein concentration

Ab concentrations were estimated using the UV/VIS spectrophotometer NanoDrop 2000c with the settings "Protein 260/280" and "IgG". However, as our antibody preparations were only crudely purified, we expected from this method only an estimation of the complete protein content. In order to monitor the antibody content of our samples, we preferred to conduct sodium dodecyl sulfate polyacrylamide gel electrophoresis (SDS-PAGE-electrophoresis) on 12 % acrylamide gels and visualize protein bands with Coomassie stain. For the SDS-PAGE-electrophoresis a 10 ml separating gel was poured by using a vertical gel system (Hoefer, Holliston, USA, catalog no. SE640) and 5 ml of stocking gel was added on top. A suitable comb was inserted, the gel was covered with a layer of dH_2O, sealed in foil, and kept at 4 °C over night. The samples were diluted in cracking buffer to reach a concentration of 15 µg protein in a volume of 25 µl, boiled for 5 min at 95 °C, and spinned down by short time centrifugation. Then the water was discarded from and the comb taken out of the gel. The pockets were rinsed with electrophoresis buffer 1x and the samples were carefully added. The gel was inserted into the electrophoresis chamber filled with electrophoresis buffer 1x and run at 200 V until the blue band of the cracking buffer reached the lower margin of the separating gel. The gel was stained in Coomassie staining bath for 20 min and incubated in destaining buffer over night at RT before scanning it.

Autofluorescent properties of ab samples were checked by photospectroscopy of diluted samples in silica glass cuvettes on a LS50B photospecrometer (Perkin Elmer, Waltham, USA).

2.2.4 Antibody neutralization with cyclic peptides

Cyclic peptides (CPs) were constructed by fluorenylmethyloxycarbonyl chloride (Fmoc) solid phase synthesis by Peptide Specialty Laboratories (Heidelberg) (Tab. 2). The 18C/C/S and 18C/S/C peptides were synthesized on an amide carrier with N-[(9H-fluoren-9-ylmethoxy)carbonyl]-L-glutamic acid (Fmoc–Glu(OH)-ODmab). The cyclization was realized via the sidechain of glutamate resulting in a glutamine residue. The remaining CPs were synthesized on a Fmoc-Glu(Wang resinLL)-ODmab (Merck Biosciences, catalog no. 856124). The glutamate residue was coupled to the resin via its sidechain. Its ODmab-group on the alpha C-atom was selectively cleaved off with 2% hydrazinhydratin

dimethylformamide (DMF) allowing for cyclization of the fully protected peptide on the resin with the free amino-group of the amino-terminus by releasing the carboxy-sidechain of the gulatamate residue and cleaving of all protecting groups. Purity and molecular mass of CPs was deduced by matrix-assisted laser desorption/ionization (MALDI) mass spectroscopy. The freeze-dried CPs were reconstituted in water and stored at -20 °C for further use.

Ab blockade was achieved using coincubation of the purified abs with linear or cyclic peptides at 40-fold molar excess (Tab. 2). The mixture was incubated with gentle shaking for 16 h at 4 °C and stored at 4 °C until further use.

Cyclic peptides	**Amino acid sequence**
18C/C/S	ADEARRCYNDPKCSDFVQ
18C/S/C	ADEARRCYNDPKSCDFVQ
22AA β_1EC_{II}	RAESDEARRCYNDPKCBDFVTG
E202A	RAASDEARRCYNDPKCBDFVTG
S203A	RAEADEARRCYNDPKCBDFVTG
D204A	RAESAEARRCYNDPKCBDFVTG
R207A	RAESDEAARCYNDPKCBDFVTG
R208A	RAESDEARACYNDPKCBDFVTG
N211A	RAESDEARRCYADPKCBDFVTG
D212A	RAESDEARRCYNAPKCBDFVTG
P213A	RAESDEARRCYNDAKCBDFVTG
K214A	RAESDEARRCYNDPACBDFVTG
22AA β_2EC_{II}	AINCYANETCCDFFTGRATHQE
Linear peptides	**Amino acid sequence**
18AA β_1EC_{II}	ADEARRCYNDPKCCDFVQ
25AA β_1EC_{II}	ARAESDEARRCYNDPKCCDFVTNRQ
25AA β_1EC_{II} scr	SFAVRDERACRKYQTACDDCNRNEP

Tab. 2: Peptides. *"B" is an abbreviation for the non-standard AA α-aminobutyric acid, the rest of the amino acids is abbreviated by the commonly used one letter code, scr = scrambled.*

2.2.5 Enzyme-linked immunosorbent assay

Enzyme-linked immunosorbent assays (ELISA) were performed as previously described.[112] In brief, all incubation steps were carried out in a 37 °C warm water bath with closed lid and 50 µl per well of the indicated solution. All washing steps were performed using 300 µl of the indicated solution per well. F96 Maxisorp microtiter plates (Nunc, Langenselbold, catalog no. 456537*) were incubated with 50 µl coating buffer per well at 4 °C over night. Wells intended for standard determination remained uncoated. Then all wells were washed thrice with PBS + 0.1 % Tween. Standards were prepared by diluting a purified antibody of the same species as tested (e.g. ChromPure rat IgG) in the following concentrations in coating buffer: 10, 2, 1, 0.4, 0.2, 0.1, 0.04, 0.02, 0.01, 0.004, 0.002, 0.001, 0.0001 µg/ml. All wells were blocked with fat-free milk for 2 h. Sera were diluted 1/200 in PBS + 0.1 % Tween on ice in a non-binding microtiter plate (Corning, Corning, USA, catalog no. 3649) and tested for reactivity in final dilutions of 1/500, 1/1000, 1/2000, 1/4000, 1/6000, 1/8000, 1/10000, and 1/20000. Incubation time was 2 h. Subsequently each well was washed thrice with blocking milk and 50 µl of the biotinylated secondary antibody (diluted 1/7000 in blocking milk) was added. The plate was incubated at 37 °C for 1.5 h and subsequently washed twice with blocking milk. 50 µl of streptavidin-peroxidase (POD) (diluted 1/4000 in blocking milk) was added at 50 µl per well and the plate was incubated for 1 h. The plate was washed thrice with PBS + 0.1 % Tween. Then 50 µl of 4.8 mM o-phenylenediamine (OPD) and 1.67 $^{0}/_{00}$ (v/v) H_2O_2 dissolved in substrate buffer were added to each well. The plate was incubated for 30 min at 37 °C and the reaction was stopped by adding 50 µl of 3 M sulphuric acid to each well. Optical densities were determined at 490 nm with a SpectraMax 340 plate reader (Molecular Devices, Sunnyvale, USA).

2.2.6 Radioligand binding

Membrane proteins of HEK293A and HEKβ_1E_1 cells were prepared by washing a dish of confluently grown cells with ice cold PBS solution and subsequent detachment by scratching in 5 ml ice cold TE buffer II. Cells were transferred into 15 ml reagent tubes and were broken up by two 15 sec long turaxing steps on ice. The suspension was centrifuged (700 g, 4 °C, 5 min) to pellet and discard large cell debris. The supernatant was centrifuged again (37000 g, 4 °C, 30 min). The resulting pellet containing small membrane fragments was reconstituted in 2 ml ice-cold Tris buffer II, further refined in a dounce potter, and protein concentration was determined.

Washed membrane protein (5 µg) was incubated (30 min, 30 °C) with 200 pM of the nonselective ^{125}I-labled β-AR antagonist cyanopindolol ([^{125}I]-CYP, 2,200 Ci/mM, Perkin Elmer, Waltham, USA, catalog no. NEX174). Nonspecific binding was determined in the presence of saturating concentrations of [^{125}I]-CYP (240 pM) and unlabled alprenolol (5 µM). To analyze the proportion of β_1-AR/β_2-AR subtypes, incubations with 50 pM [^{125}I]-CYP were supplemented with various concentrations of the β_2-AR selective antagonist ICI 118551 (ICI) or the β_1-AR selective antagonist bisoprolol, respectively. The reactions were filtered (Millipore, Billerica, USA, catalog no. APFF02500) soaked in 0.33 % polyethylenimin and the filters were washed thrice with Tris buffer II. Filter-bound radioactivity was measured by γ-counting (Wallac 1480 Wizard 3'', Perkin Elmer, Waltham, USA). The inhibitory equilibrium constant (K_I) can be derived from the equation of Cheng-Prussow $K_I = \frac{[I_{50}]}{1+\frac{[L]}{K_L}}$ with [I_{50}] being the concentration of the antagonist which inhibits 50 % of specific ^{125}I-cyanopindolol binding, [L] being the known ^{125}I-cyanopindolol concentration and K_L being the equilibrium constant of ^{125}I-cyanopindolol binding.[198] Radioligand-binding and competition curves were fitted to the data using GraphPad Prism version 4.0 (GraphPad Software, San Diego, USA).

2.2.7 Live-cell FRET analysis

For FRET-measurements in living cells expressing (either transiently or stably) Epac1-camps five different experimental setups were used.

2.2.7.1 Zeiss Axiovert 200 setup

For measurements employing the Zeiss Axiovert 200 setup, the cells were seeded on PDL-coated round glass coverslips (diameter 24 mm, Hartenstein, Wuerzburg, catalog no. DKR5) and incubated with 400 µl FRET-buffer supplemented with 0.1 µM ICI at RT. The Zeiss Axiovert 200 microscope is equipped with an Plan-Neofluar oil immersion 63x objective (Zeiss, Jena), a beam splitter 505 DCXR (AHF Analysetechnik, Tuebingen), a CoolSNAP HQ CCD-camera (Visitron Systems, Puchheim) and a Polychrome IV (TILLPhotonics, Martinsried) for sample illumination. The cells were illuminated at 436 ± 10 nm and the emission intensities at 535 ± 20 nm and 480 ± 15 nm were monitored online using MetaFluor 5.0 (Visitron Systems, Puchheim) and analyzed with OriginPro 8G (Origin Lab Corporation, Northampton, USA). Emissions at 535 nm were corrected for CFP bleedthrough (57 %) and direct excitation of YFP (7 %) as determined from HEK cells expressing either CFP or YFP alone.[199] The change in YFP/CFP emission – also termed

FRET ratio – after adding 100 µl of the various ab preparations was compared to the change induced by adding (-) iso in a final concentration of 2 µM. The FRET ratio changes of up to 10 cells were determined for each field of view.

2.2.7.2 iMIC setup

In order to perform FRET-measurements in a miniaturized manner, we used the iMIC 2000 setup (TILLPhotonics, Martinsried, catalog no. 000-530-13652) working with PDL-coated 96-well-plates (IBIDI, Martinsried, catalog no. 89621). The cells were incubated with 200 µl of FRET-buffer with 0.1 µM ICI per well at 37 °C without CO_2. FRET-measurements were performed using a Polychrome 5000 (TILLPhotonics, Martinsried, catalog no. 0000-510-13397) and an U Plan Fluorite 10x Olympus (TILLPhotonics, Martinsried, catalog no. 0000-330-14360) objective, a Dichrotome iMIC Dual Emission Modul (TILLPhotonics, Martinsried, catalog no. 000-530-14565) with a CFP/YFP filter set, a Interline Transfer CCD Camera IMAGO Type QE (TILLPhotonics, Martinsried, catalog no. 0000-540-12149), the TillvisION v4.5.59 for single-well measurement mode (TILLPhotonics, Martinsried). Approximately 500 cells were imaged per experiment and well, and a mean fluorescence intensity value was calculated for each timepoint measured. As described for the FRET-measurements above the changes in YFP/CFP emission were monitored after adding ab (50 µl, corresponding to a 5-fold dilution) and compared to the response to 2 µM full agonist (-) iso. The setup described does not permit the direct excitation of YFP using the single-well measurement mode, however. Therefore, only the CFP bleedthrough was corrected for (40 %).

Recent implementation of the LiveAquisition 1.6.0.14 software (TILLPhotonics) made it possible to acquire FRET images in multiple wells in sequence and to analyze the acquired data online using the Arivis 2.5.5 browser (Arivis Multiple Image Tools, Rostock). Eight wells were measured per experiment and re-identification of the respective image frames was achieved by keeping the corresponding XYZ-marker settings.

2.2.7.3 NOVOstar reader

To improve automatization of the FRET assay, we tested the NOVOstar plate reader (BMG Labtech, Offenburg) allowing for an automated pipetting of samples and measuring multiple wells of a 96-well-plate in one single experiment. The system is equipped with a high energy xenon flash lamp for illumination and a CFP/YFP filter system with a BrightLine HC 438/24 excitation filter (AHF Analysetechnik, Tübingen, catalog no. F39-438), a

BrightLine HC 483/32 (AHF Analysetechnik, Tübingen, catalog no. F37-483), and a BrightLine HC 542/27 (AHF Analysetechnik, Tübingen, catalog no. F99-115) emission filter with a diameter of 15 mm. CFP and YFP emissions are detected sequentially. The setup does not allow for direct imaging of the cells or focused measurements. For our experiments the cells were seeded in PDL-coated 96-well-plates (IBIDI, Martinsried, catalog no. 89621) and incubated in 150 µl of FRET-buffer supplemented with 0.1 µM ICI per well at 37 °C without CO_2 supply during the experiments. For our measurements the DDE interface software of the NOVOstar was employed, data were analyzed using Microsoft Office Excel 2007 (Microsoft, Redmond, USA). During one cycle, measurements were performed of each well, and the exact position of each well was retrieved in consecutive cycles. Addition of samples to analyze was facilitated by the built-in multifunctional pipettor.

2.2.7.4 Pathway 855 setup

The Pathway 855 setup (BD Biosciences, Franklin Lakes, USA) allows for automated measurement and sample pipetting as well as imaging and data processing of individual cells. The setup is equipped with a Photofluor Metall Halide lamp as a light source, a CFP/YFP filter set containing an excitation filter Bright Line HC 427/10 nm (AHF Analysetechnik, Tübingen, catalog no. F39-427), an emission filter Bright Line HC 542/27 nm (AHF Analysetechnik, Tübingen, catalog no. F37-542), and a dichroic mirror HC Dualband 440/520 nm (AHF Analysetechnik, Tübingen, catalog no. F73-417). For imaging an Olympus UPLAPO 10x objective and a cooled CCD camera were used. Cells were seeded on a PDL-coated 96-well-microplate (IBIDI, Martinsried, catalog no. 89621), incubated with FRET-buffer containing 0.1 µM ICI-118551 and 1 µM Hoechst for 30 min, washed twice with FRET-buffer and incubated at 37 °C and 5 % CO_2 supply in 150 µl FRET-buffer supplemented with 0.1 µM ICI 118551 during the measurements. Measurement cycles were stacked similarly to the protocol used for the NOVOstar setup. As the Pathway 855 setup is not equipped with a beam splitter, CFP and YFP measurements are taken in rapid succession. A single measurement with a Bright Line HC 380/10 nm excitation filter (BD Biosciences), a 435 nm long pass emission filter (BD Biosciences), and a 400 nm long pass dichroic mirror (BD Biosciences) was applied at the end of each experiment to image Hoechst staining and allow for segmentation of the respective cells. The YFP channel is directly excited at the end of the experiment using a Bright Line HC 504/12 nm excitation filter (AHF Analysetechnik, Tübingen, catalog no. F39-504) and the aforementioned 542/27 nm emission filter and 440/520 nm dichroic mirror in order to obtain the required signal for FRET correction. The FRET signal could be corrected for 78 % CFP bleedthrough

in the YFP channel and 14 % direct excitation of the YFP channel only by manual data analysis using Windows Excel. For our Pathway 855 measurements the BD Attovision software was used, obtained data were analyzed using the BD Image Data Explorer.

2.2.7.5 Flow cytometry

Cell-suspensions for flow cytometry were obtained by detaching stable HEKβ_1E_1 cells from the surface of culture dishes with trypsin EDTA. Detached cells were sedimented by centrifugation (200 g, 2 min) and transferred into FRET buffer. Cells were incubated at 37 °C in the presence of (a) buffer, (b) 10 µM (-) iso, or (c) purified abs prior to analysis by flow cytometry. Cells were excited with a 405 nm Coherent VioFlame PLUS violet diode laser at 25 mW and emission signals were aquired with a 450/50 nm and a 530/30 nm filter on a LSR II flow cytometer (BD Biosciences, Franklin Lakes, USA). Data was aquired and processed using the BD FACSDiva software (BD Biosciences).

2.2.8 Statistical analyses

For comparison of data statistical analyses were performed with Windows Excel (Windows, Seattle, USA) using the unpaired two-tailed Student's T-test. $p < 0.05$ was considered significant, $p < 0.01$ highly significant. Data are given as mean plus or minus standard error of mean (SEM) except where indicated.

To evaluate the different assay methods, we employed the Z-factor, a statistical parameter that assesses the suitability of a specific assay for high-throughput screening.[200, 201] The Z-factor can be derived from the positive and negative controls' means and standard deviations ($\hat{\mu}_p$, $\hat{\mu}_n$, $\hat{\sigma}_p$, and $\hat{\sigma}_n$): $estimated\ Z - factor = 1 - \frac{3\,(\hat{\sigma}_p + \hat{\sigma}_n)}{|\hat{\mu}_p - \hat{\mu}_n|}$. A Z-factor value of 0.9 to 1.0 is considered as ideal in particular for high-throughput diagnostic assays, values between 0.7 and 0.9 are are acceptable for good diagnostic assays, values between 0.5 and 0.7 warrant assay improvement, assays with a Z-factor below 0.5 essays are not recommended for high-throughput screening.

Correlation analysis was performed using the Pearson correlation coefficient for parametric data and a linear fitting algorithm.

3 Results

3.1 Primary murine adult cardiac myocytes from a transgenic Epac1-cAMP sensor mouse

A prerequisite for the reliable and reproducible detection of conformational aabs capable of modulating the function of membrane β_1-AR is the expression of this recombinant receptor in cells that respond to physiological changes in a defined and quantifiable manner. One valuable cell system to analyze the effects of such conformational β_1-AR aabs on the human heart in the context of DCM would be primary ventricular cardiac myocytes from rodents in which the β_1-AR is homologous to humans.

Adult murine cardiac myocytes from an Epac1-camps expressing transgenic mouse line were prepared and FRET measurements on single cardiac myocytes were performed using the iMIC setup 2 h after seeding of the cell preparations on laminin-coated 96-well-plates. After registration of the baseline conditions (stimulation of the cell preparation with monochromatic light at 436 nm), potentially functionally active β_1-AR abs were added to the cells, and the change in the emission light intensities at 480 nm and 535 nm were recorded. For all experiments the maximal response of cardiac myocytes upon application of the β_1-AR agonist (-) iso (2 µM) was determined after 22 min of ab incubation (Fig. 4 a). For quantification of the functional effects of various conformational aabs tested, the FRET ratio change before and after aab application was calculated and expressed as a percentage of the FRET ratio change. Aabs prepared from a female DCM-patient achieved a FRET-ratio change of 24.7 ± 1.6 % SEM compared to the maximum obtained with 2 µM (-) iso (n = 5 experiments). Antibody preparations from an age-matched healthy female (control) changed the FRET-ratio only by 8.9 ± 2.8 % SEM (n = 14 experiments) yielding a highly significant difference between both samples (p = 0.002, Fig. 4 b).

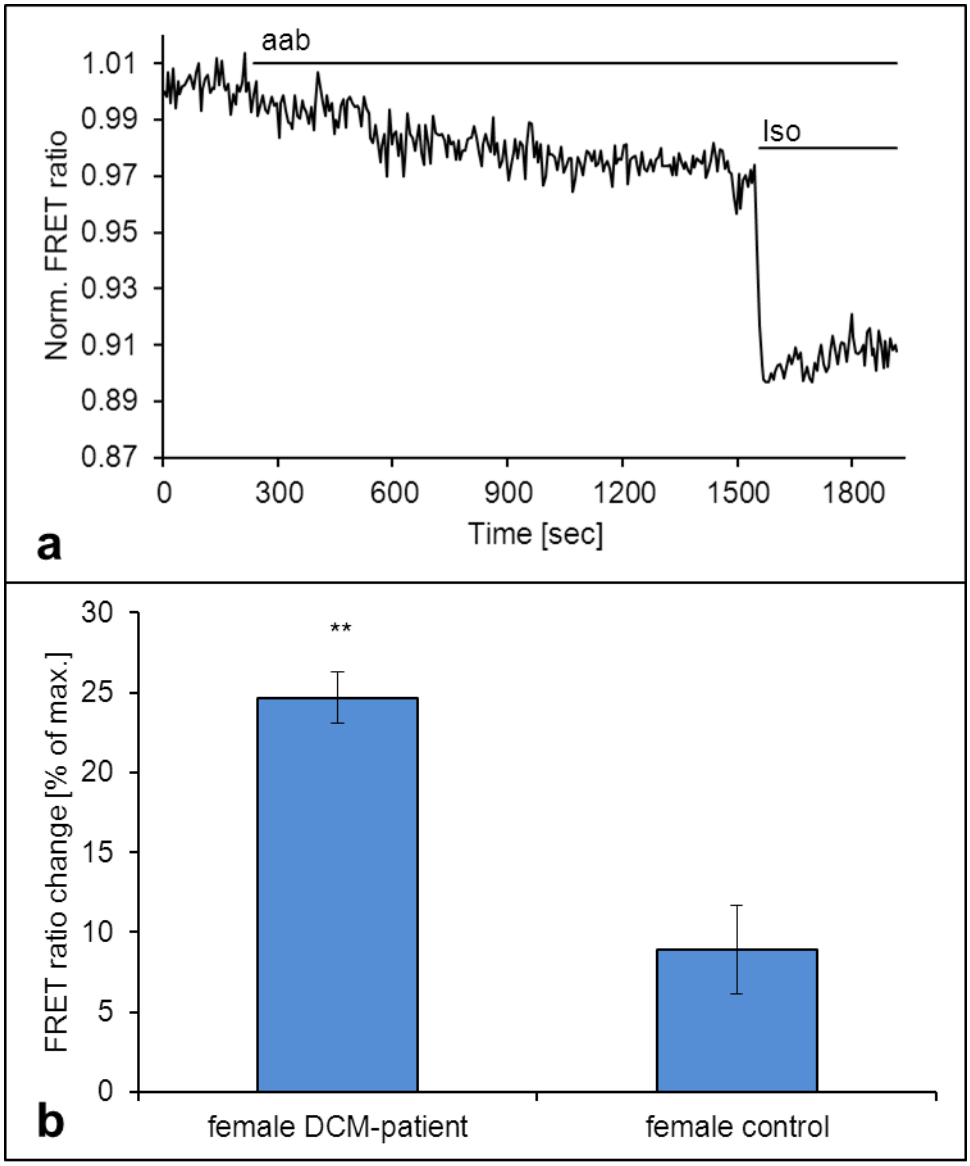

Fig. 4: FRET measurements of human ab preparations using adult murine cardiac myocytes. a) *Representative FRET measurements using adult murine cardiac myocytes expressing Epac1-camps upon incubation with aabs of a female DCM patient for 20 min and maximal stimulation with 2 µM (-) iso after reaching a plateau.* **b)** *FRET-responses of adult murine cardiac myocytes expressing Epac1-camps achieved with ab-preparations of a female DCM-patient or a healthy female control subject. The FRET-ratio change is expressed as % of maximal stimulation with (-) iso. (Error bars represent ± SEM, ** = p < 0.01).*

. Although isolated cardiac myocytes from rodents revealed agonist-like functional effects induced by ab preparations of human DCM patients in a reproducible manner, primary cells are not an ideal system for routine measurements, as there are large variations between individual animals and preparation days and the animal expenditure is undesirable. A functional assay based on a cell line that is expandable in culture was consequently aimed at.

3.2 Human embryonic kidney cell line stably expressing β_1-AR and Epac1-cAMP sensor

Firstly, the coding sequence of the human β_1-AR was stably expressed in HEK293A cells by transfection with the plasmid vector pBC-β_1 using the Effectene® transfection method and the antibiotic geneticin for selection. Secondly, upon establishment of a stable clonal HEKβ_1 cell line the cAMP-sensor Epac1-camps was transiently transfected into these cells with either the Effectene® or the calcium phosphate transfection method using the pcDNA3.1-Epac1-camps vector. 48 h after transient transfection of the sensor the cells were assessed by fluorescent microscopy for Epac1-camps expression and in case of positivity subsequently used for the assays. FRET measurements were performed in PDL-coated 96-well-plates on the iMIC setup in the presence of FRET buffer. After determination of the baseline measurement, cells were challenged with 2 µM (-) iso and the decrease in YFP/CFP FRET ratio was measured (Fig. 5). The response of HEKβ_1 cells transiently expressing Epac1-camps on (-) iso was 23.6 ± 16.2 % SD FRET ratio change (± 5.27 % SEM, n = 8, measurements on 200 - 500 cells per experimental condition). These cells were considered not suitable for routine measurements of patient samples due to their highly variable response upon (-) iso stimulation. Therefore, we generated a HEK293A cell line stably expressing both the human β_1-AR and Epac1-camps. The vector used for the stable transfection was pCEP4Epac1-camps under selection of the antibiotic hygromycin. The stable clonal cell line HEKβ_1E_1 routinely reacted to maximal (-) iso challenge with a FRET ratio change of 14.9 ± 1.3 % SD (± 0.45 % SEM, n = 8 measurements on 200 - 500 cells each, Fig. 5).

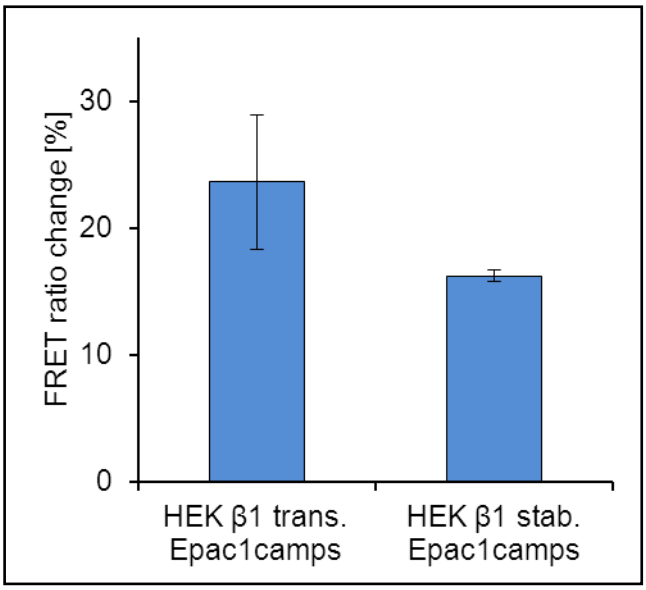

Fig. 5: Comparison of transient vs. stable expression of Epac1-camps. *FRET ratio change of HEK293A cells stably expressing β_1-AR and either transiently (left) or stably (right) expressing Epac1-camps upon stimulation with 2 µM (-) iso. 8 experiments on 200 to 500 cells were performed for each condition, error bars represent ± SEM.*

The clonal cell line HEKβ_1E_1 has been deposited at the "Deutsche Sammlung für Mikroorganismen und Zellkulturen GmbH" (Braunschweig) under the accession no. HEK-293 – DSM ACC 2985 and the University of Würzburg has filed for patent protection of this cell line (DE 102009 019578.5).[202]

Representative images of HEKβ_1E_1 cells illuminated with monochromatic light of 436 nm using the 480 ± 15 nm or the 535 ± 20 nm filter for monitoring CFP or YFP, respectively, were taken with the Zeiss Axiovert 200 setup (Fig 6). Cells were regularly checked for their clonal expression of the Epac1-camps FRET sensor using CFP excitation and transmitted light.

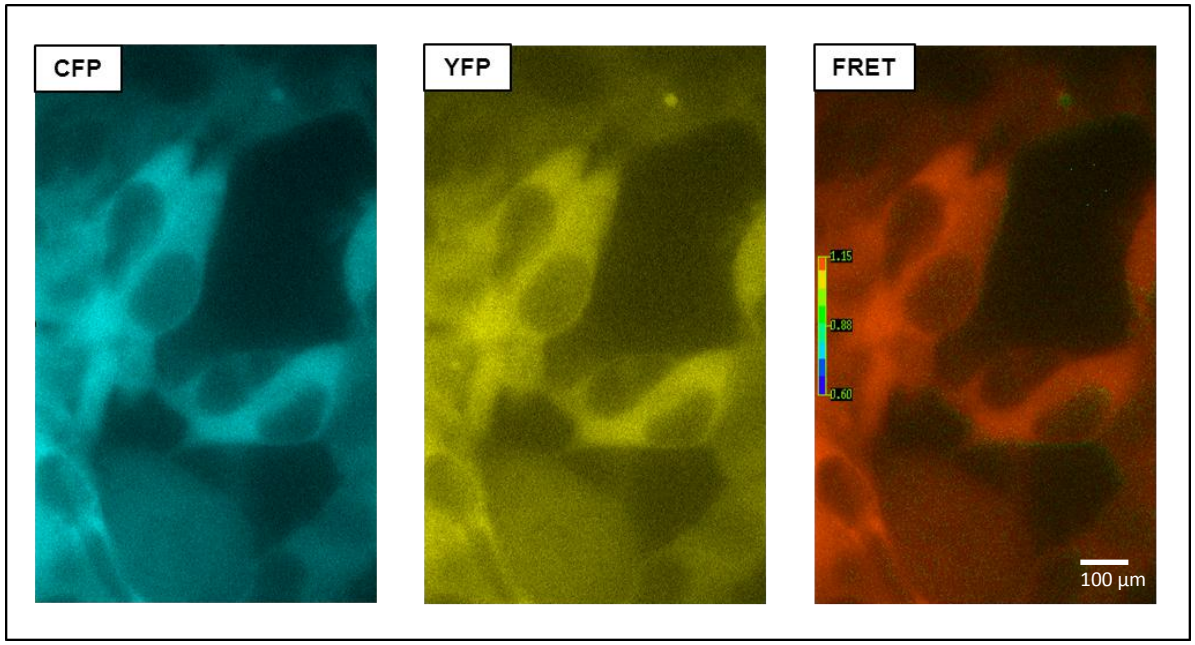

Fig 6: Fluorescent properties of HEKβ$_1$E$_1$ cells. *HEKβ$_1$E$_1$ cells emitting light in the YFP (535 ± 20 nm) and the CFP (480 ± 15 nm) channel upon excitation with monochromatic light of 436 nm. The YFP/CFP FRET ratio is depicted in pseudocolor, exposure time 15 msec, magnification 630x.*

Expression of β_1-AR in HEKβ_1E$_1$ cells was determined by radioligand binding (Fig. 7). Radioligand-competition experiments were conducted with the β_2-AR specific antagonist ICI or the β_1-AR specific antagonist bisoprolol. A β-AR subtype-specific drug has high affinity to its corresponding (specific) receptor subtype at a low concentration (left-hand part of the bi-sigmoidal curves) and binds only at higher concentrations also to the other subtype (right-hand part of the bi-sigmoidal curves). The curves demonstrate competition of [^{125}I]-CYP with low ICI concentrations at the β_2-AR, and with higher ICI concentrations also at the β_1-AR (Fig. 7 b). In contrast, [^{125}I]-CYP competes with low bisoprolol concentrations at the β_1-AR, and with higher concentrations also at the β_2-AR (Fig 7 a). The K_I value for the stably expressed β_1-AR was calculated and the β_1-AR/β_2-AR ratio was estimated. Total amount of β-AR expressed in the cell membrane were determined from saturation curves obtained with alprenolol and amounted to 0.4 ± 0.01 pmol/mg, which is higher than the physiological amount in cardiomyocytes (100-120 fmol/mg) (Tab. 3). The results obtained for bisoprolol and ICI 118551 in HEKβ_1E$_1$ cells were comparable to previous reports.[203]

An increase in the expression of membrane β_1-AR from 0.4 pmol/mg to 14 pmol/mg membrane protein in a stable HEKβ_1E$_1$ cell line did not increase the FRET signal (14.9 ± m 1.3 %, Fig. 5) , yielding 12.5 ± 4 % SEM (n = 4) FRET ratio change achieved with 10 µM (-) iso measured on the iMIC setup.

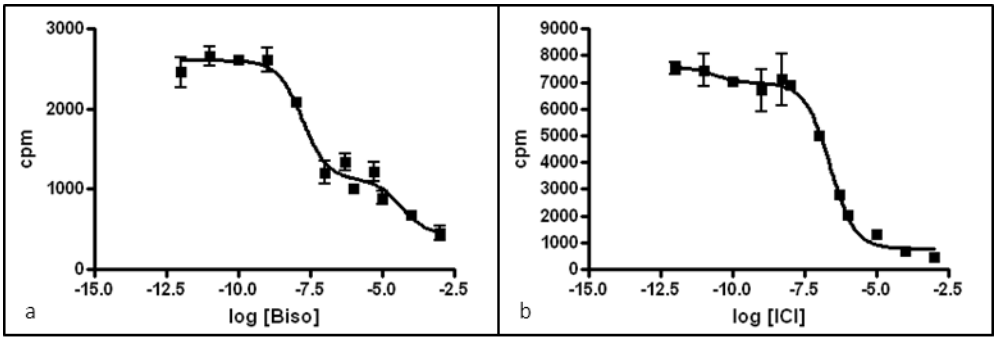

Fig. 7: Representative ^{125}I-cyanopindolol binding competition curves using a) bisoprolol or b) ICI 118551. *Experiments were performed in duplicate, error bars represent ± SEM. Curves were fitted to the data using two-sided non-linear regression analyses, cpm = counts per minute.*

Ligand	Receptor subtype	K_I [nM]	95 % Confidence Limit [nM]	Ligand binding sites [pmol/mg, %]
alprenolol	β_1-AR + β_2-AR			0.4 ± 0.01
bisoprolol	β_1-AR	4.3	2.1 – 8.7	
	β_2-AR	421	29.2 - 35200	
	β_1:β_2-AR			63 % : 37 %
ICI 118551	β_1-AR	1220	458 - 3280	
	β_2-AR	0.320	0.02 - 9.3	
	β_1:β_2-AR			68 % : 32 %

Tab. 3: Binding and expression characteristics of HEKβ_1E_1 cells derived from radioligand competition experiments.

Stable HEKβ_1E_1 cells responded to catecholamine stimulation in a physiological manner as was determined by a concentration-response curve of increasing (-) iso concentrations covering the naturally occuring range measured on the iMIC setup. Cells were stimulated with the chosen concentrations of (-) iso followed by a maximal stimulation of the cells with 10 M (-) iso. The cAMP response of the cells was expressed as % of the maximal response. Values were related to the respective (-) iso concentrations and the half maximal effective concentration (EC_{50}) of (-) iso was determined by semi-logarithmic plotting to 28.9 pM (Fig. 8) which is in the expected range of previously reported results in HEKβ_1 cells transiently expressing the Epac1-cAMP sensor.[144]

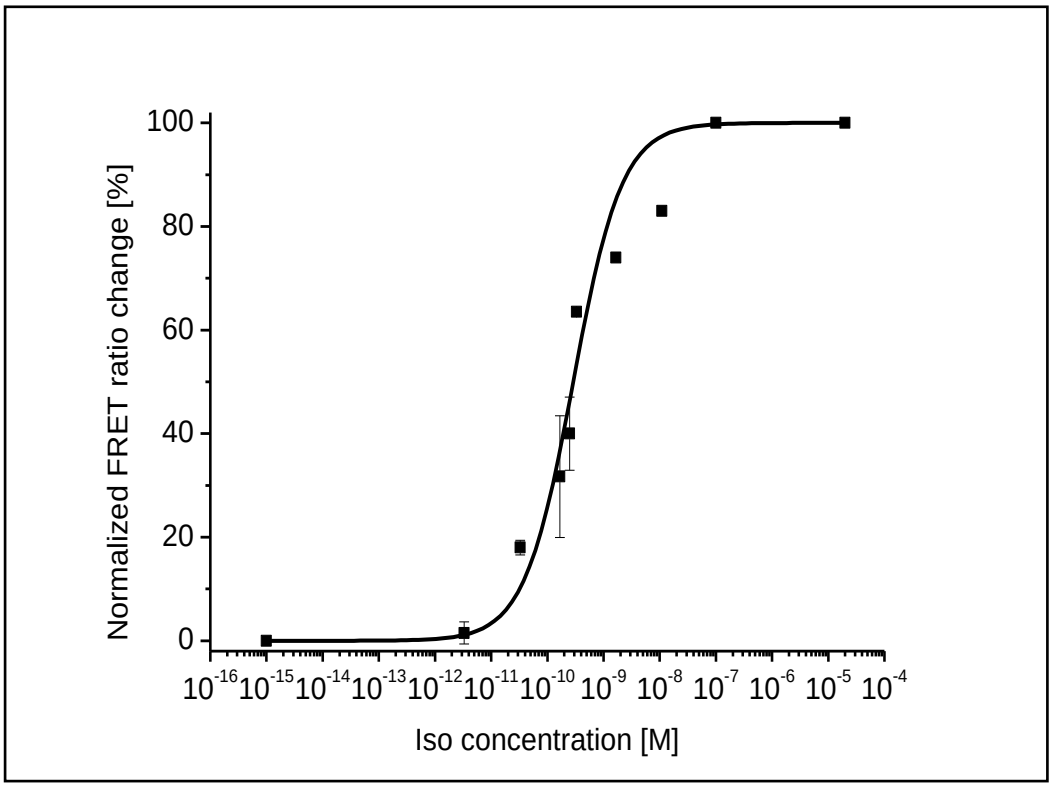

Fig. 8: Concentration-response-curve of FRET ratio changes of stable HEKβ_1E_1 cells after exposure to different concentrations of (-) iso.

The response of HEKβ_1E_1 cells to β_1-AR stimulation by (-) iso could be reverted by addition of the β_1-AR specific β-blocker bisoprolol (Fig. 9) as shown in a representative FRET curve of HEKβ_1E_1 cells determined using the Zeiss Axiovert 200 setup.

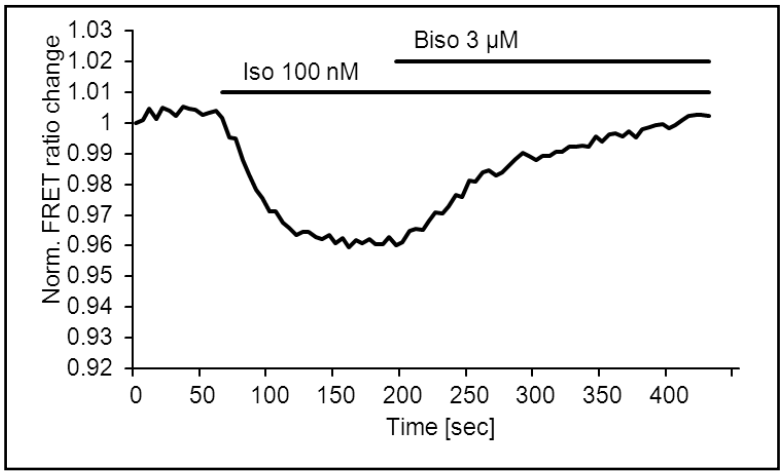

Fig. 9: Response to β_1-AR agonist and antagonist. *FRET measurement of HEKβ_1E_1 cells after stimulation with 100 nM (-) isol followed by application of the β_1-AR selective beta-blocker bisoprolol (3 µM).*

3.3 Antibody purification

Ab preparations had to fulfill certain pre-requisites in order to be reliably tested in the live-cell FRET assay using HEKβ_1E_1 cells. Preparation methods should be limited to only few handling steps to reduce the risk of ab damage and/or loss of functionality. Ab recovery, in particular of the IgG3 fraction, which has previously been identified as the Ig fraction potentially relevant for DCM,[204] should be optimized, and confounding serum components influencing the detection of conformational β_1-AR abs had to be reduced to a minimum – not interfering with the FRET assay.

Human serum exhibits autofluorescence when excited with monochromatic light at 430 nm (Fig. 10). As this would significantly affect fluorescence detection in the spectral range necessary for CFP and YFP (480 and 535 nm, respectively), it is not possible to utilize crude serum for live-cell assays. Additionally, human serum may contain the catecholamines epinephrine and norepinephrine and/or traces or metabolites of drugs (e.g. beta-blockers) interfering with the adrenergic system bearing the risk of false positive or negative results in functional assays.

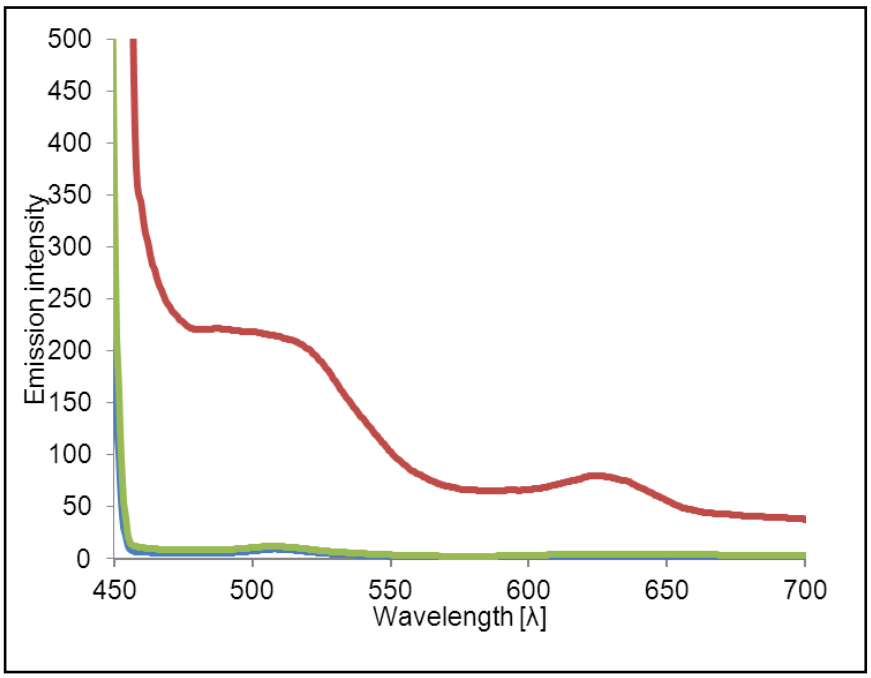

Fig. 10: Autofluorescent characteristics of serum. *Photospectrometrical analysis of crude human serum (red), abs prepared by caprylic acid precipitation from the same serum (green), and FRET buffer alone (blue) excited at 430 nm.*

With caprylic acid precipitation (CAP) almost all serum proteins are precipitated, whereas IgG remains in the supernatant. With this precipitation method (and dialysis against FRET-buffer) it was possible to overcome the problem of autofluorescence (Fig. 10) and to get rid of endogenous catecholamines and (exogenous) potentially interfering drugs and/or drug-metabolites. With SDS-PAGE separation the high purity of caprylic acid precipitated samples could be demonstrated. Compared with crude serum, fewer protein bands, particularly in the molecular weight (MW) range of 50 to 250 kDa, were observed (Fig. 11). Furthermore, a relative reduction of a protein band coresponding to the molecular weight of albumin (human 67 kDa,[205] rat 65 kDa[206]) compared to the bands with the characteristic MW of the Ig heavy (human HC ~50 kDa,[207] rat HC ~55 kDa[208]) and light chains (rat LC ~23 kDa[207, 208]) was achieved, indicating an enrichment of Ig through caprylic acid precipitation.

Additional purification of ab samples is thought to be achieved by ammoniumsulphate precipitation (ASP) of the Ig fraction and subsequent reconstitution of the pelleted protein. However, our results show that this purification method on its own is not superior to CAP; nevertheless, when combined with CAP either before or after ASP further reduced the protein band assigned to albumin (Fig. 11).

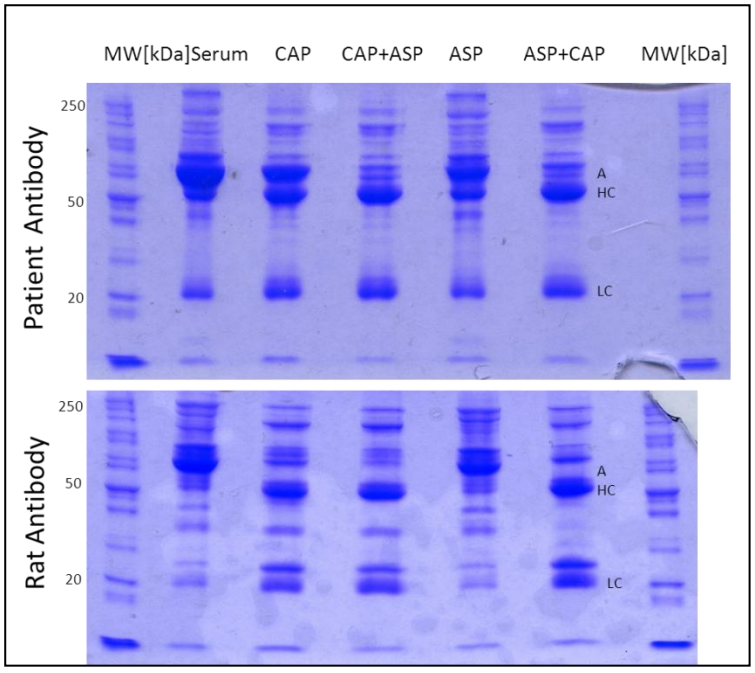

Fig. 11: IgG purification. *SDS-PAGE of crude serum, caprylic acid precipitation (CAP), caprylic acid and subsequent ammoniumsulphate precipitation (CAP+ASP), ammoniumsulphate precipitation (ASP), ammoniumsulphate and subsequent caprylic acid precipitation (ASP+CAP). Representative serum samples from a female DCM-patient (upper panel) and from an immunized DCM rat (lower panel) were utilized. Coomassie blue stain, 15 µg of denatured protein was loaded per lane, A = albumin, HC = Ig heavy chain, LC = Ig light chain.*

Despite the slightly increased purity of the IgG fraction in serum samples treated with both CAP and ASP, the functional effects of IgG isolated with both methods combined compared to caprylic acid precipitation alone were not more pronounced in the live-cell FRET assay (iMIC setup, Fig. 12). Therefore, in clinical or laboratory routine ab preparation by ASP will not be applied; however, this procedure might be useful in case abs must be concentrated, as the pelleted Igs might be reconstituted in a smaller volume of buffer.

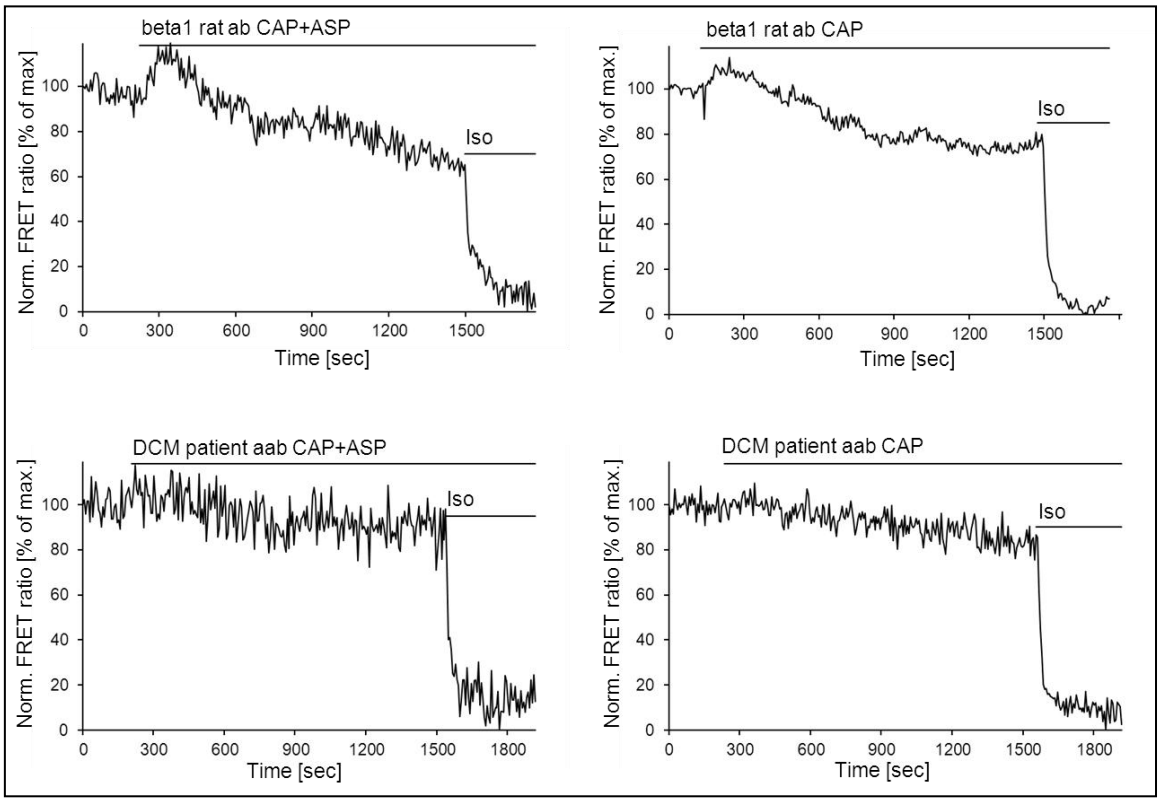

Fig. 12: FRET-analysis of different IgG preparation protocols. *Comparison of caprylic acid followed by ammoniumsulphate precipitation (left, CAP+ASP) to caprylic acid precipitation alone (right, CAP). Ab preparations from the serum of an immunized DCM rat (upper panels) or a female DCM patient (lower panels) were tested in the live-cell FRET assay. For the maximal FRET response 2 µM (-) iso was added after completion of the ab-response.*

Another method of ab preparation from sera is their adsorption on thiophilic agarose columns and subsequent elution. We tested ab purification using thiophilic agarose according to (a) the manufacturer or (b) to a previously published protocol. However, none of these purification methods was superior to CAP in terms of purity, IgG enrichment (Fig. 13), and functional effects in the live-cell FRET assay (iMIC setup, Fig. 14). Aabs from a female DCM patient prepared by CAP exhibited 16.3 ± 2.4 % FRET signal, aabs from the same patient prepared by TAA according to (a) or to (b) established in our lab[197] yielded a FRET signal of 14.8 ± 1.9 % and 14.6 ± 2.1 %, respectively.

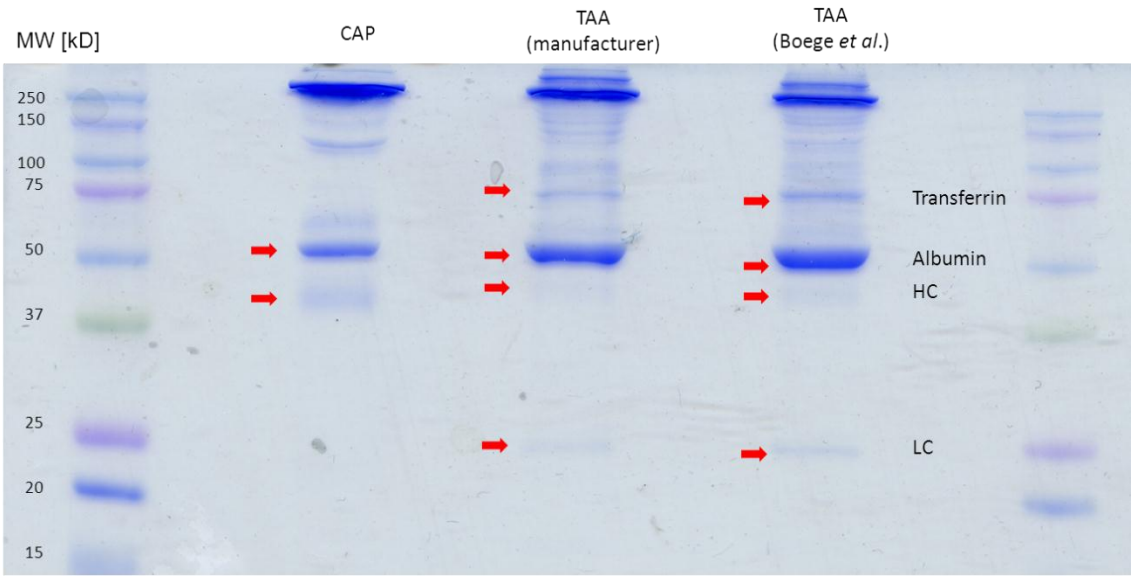

Fig. 13: SDS-PAGE of caprylic acid and thiophilic acid precipitation purified IgG. *SDS-PAGE of aab preparations from a female DCM patient by caprylic acid precipitation (CAP) or thiophilic agarose adsorption (TAA) according to (a) the manufacturer or (b) a previously published protocol. 15 µg of denatured protein was applied per lane with Coomassie blue stain; bands corresponding to transferrin (T),[207] albumin (A), and Ig heavy (HC) and light chain (LC) are indicated by arrows.*

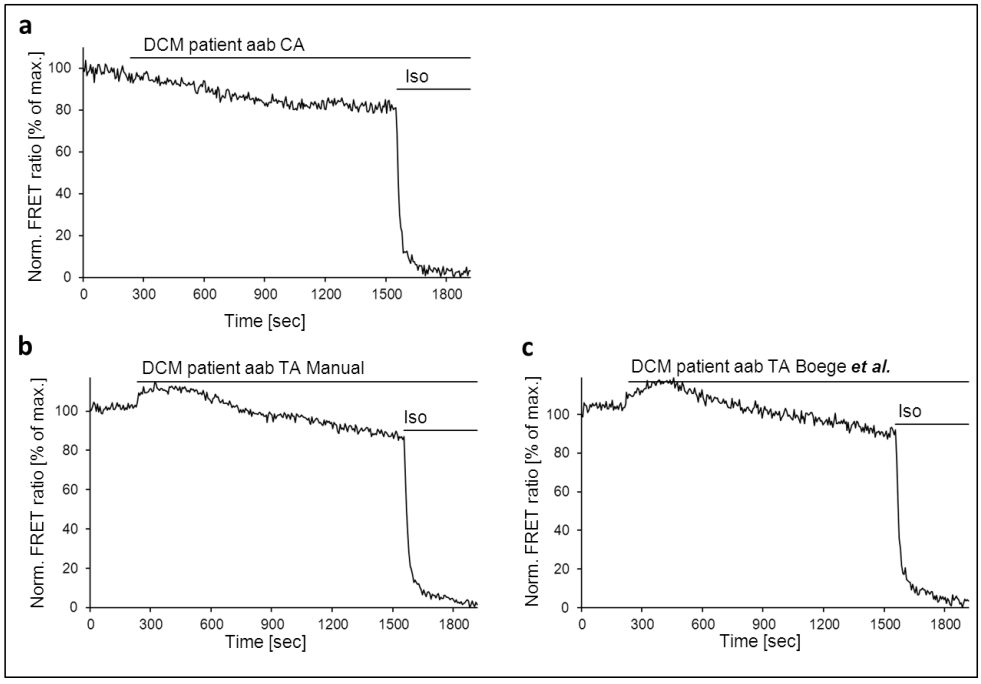

Fig. 14: FRET activity of IgG isolated by caprylic acid precipitation (CAP) or thiophilic agarose adsorption (TAA). *Comparison of CAP **a**) to TAA (lower panels) according to **b**) manufacturer's protocol (left) or **c**) to Boege* et al.[197] *(right). Aabs from serum of a female DCM patient were applied in the FRET assay and 100 µM (-) iso was added after completion of the antibody-response.*

3.4 Mono- and polyclonal anti-β_1-AR-abs

Having established a clonal cell line allowing for a reproducible online measurement of cellular cAMP levels upon β_1-AR activation and an appropriate IgG isolation protocol, we measured the effects of different conformational anti-β_1-AR abs (Tab. 4). A polyclonal rabbit anti-β_1EC_{II} ab exhibited FRET signals of 30.63 ± 3.85 % of maximal FRET responses obtained with 2 µM (-) iso set to 100 %.

To establish a large-scale functional FRET assay for the screening of patients for stimulating anti-β_1-AR aabs it is essential to have a reliable positive control. Because a continuous supply of such a positive control (including a constant quality for several years) is required, the best strategy would be to employ a monoclonal ab for this purpose. We tested a commercially produced monoclonal mouse and several monoclonal rat anti-β_1EC_{II} abs (self-generated by fusion of B-cells from successfully immunized Lewis rats with immortalized plasma cells). In the FRET assay using the iMIC setup. MAB from the self-generated clones 13F6 and 10E1 yielded reproducible strong cAMP signals in the assay, whereas those from clone 1D4 had a clearly lower functional activity. Isotypic monoclonal rat ab served as control and yielded less than 10 % FRET signal. The commercially produced mouse anti-β_1EC_{II} MAB (26-6-7) exhibited 27.25 ± 2.89 % FRET signal in the functional FRET assay.

	FRET ratio change [% of max.]	**SEM**	**n**
Monoclonal abs			
Rat 10E1	27.37	1.53	3
Rat 13F6	34.52	3.41	5
Rat 1D4	12.33	4.15	4
Rat isotype	8.60	6.79	3
Mouse 26-6-7	27.25	2.89	13
Polyclonal abs			
Rabbit	30.63	3.85	11

Tab. 4: Rodent antibodies. *List of abs tested for functional sympathomimetic activity in the live-cell FRET assay (iMIC setup).*

3.5 Anti-β_1-aab detection in sera from patients with heart failure

Selected patient collectives suffering from various cardiac disorders were analyzed. Control sera were obtained from healthy volunteers without evidence for, or history of, cardiac disease. DCM patients from the outpatients' department of the University Hospital

Würzburg had significant coronary artery disease excluded (previous coronary angiography) and were stable on medication according to current CHF treatment guidelines[209] for at least 3 months. At the time of visit blood was drawn, centrifuged (4000 g, RT, 15 min) and the serum fraction immediately placed on ice for further aab preparation (CAP, dialysis) and testing. On the same day the patients underwent echocardiography to assess left ventricular (LV) diameters and function according to ASE guidelines[210] (biplane volumetry, Simpson). The mean value of FRET signals (corresponding to ab-induced cellular cAMP increases) achieved by aabs prepared from patients with hypertensive heart disease (HHD, 18.19 ± 1.76 % SEM, n = 6), ischemic cardiomyopathy (ICM, 18.41 ± 2.54 % SEM, n = 9), or dilated cardiomyopathy (DCM, 19.24 ± 2.60 % SEM, n = 58) did not differ significantly from each other, but differed significantly from healthy controls (5.6 ± 0.78 % SEM, n = 9, $p < 0.001$ Tab. 5). The mean value of the FRET-signals achieved with IgG preparations from healthy controls + twofold SD (10.3 %) was chosen as a cut off for sympathomimetic β_1-AR-mediated effects. None of the controls, but all of the HHD and ICM patients, as well as the majority of the DCM patients (82.8 %) were positive for activating β_1-AR aabs.

In DCM patients identified as β_1-AR aab positive, there was a significant inverse correlation between left ventricular ejection fraction (LVEF) and the receptor stimulating potential of β_1-AR aabs ($R^2 = 0.11$, n = 48, $p < 0.002$, DCM 11-58, Fig. 15). Only a limited number of ab preparations from patients with ICM were analyzed. Due to the small sample size any attempt to correlate LVEF with the extent of β_1-AR stimulation was not meaningful. LVEF in HHD patients was $\geq$ 50 %. LVEF in healthy humans was assumed to be in the normal range of 55-70%, therefore, for our statistical analysis a mean value of 62.5 % was used.

Human ab samples	FRET ratio change [% of max.]	SEM	LVEF [%]	Human ab samples	FRET ratio change [% of max.]	SEM	LVEF [%]
Healthy 1	2.47	1.04	62.5	DCM 19	15.30	1.80	55
Healthy 2	4.06	1.68	62.5	DCM 20	15.59	0.41	20
Healthy 3	4.35	1.55	62.5	DCM 21	16.23	3.53	45
Healthy 4	4.60	1.70	62.5	DCM 22	16.50	1.30	27
Healthy 5	4.63	2.39	62.5	DCM 23	16.57	3.17	50
Healthy 6	4.92	6.30	62.5	DCM 24	17.03	1.92	34
Healthy 7	7.62	1.46	62.5	DCM 25	17.13	1.91	16
Healthy 8	7.75	3.65	62.5	DCM 26	17.54	1.96	16
Healthy 9	10.02	1.07	62.5	DCM 27	17.97	0.80	45
HHD 1	13.20	2.17	50	DCM 28	18.25	1.07	30
HHD 2	13.47	4.71	50	DCM 29	18.46	5.24	24
HHD 3	17.27	1.44	50	DCM 30	18.72	1.45	29
HHD 4	19.70	4.34	50	DCM 31	18.73	0.58	52
HHD 5	22	0.3	58	DCM 32	19.19	3.83	45
HHD 6	23.50	1.70	50	DCM 33	20.00	3.24	26
ICM 1	12.26	0.07	35	DCM 34	20.58	1.45	21
ICM 2	12.87	0.92	19	DCM 35	20.86	1.64	36
ICM 3	14.72	2.43	48	DCM 36	22.34	4.86	15
ICM 4	14.94	4.12	30	DCM 37	21.50	2.27	27
ICM 5	15.60	1.84	30	DCM 38	21.71	4.98	40
ICM 6	16.65	6.60	35	DCM 39	22.57	1.48	40
ICM 7	19.19	2.19	31	DCM 40	22.72	2.01	30
ICM 8	22.49	4.44	26	DCM 41	22.78	3.68	20
ICM 9	36.95	4.36	35	DCM 42	23.66	1.84	25
DCM 1	4.94	4.94	43	DCM 43	23.84	2.64	17
DCM 2	6.39	3.12	35	DCM 44	23.88	5.00	31
DCM 3	6.44	3.40	30	DCM 45	23.98	4.36	33
DCM 4	7.69	4.08	17	DCM 46	25.07	1.08	45
DCM 5	7.80	2.74	42	DCM 47	26.22	0.79	22
DCM 6	7.86	2.02	52	DCM 48	26.55	2.87	37
DCM 7	8.18	4.63	32	DCM 49	27.35	1.49	34
DCM 8	8.26	3.01	13	DCM 50	27.36	1.70	43
DCM 9	9.11	3.51	40	DCM 51	28.05	2.64	31
DCM 10	10.00	1.79	22	DCM 52	32.06	1.25	32
DCM 11	10.89	2.56	41	DCM 53	32.55	0.13	19
DCM 12	11.06	3.62	54	DCM 54	33.03	6.02	33
DCM 13	12.07	3.27	50	DCM 55	34.15	3.27	28
DCM 14	12.20	2.22	35	DCM 56	34.38	4.80	26
DCM 15	13.90	2.30	50	DCM 57	36.61	1.38	30
DCM 16	14.37	0.73	24	DCM 58	38.41	1.32	22
DCM 17	14.40	4.95	47				
DCM 18	15.20	1.01	31				

Tab. 5: Human IgG. *FRET ratio changes induced by (a)abs of healthy subjects or patients with hypertensive heart disease (HHD), ischemic cardiomyopathy (ICM), or dilated cardiomyopathy (DCM) upon testing in the live-cell FRET assay on the iMIC setup. Left ventricular ejection fraction (LVEF) was determined by echocardiography. In patients judged anti-β_1EC_{II}-aab positive the respective FRET values are indicated in red.*

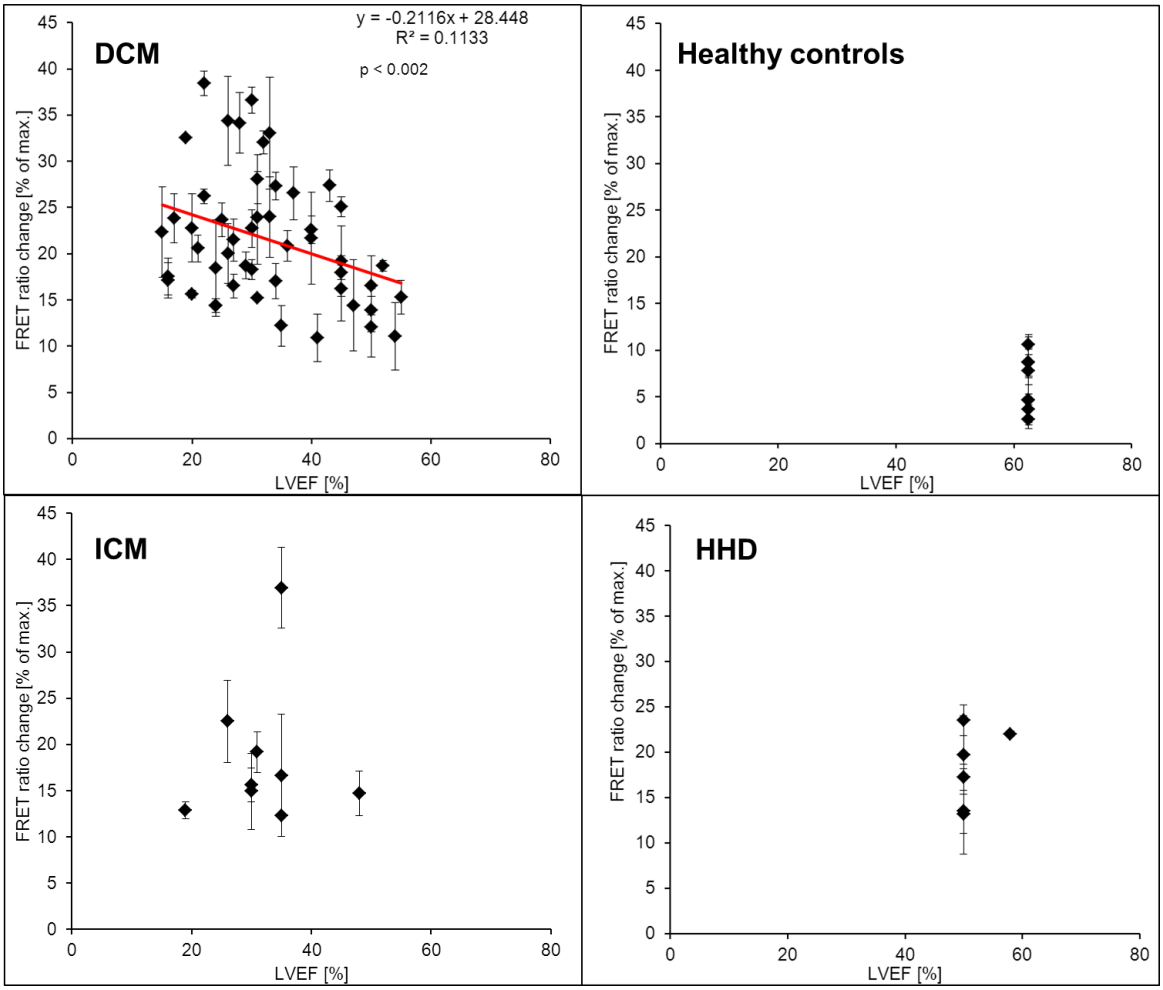

Fig. 15: Correlation of LVEF of DCM patients with the β_1-AR activating potential of aabs in the live-cell FRET assay. *Due to small sample size for healthy controls, ICM and HHD patients no correlations were calculated. Error bars represent ± SEM. For DCM patients, the inverse correlation between FRET-activity and LVEF is shown with the derived equation in red.*

3.6 Characterization of linear and cyclic peptides mimicking the β_1EC_{II}

3.6.1 Pilot experiments with rabbit anti-β_1-AR-abs

In the next step of my working programm it was my task to test whether the functional effects of conformational β_1-AR-aabs activating the receptor could be neutralized by peptides mimicking the antigenic region of the receptor. In the experiments I utilized flexible linear and cyclic peptides mimicking β_1EC_{II} for *in vitro* pre-incubation, and analyzed their respective blocking effects on (a)abs in the FRET assay. The agonistic activity of polyclonal

rabbit anti-β_1-AR abs (30.6 ± 3.9 % SEM FRET ratio change, n = 11) could be significantly reduced by pre-incubation with a 40-fold molar excess of 22AA CP (9.6 ± 2.1 % SEM FRET ratio change, p = 0.003, n = 5) but only to a lesser extent with the 22AA linear peptide corresponding to the β_1EC_{II} sequence (13.9 ± 1.1 % SEM FRET ratio change, p = 0.049, n = 3, Fig. 16). A 25AA linear peptide with a random scrambled arrangement of the AAs present in the β_1EC_{II} sequence was used as a control and was not able to block the partially agonistic effects of rabbit anti-β_1-AR-abs (24.4 ± 2.8 % SEM FRET ratio change, p = 0.43, n = 3). As a consequence from these pilot experiments for all further *in vitro* blocking experiments we employed cyclic rather than linear peptides.

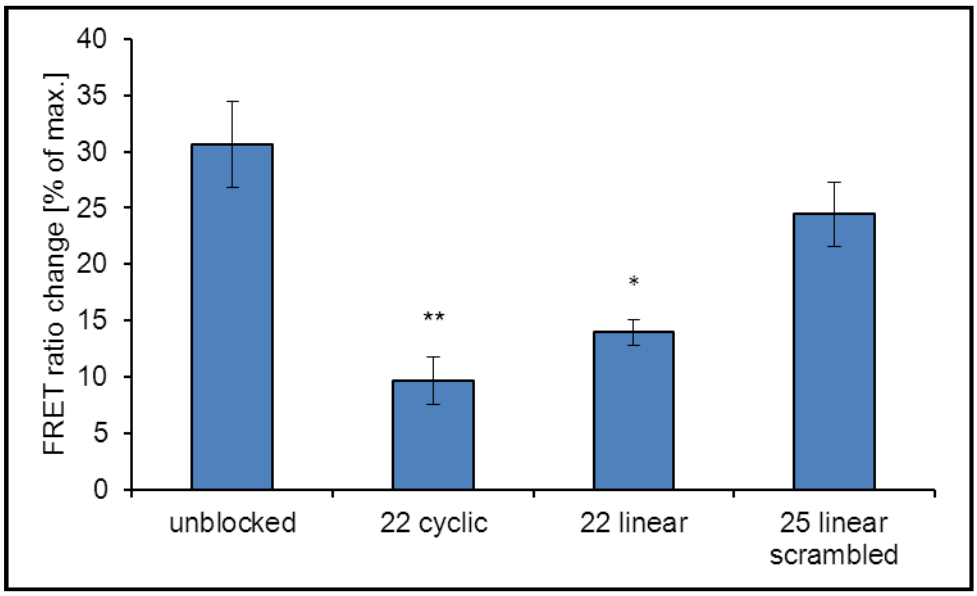

Fig. 16: Neutralization of of activating β_1-AR-abs pre-incubated with linear and cyclic peptides. *Polyclonal rabbit anti-β_1-AR abs were pre-incubated with the 22AA cyclic, or the 22AA linear peptide mimicking β_1EC_{II} and compared with a 25AA linear peptide with a scrambled sequence of the AAs constituting the β_1EC_{II}. ** = p < 0.01, * = p < 0.05 vs. unblocked, error bars depict ± SEM.*

3.6.2 Experiments with rat anti-β_1-AR-abs

Lewis rats were immunized with a β_1EC_{II}-GST fusion peptide and developed anti-β_1EC_{II} abs. After 6-9 months of monthly immunization, anti-β_1EC_{II} positive rats also developed a cardiac DCM phenotype as determined by echocardiography and by invasive measurements (left heart catheterization, data not shown). As in these rats the immune-response against β_1EC_{II}-GST was expected to be polyclonal, we intended to analyze

whether the known EC_{II} interloop disulfide bridge between C209 and C215 is important for epitope recognition by the generated rat anti-β_1EC_{II}-abs.

In the experiments I deduced the immunoreactivity of rat sera after pre-incubation with CPs possessing either a disulfide bridge between C209 and C215 (18C/C/S) or between C209 and C216 (18C/S/C). In the β_1-AR, the C216 residue engages in a disulfide bridge with the transmembrane region III in direct vicinity of the first extracellular loop EC_I. In 12 rats pre-incubation of sera with either peptide did not alter ab-binding to β_1EC_{II}, 5 rats had abs that could be blocked by either peptide and therefore featured reduced ab-binding in ELISA experiments. Very few (4 %) rat-ab-samples were blockable by 18C/S/C only. However, the overwhelming majority of DCM-rats (78 animals, 79 %) had developed anti-β_1EC_{II}-abs that were blocked by 18C/C/S only, and not by 18C/S/C (Fig. 17).

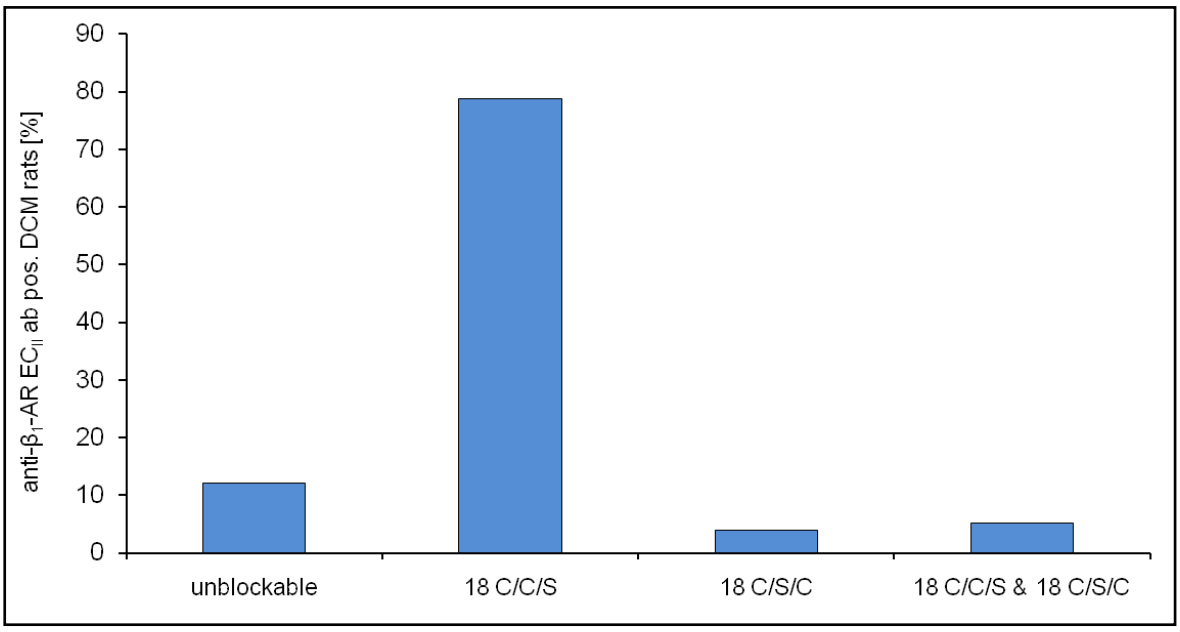

Fig. 17: ELISA data of CP-incubated rat sera. *Sera with anti-β_1EC_{II} abs from 99 rats immunized with β_1EC_{II}-GST that could be blocked by 18C/C/S, 18C/S/C, both cyclic peptides, or none of them as confirmed by ELISA binding experiments (Schlipp* et al*. in preparation).*

3.6.3 Neutralization of functional ab-effects

After analyzing their blocking capacity in ELISA, the next step was to determine whether these peptides were also able to circumvent an ab-mediated activation of the native receptor situated in a cell membrane. The activating potential of abs was detected indirectly by FRET-experiments measuring the production of cellular cAMP upon stimulation of the receptor. For these experiments the iMIC setup was used.

After stable baseline for 4 min, either unblocked or over night peptide-incubated ab samples were added to the cells. In pre-experiments we determined the maximal reaction time for conformational receptor-abs in the FRET assay to be 20 min. Therefore, the reference value for maximal stimulation of the receptor was routinely determined by adding the full β_1-AR agonist (-) iso to the cells after 22 min. Adding (-) iso to the cells also serves (a) to demonstrate viability of the cells employed in the respective assay, and (b) to furnish a basis for the calculation of the relative activatory potential of abs in relation to (-) iso. In our experiments, the time-course of the YFP/CFP emission ratio was routinely followed in about 200-500 cells per assay. The activation potential of the sample was then expressed as maximal FRET ratio change achieved by the respective antibody (blocked or unblocked) compared to the maximal (-) iso response normalized to 100 %.

An anti-β_1EC_{II} polyclonal rabbit IgG preparation yielded 18.7 % FRET activity (± 1.2 % SEM, n = 6). Pre-incubation with the 18C/C/S peptide significantly reduced its activity to 9.4 % (± 2.2 % SEM, n = 5), whereas pre-incubation with the 18C/S/C peptide had almost no effect (18 ± 2 % SEM of maximal response, n = 4, Fig. 18).

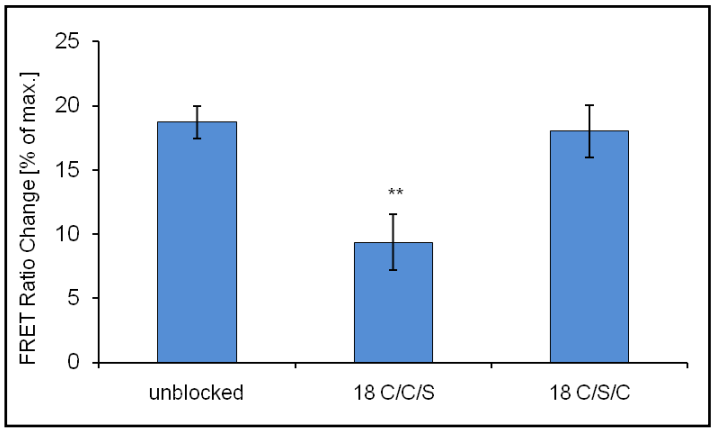

Fig. 18: FRET data of CP-incubated rabbit IgG. *FRET signals obtained with polyclonal rabbit anti-β_1EC_{II} (unblocked, left) pre-incubated with 18C/C/S CP (middle) or 18C/S/C CP (right) at 40-fold molar excess. FRET experiments were performed at least in triplicate with ~ 500 cells per experiment, error bars represent ± SEM, ** = p < 0.01 compared with unblocked IgG (Schlipp* et al.*, in preparation).*

3.7 Fine-mapping of the functionally relevant anti-β_1EC_{II}-(a)ab epitope

Since the blocking or neutralizing efficiency of the aforementioned different peptides also provides some information on the conformation of the targeted structure, we then attempted to employ these peptides in order to map the functionally relevant receptor epitope recognized and bound by abs implicated in the induction or promotion of a DCM phenotype. In this aim, sera from 20 immunized DCM-rats positive for activating β_1EC_{II} abs were individually blocked with either β_1EC_{II}-22AA-CP (the CP mimicking β_1EC_{II}) or a series of sequentially alanine-mutated 22AA-CP (E202A, S203A, D204A, R207A, R208A, N211A, D212A, P213A, K214A) in a so-called ala-scan approach. If a conformationally relevant peptide residue within the CP is exchanged for alanine, the resulting "damaged" peptide should no longer be able to bind to and block ab-mediated β_1-AR activation. The average neutralizing potential of the alanine-mutated CPs was determined first by ELISA competition assay using the linear β_1EC_{II}-25AA-peptide as an antigen (Fig. 19). An unblocked antibody-sample binding to the β_1EC_{II}-25AA-peptide would equal 0 % blocking capacity; a peptide fully blocking ab-binding to the antigen would be classified as having 100 % blocking capacity. The CPs corresponding to β_1EC_{II}-22AA-CP E202A, S203A, D204A, R207A, and R208A exerted a blocking capacity of approximately 80 % each. The blocking capacity of the peptides N211A, D212A, and P213A decreased gradually yielding 53.5 %, 44.8 %, and 21.2 % reduction in ELISA reactivity, respectively. The CP K214A blocked the ELISA signal by 53.7 % comparable to N211A. Thus, for the anti-β_1EC_{II} abs induced in Lewis rats which had developed DCM the "NDPK" motif within the CP seems to represent an essential epitope being recognized and bound by disease-inducing abs.

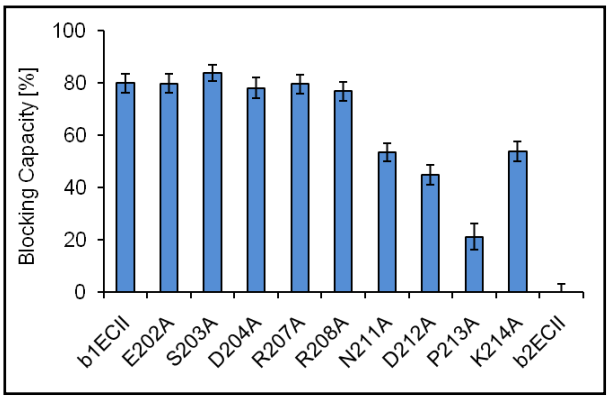

Fig. 19: ELISA data of rat sera incubated with ala-mutated β_1EC_{II}-22AA-CP. *Sequentially ala-mutated 22AA-CPs mimicking β_1EC_{II} were used to block abs from anti-β_1EC_{II} positive immunized rats (triplicate). CPs mimicking β_2EC_{II} (b2ECII), β_1EC_{II} (b1ECII), or sequentially alanine-mutated versions of a 22AA β_1EC_{II}-CP were employed. Sera were measured individually and normalized to unblocked samples (0 %, error bars represent $\pm$ SEM, n = 20, Schlipp* et al., *in preparation).*

In order to confirm this observation, we analyzed the neutralizing potential of the different CP mutants by testing other available anti-β_1EC_{II}-(a)abs using a two-tier approach: ELISA and FRET microscopy. Results are depicted as % of reduction of the signals obtained with an unblocked ab-preparation of anti-β_1EC_{II} generated either in mice (MAB), in rabbits (PAB) or, again, those generated in rats (PAB, Fig. 20).

In the mouse MAB the residues RRNDPK seem to be important for the recognition of the linear 25AA β_1EC_{II} peptide in ELISA, but only the residues NDPK appear to be relevant in the functional FRET assay. Rabbit anti-β_1EC_{II}-PAB were insufficiently blocked by peptides mutated in the NDPK motif in the ELISA approach and only by PK-mutated CP in the functional FRET assay. For rat anti-β_1EC_{II}-PAB in both assays mutations in the DPK motif hindered CPs from binding and blocking ab-induced β_1-receptor activation. In addition, the N211A mutant showed a slightly reduced blocking capacity, when preincubated with rat PAB in the functional FRET assay.

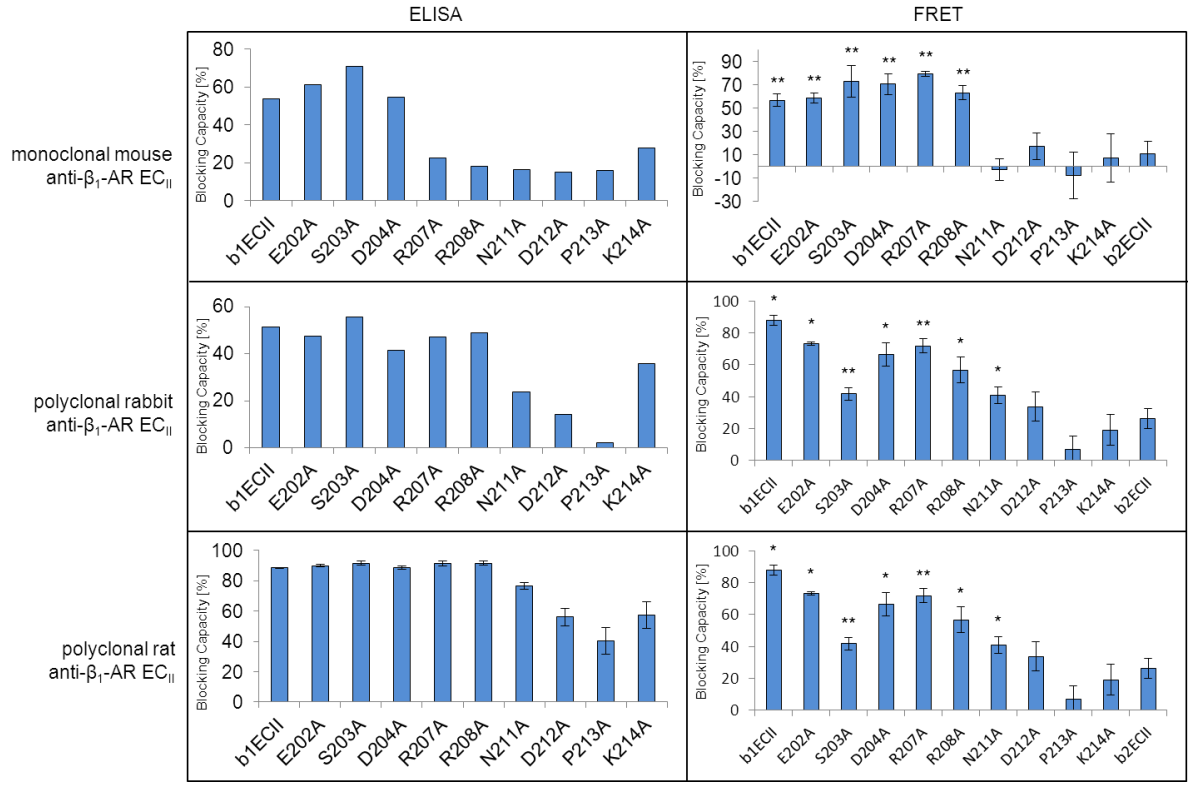

Fig. 20: ELISA and FRET data of different anti-β_1-AR abs incubated with ala-mutated β_1EC_{II} 22AA-CPs. In vitro *blocking capacity of cyclic peptides tested with various abs. Monoclonal mouse anti-β_1EC_{II}- (top), polyclonal rabbit anti-β_1EC_{II} (middle), and polyclonal rat anti-β_1EC_{II}-IgG preparations (bottom) were incubated with cyclic peptides mimicking β_2EC_{II} (b2ECII), β_1EC_{II} (b1ECII), or sequentially alanine-mutated versions thereof. These samples were tested for binding to β_1EC_{II} by ELISA (left), and physiological activity in FRET experiments (right) with β_1-AR-expressing cells. The extent to which the various cyclic peptides blocked the signal compared to unblocked ab preparations set at 100 % is referred to as "blocking capacity". ELISA and FRET experiments were performed at least in triplicate. In the FRET assay approximately 500 cells per experiment were used, error bars indicate ± SEM, * = $p < 0.05$, ** = $p < 0.01$ vs. unblocked ab preparations (Schlipp* et al., *in preparation).*

Taken together the two assays used to determine ab binding (ELISA) and functional ab activity (FRET assay) yielded slightly diverging results for the blocking capacities of different 22AA-CP ala-mutants; however all different conditions unmasked one-and-the-same epitope seemingly crucial for target recognition and target activation.

3.8 Monitoring of cyclic peptide therapy in the rat

FRET experiments (Zeiss Axiovert 200 setup) using stimulatory IgG prepared from rats with immune DCM revealed that the effect induced by agonist-like β_1-AR agonistic abs from an immunized animal clearly differed from that of a non-immunized control animal, and could only partially be abolished by adding 5 µM bisoprolol (Fig. 21). However, similar to the tested rabbit anti-β_1EC_{II}-abs (Fig. 16), the stimulatory effects of abs from immunized Lewis

rats could be blocked efficiently (> 60 %) with either a 22AA CP mimicking the **β_1EC_{II}**, or – less efficiently (~ 50 %) – with a linear 25AA peptide. The **β_2EC_{II}**-mimicking 22AA cyclic control peptide had no effect on stimulating anti-β_1-abs.

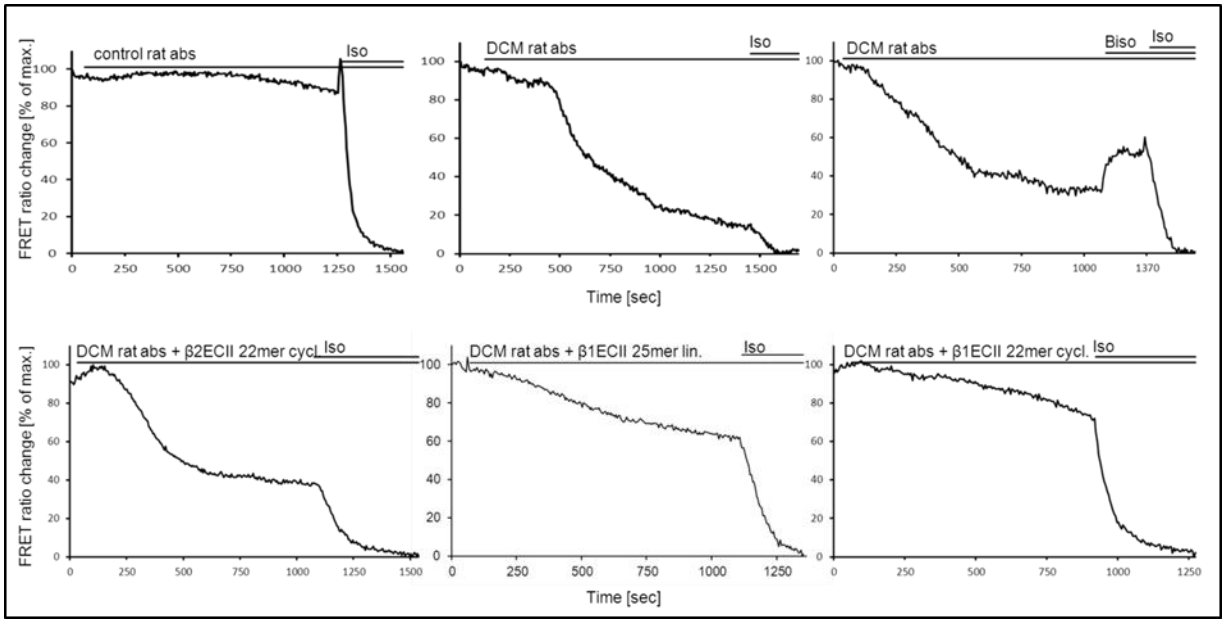

Fig. 21: Functional effects of rat abs in the FRET assay. *Abs from an anti-β_1-ab positive immunized but not from a non-immunized control animal significantly reduced the YFP/CFP FRET ratio compared to the maximal effect induced by 2.5 µM (-) iso; this effect could only partially be reverted by the addition of 5 µM bisoprolol (Biso); 20 µM of (-) iso were used to induce the maximal effect (upper panels). A 22AA cyclic, and to a lesser extent a 25AA linear peptide, mimicking β_1EC_{II}, but not a 22AA cyclic peptide mimicking β_2EC_{II}, were able to neutralize the activating effect of rat anti-β_1EC_{II} (lower panels, Boivin* et al. *in preparation).*

In vitro blockade of rat abs by CP was repeated using the same FRET assay employing the iMIC system. IgG prepared from control animals showed a negligible effect (4.4 %), whereas anti-β_1EC_{II} abs from immunized animals yielded FRET-activities of more than 20 % - indicating increased β_1AR-mediated cAMP production (Fig. 22a)). By *in vitro* incubation of the anti-β_1EC_{II}-abs with β_1EC_{II}-CP FRET activity could be reduced to 3 %.

In the last step we used our rat model to investigate whether *in vivo* administration of β_1EC_{II}-mimicking peptides to immunized antibody-positive animals would have an effect on the adrenoceptor-activating potential of their IgG fractions. In fact, comparison of the activatory potential of IgG isolated from β_1-AR-ab positive rats before and 24 hours after a single injection of 1.0 mg/kg (body weight) of the β_1EC_{II}-mimicking CP revealed a significant blocking effect of the EC_{II} peptide also *in vivo*, yielding ~ 60 % reduction of the initially observed FRET signals (Fig. 22b).[53]

Monthly treatment of immunized β_1-ab-positive DCM-rats with 1 mg/kg body weight (BW) CP after 12 injections led to a long-term reduction in the FRET-responses achieved with their IgG fractions. FRET signals obtained with abs from 5 immunized DCM-rats treated with CP (13.45 ± 1.34 % SEM) were significantly reduced compared to IgG from sera of 7 immunized but untreated DCM-rats (29.81 ± 4.80 % SEM). IgG prepared from control animals yielded almost negligible FRET signals in the range of the background (7.49 ± 1.08 % SEM, n = 6, Tab. 6, Fig. 23).

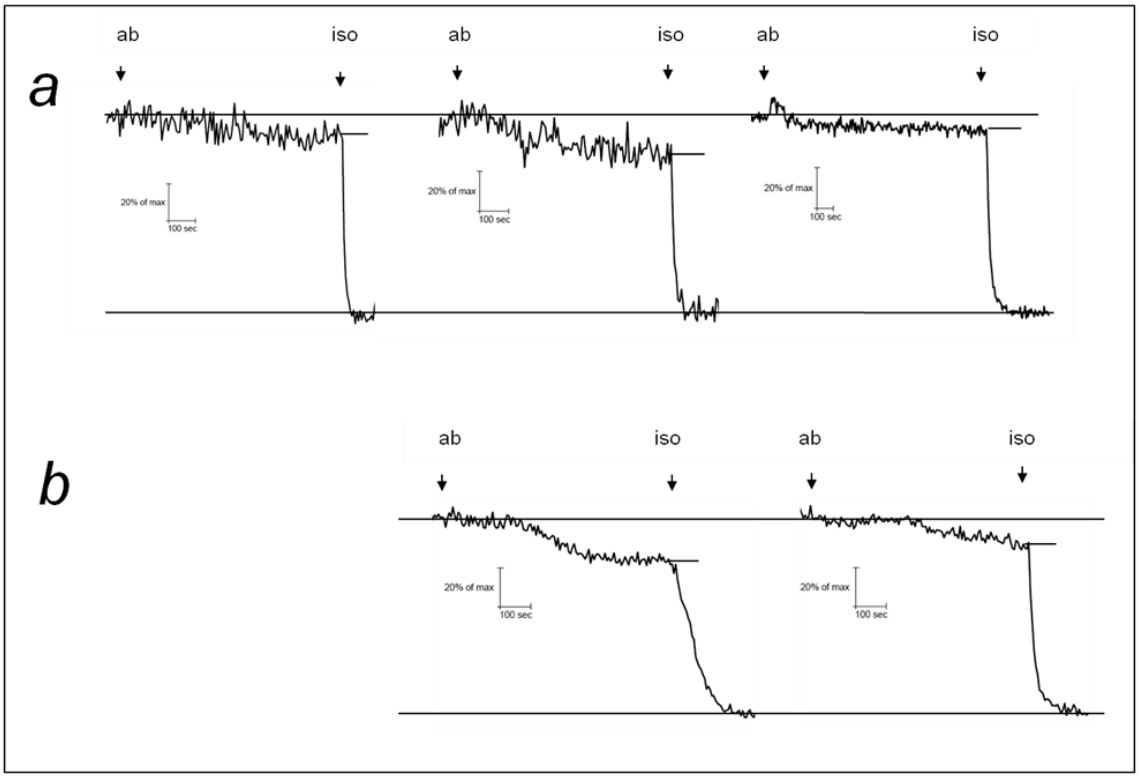

Fig. 22: Blocking capacity of β_1EC_{II}-mimicking peptides monitored by functional FRET assay *(**a**)* in vitro *and (**b**)* in vivo*. Arrows in the graphs indicate the time points of adding either IgG-antibodies (ab) or 3 µmol/L (-) iso. **a**: IgG prepared from control animals had only negligible effects on β_1-AR activity in our FRET assay (5 % activation, left), whereas IgG isolated from a representative immunized anti-β_1-ab-positive rat yielded 22 % of the maximal receptor-activation achieved with 3 µmol/L (-) iso, set to 100 % (middle). After* in vitro *pre-incubation of the same IgG-fraction with β_1EC_{II}-mimicking peptides (12 h, 4 ºC, rotating incubator, 40-fold molar excess) its activating potential was almost fully abolished (3 % residual activation, right). **b**: IgGs isolated from another β_1-ab positive immunized rat yielded 25 % of the maximal (-) iso effect in our cell-based FRET assay (left). 24 h after a single* i.v. *(*in vivo*) application of 1 mg/kg (body weight) of the β_1EC_{II}-mimicking peptide, the activating potential of IgG-fractions from the same animal was reduced by about 60 % (10 % residual receptor activation, right,* Jahns, R.; Schlipp, A.; Boivin, V.; Lohse, M.J.: Targeting Receptor Antibodies in Immune Cardiomyopathy, Semin Thromb Hemost 2010; 36: 212-218, reprinted with permission).[53]

Immunized rats	FRET ratio change [% of max.]	SEM
K2R1S5 control	4.81	0.41
K3R1S5 control	6.47	2.90
K1R1S5 control	5.97	1.97
K2R4S5 control	8.34	2.51
K1R5S5 control	6.70	3.35
pooled control rat	5.05	1.88
K2R2S5 beta1	30.3	2.4
K5R3S5 beta1	16.75	5.15
K5R5S5 beta1	14.50	5.00
K7R2S5 beta1	35.87	5.12
K11R2S5 beta1	49.75	1.45
K15R3S5 beta1	34.16	6.21
K30R4S5 beta1	23.50	2.37
K9R3S5 beta1 treated 18C/C/S	14	0.2
K12R3S5 beta1 treated 18C/C/S	17.43	4.16
K13R2S5 beta1 treated 18C/C/S	8.7	1.2
K20R2S5 beta1 treated 18C/C/S	14.6	1.90
K20R4S5 beta1 treated 18C/C/S	12.85	1.75

Tab. 6: Functional effects of rat antibodies. *FRET ratio changes (iMIC setup) induced by abs prepared from non-immunized control rats or rats immunized with β_1EC_{II}-GST fusion proteins (beta1), either treated or not with monthly injections of 1 mg/ml (BW) 18 C/C/S* i.v.

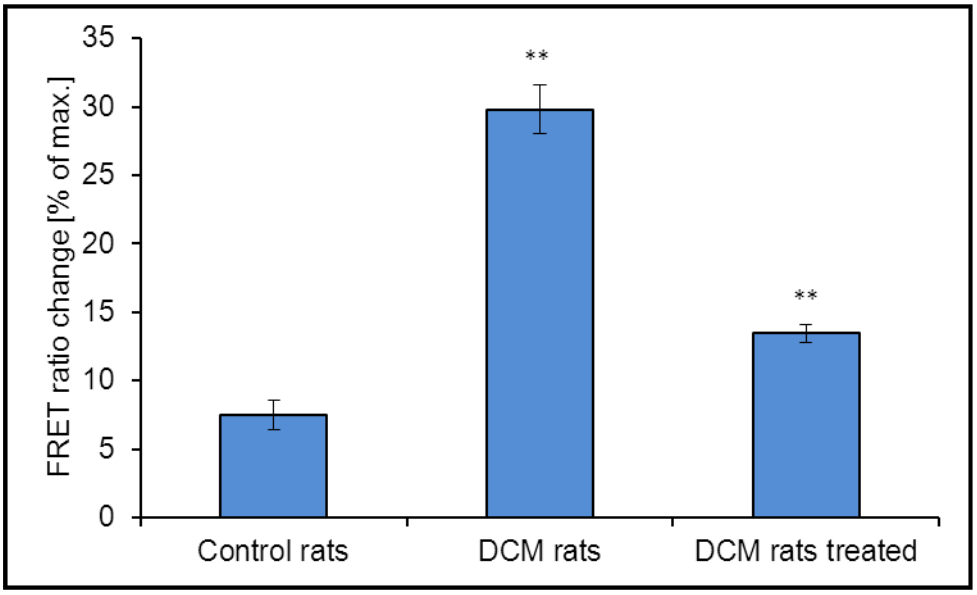

Fig. 23: Effect of repetitive 18C/C/S-CP injections on the stimulatory potential of anti-β_1EC_{II} from DCM rats determined by FRET. *Anti-β_1 EC_{II} prepared from immunized animals induced FRET signals of 29.26 ± 4.62 % SEM (n = 7) ** = p < 0.01 vs. control rats. The stimulatory potential was significantly reduced in IgG prepared from anti-β1-immunized animals treated monthly with 1 mg/kg (BW) 18C/C/S-CP for 12 months (13.52 ± 1.42 % SEM, n = 5) ** = p < 0.01 vs. DCM rats). IgG isolated from control animals injected with NaCl changed the FRET ratio only by 6.22 ± 1.52 % SEM (n = 6). Error bars represent ± SEM of 5 to 7 independent experiments.*

3.9 Blockade of partially agonistic human anti-β_1-AR-aabs with cyclic peptides

In order to block the functional effects of human anti-β_1-AR aabs we pre-incubated human IgG-preparations with peptides mimicking the epitope recognized and bound within the EC_{II} of the receptor *in vitro*. We tested various concentrations of the β_1EC_{II}-mimicking peptides to determine the concentration that optimally neutralized the functional aab-effects. In addition, several molecular ratios between aabs and the peptide were tested. Each ab possesses two antigen-recognizing highly variable domains (Fab), which potentially bind to the blocking peptide. We used peptides at 0.4-, 4-, or 40-fold molar excess, thus theoretically blocking each Fab domain 0.2-, 2-, or 20-fold, respectively. Two aab preparations from a female and a male DCM patient, which had previously been judged positive for (agonist-like) activating β_1-AR-aabs, were preincubated with the β_1EC_{II}-mimicking cyclic peptide and tested in the live-cell FRET assay (iMIC setup, Fig. 24). The FRET-signals achieved with IgG prepared from the female DCM patient could be dose-dependently reduced with 0.4-, 4-, and 40-fold molar excess of 22AA-CP, whereas neutralization of the functional effects of IgG prepared from the male DCM patient required at least a 40-fold molar excess of 22AA CP ($p < 0.05$). Addition of the peptide alone to the HEKβ_1E_1-cells had only marginal effects in the FRET assay (6.4 ± 2.79 % SEM, n = 6). As a consequence, for all further blocking experiments with human IgG-preparations a 40-fold molar excess of the CPs was used.

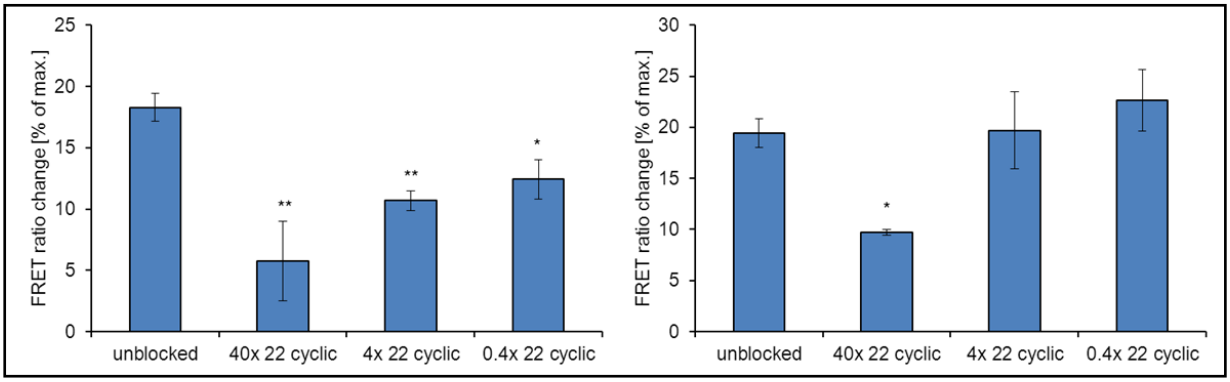

Fig. 24: Neutralization of functional ab-effects with a 22AA cyclic peptide. *Aab preparation of a female (left) and a male DCM-patient (right) incubated with 0.4-, 4-, or 40-fold molar excess of a β_1EC_{II} mimicking 22AA peptide. ** = $p < 0.01$, * = $p < 0.05$ vs. unblocked, error bars represent ± SEM of 6 independent experiments.*

Next, we tested the mutated 22AA-CPs of the ala-scan using anti-β_1-AR-aabs isolated from sera of DCM-patients for their capacity of neutralizing the stimulatory aab-effects. Unblocked patient IgG-preparations induced a strong FRET signal, which was only

slightly diminished by pre-incubation of the aabs with the P213A-CP mutant, but was almost completely abrogated by preincubation with the non-mutant 22AA-β_1EC_{II}-CP (Fig. 25).

Generally, with IgG-preparations from DCM-patients judged β_1-AR-ab "positive", β_1EC_{II}-GST immunized animals, and/or with anti-β_1EC_{II} MABs a FRET ratio change of more than 20% was achieved compared to the maximal signal obtained with the full agonist (-) iso. Control samples from healthy subjects (not containing anti-β_1-AR-abs) generally showed less than 10 % FRET ratio change compared to the maximal (-) iso effect. FRET signals less than 10.3 % of the maximum achieved with (-) iso were generally considered anti-β_1-AR-ab negative (based on the mean values of the controls: 6 ± 4.8 % SD, Tab. 5).

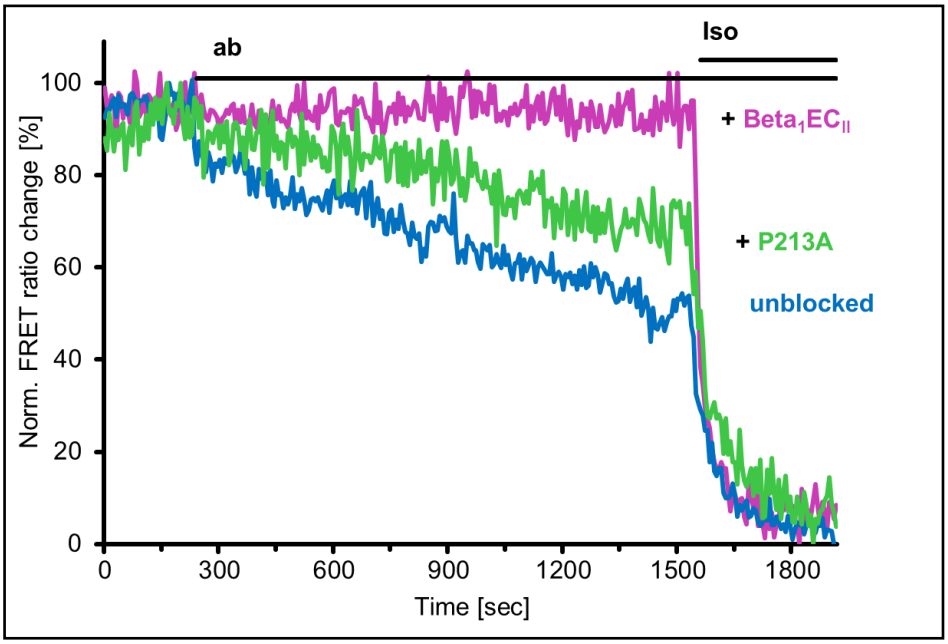

Fig. 25: FRET experiments using a representative human anti-β_1-aab incubated with different β_1EC_{II}-mimicking CPs. *Representative example of normalized FRET ratio changes upon addition of an unblocked aab preparation from a male DCM patient (blue), the same aab preparation either blocked with 40-fold β_1EC_{II}-22AA-CP (purple), or with the 22AA-CP mutant P213A (green). Addition of the aabs and of the full β_1-AR agonist (-) iso (2 µM) are indicated by bars (Schlipp* et al., *in preparation).*

Neutralization of the unblocked aab samples (set to 0%) and direct comparison with the results obtained by pre-blocked samples in the functional FRET assay revealed a strong difference in the blocking capacities of different alanine-mutated CPs (Fig. 26). A female DCM-patient had anti-β_1-AR-aabs that could be blocked by the alanine-mutated peptides E202A, S203A and R207A, unmasking the AAs D*RNDPK within the EC_{II} domain as potentially essential components of the epitope required for receptor activation. Peptides mutated in only one of these essential AAs were no more able to neutralize the aabs and to prevent their stimulatory effects. IgG prepared from a male DCM-patient could be neutralized

efficiently by the CP mutants E202A, S203A, D204A, and R207A, confirming that the RNDPK-epitope contains AAs essential for receptor activation. For the assay, the non-mutated β_1EC_{II}-22AA-CP and the β_2EC_{II}-CP were used as positve and negative controls, respectively. β_1EC_{II}-CP fully blocked aabs of both patients, whereas β_2EC_{II}-CP had no effect on the activating potential of both aab preparations.

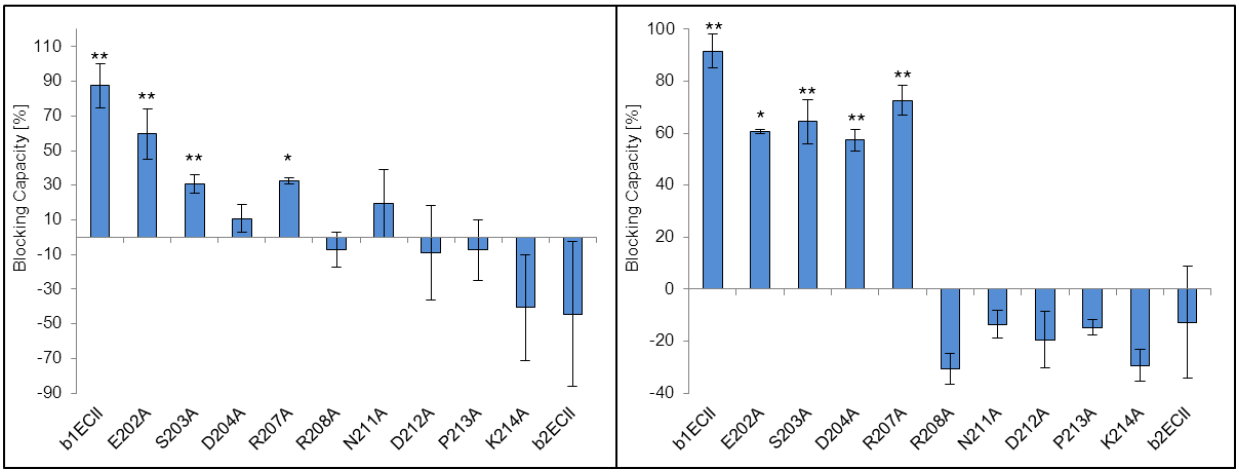

Fig. 26: FRET experiments using human β_1-aabs incubated with β_1EC_{II}-mimicking CP mutants. *FRET ratio changes induced by aabs from a female (left) and a male (right) DCM patient in β_1-AR and Epac1-camps expressing HEK293-cells. Aab preparations were incubated with a 40-fold excess of cyclic peptides mimicking β_2EC_{II} (b2ECII), β_1EC_{II} (b1ECII), or sequentially alanine-mutated versions thereof and their functional activity was tested in FRET experiments. The extent to which the various cyclic peptides blocked the signal compared to unblocked ab preparations is depicted. FRET experiments were performed at least in triplicate with approximately 500 cells per experiment, error bars depict ± SEM, * = $p < 0.05$, ** = $p < 0.01$ compared with unblocked ab preparations (Schlipp* et al., *in preparation).*

3.10 Large-scale application of the live-cell FRET assay

In light of the need for a routine screening method for cardio-noxious agonist-like β_1-AR-aabs in larger chronic heart failure (CHF) populations, a large-scale functional FRET assay is required. Therefore we tested the FRET approach in several available setups.

3.10.1 iMIC

A recent improvement in the application-software facilitated large-scale FRET measurements with the iMIC setup (sequential measurement of several wells in a multiwell-plate). Initial experiments showed clearly distinguishable FRET signals in (-) iso stimulated HEKβ_1E_1-cells (5.82 ± 0.22 % SEM, n = 3) compared to control wells (buffer only, -0.01 ± 0.31 % SEM, n = 4, Fig. 27a). However, due to hardware problems (loss of the focus)

maximal FRET signals only achieved ~ 6 % with the large-scale setting compared to ~ 15 to 20 % FRET signals obtained in single well measurements with the same setup. This might explain the difficulties we had and why we could not detect the rabbit anti-β_1EC_{II}-PAB – previously judged positive in the single well mode – when using multiwell FRET measurements (8.98 ± 0.34 % SEM of max., n = 4, Fig. 27b)

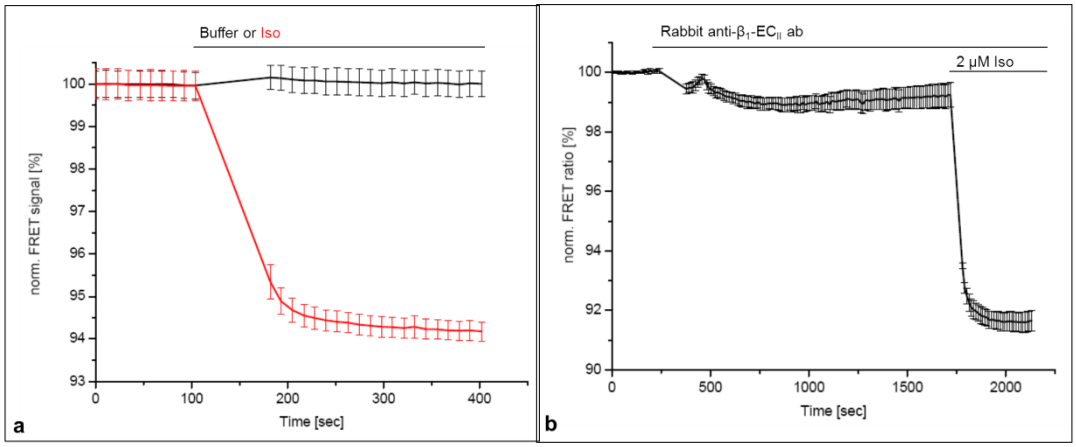

Fig. 27: Large-scale FRET measurements using the multi-well mode in the iMIC setup. *(-) iso induced FRET signals **a)**, red, n = 3) were clearly distinguishable from controls (buffer, **a)**, black, n = 4) using a multiwell mode (measuring 7 wells in parallel). Polyclonal rabbit anti-β_1EC_{II}-abs previously judged positive for activating anti-β_1-AR-abs achieved only a 8.98 ± 0.34 % FRET response compared to the maximal response induced by 2 µM (-) iso **b)** (n = 4, error bars indicate ± SEM).*

3.10.2 NOVOstar reader

The NOVOstar fluorescent plate reader is able to pipet samples automatically and to perform FRET measurements in up to 96 wells simultaneously. However, pilot experiments with addition of buffer as a negative and 3.3 µM (-) iso as a positive control (Fig. 28) revealed that the device was prone to major artifacts in all pipette settings tested. The signal-to-noise ratio was rather low and the difference in FRET ratios obtained between negative and positive controls was not acceptable. Negative controls yielded a FRET signal of 1.66 ± 0.23 % SEM (n = 8) and positive controls achieved only FRET signals of 3.94 ± 0.51 % (n = 8, Fig. 28). Z-factor calculation with $\hat{\sigma}_p$=0.6411, $\hat{\sigma}_n$=1.4295, $\hat{\mu}_p$=3.9375, and $\hat{\mu}_n$=1.6563 yielded a value of -1.7230 indicating that the assay is not suited for routine application.

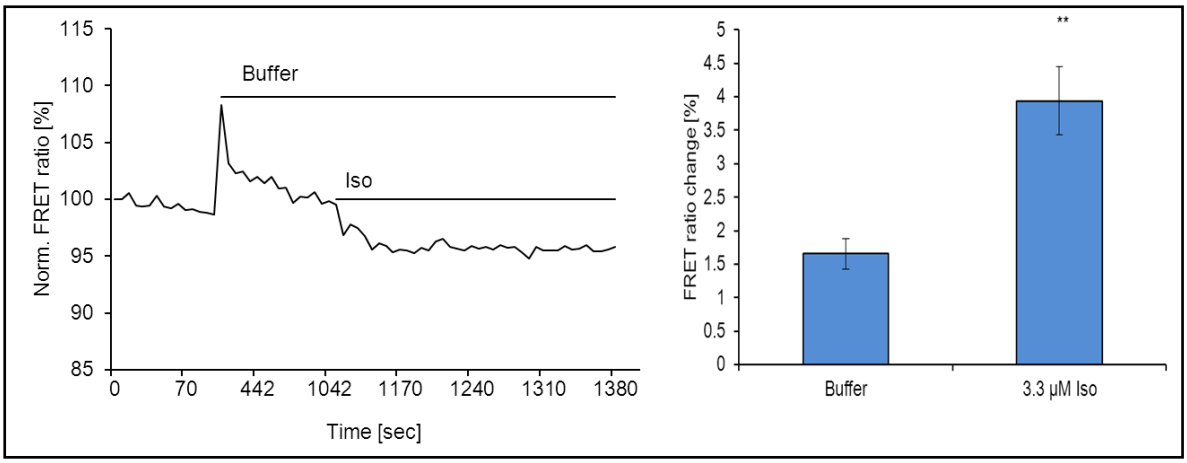

Fig. 28: Live-cell FRET assay performed on the NOVOstar plate reader. *Representative curve showing the effect of adding either buffer or 3.3 µM (-) iso on the FRET ratio obtained (left). The bar graph on the right depicts the mean ± SEM of n = 8 independent experiments (** = p < 0.01).*

3.10.3 Pathway 855 setup

FRET measurements using the Pathway 855 setup is facilitated by the option to perform (sequential or parallel) multi-well experiments, an automated sample addition, autofocus, and a software feature allowing for automated cell separation (Fig. 29) and analysis.

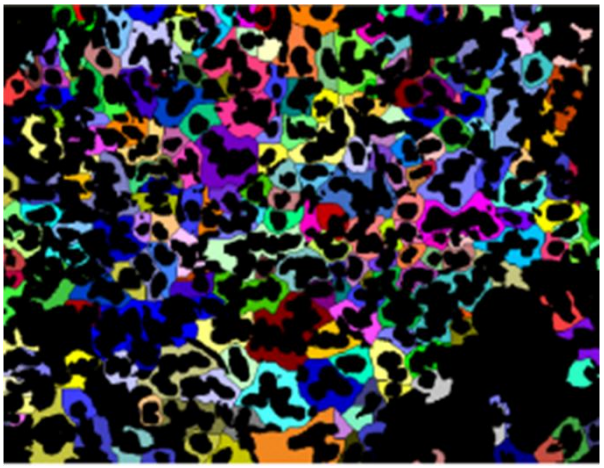

Fig. 29: Automated detection individual cytosolic compartments of HEKβ_1E_1 for FRET analysis using the Pathway 855 setup.

Using the Pathway 855 setup, we were able to generate concentration-response curves for (-) iso in our live-cell FRET assay (Fig. 30). FRET experiments were performed simultaneously in 24 wells. Blank values (FRET-activity determined in wells without any

sample addition) were subtracted from values serving to calculate the (-) iso concentration-response curve. In each well the addition of an increasing (-) iso concentration to the cells was followed by a maximally activating concentration of (-) iso (100 µM). The FRET-signal achieved with each of the lower concentrations was expressed as a percentage of the respective FRET signals after maximal stimulation. The concentration-response-curve shown in Fig. 30 is based on experiments in 96 wells (in total approximately 15000 cells) on 4 different days.

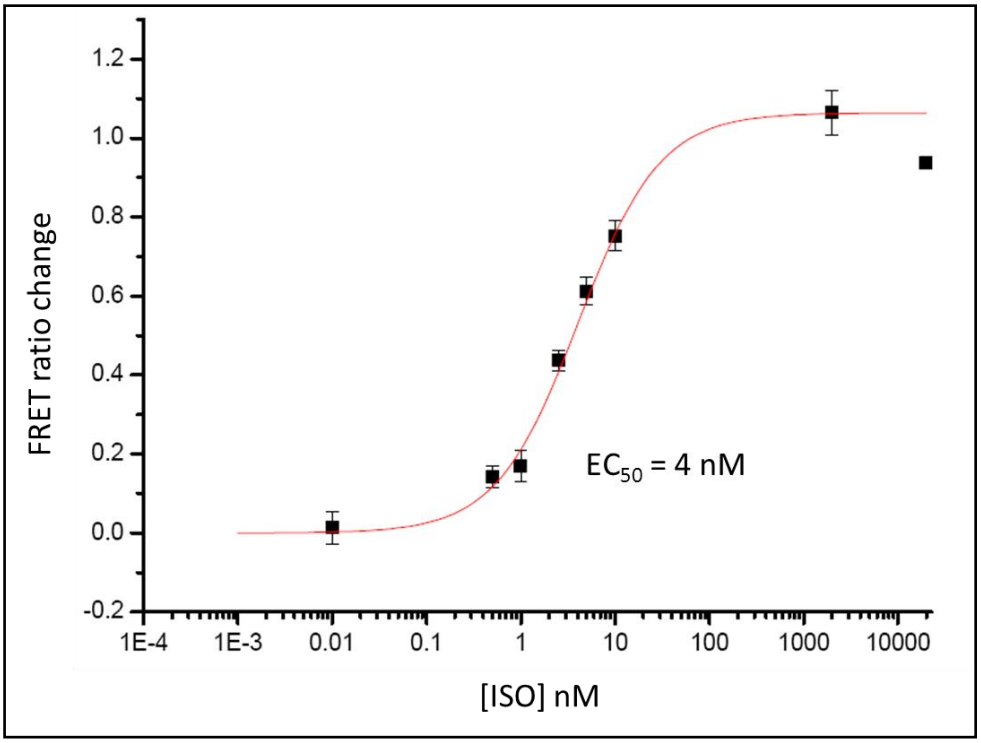

Fig. 30: Concentration-response curve for (-) iso in the live-cell FRET assay using the Pathway 855 setup. *The EC_{50} value was calculated to 4 nM corresponding to a shift to higher concentrations in comparison to data obtained on the iMIC setup (Fig. 8). Mean values ± SEM of 4 independent experiments are shown (96-well format, each point in the graph corresponding to ~ 15 000 single cells).*

The (-) iso concentration-response curve as well as a Z-factor of 0.91 (with $\hat{\sigma}_p$=0.0097, $\hat{\sigma}_n$=0.0269, $\hat{\mu}_p$=1.4178, and $\hat{\mu}_n$=0.1481) encourage a potential large-scale application of the live-cell FRET assay employing the Pathway 855. However, in FRET-experiments with ab-preparations previously judged positive, it was not possible to reveal a significant difference between control abs (human IgG from healthy control subjects) and agonist-like anti-β_1-AR-abs (mouse and rat MAB, rabbit PAB, Fig. 31).

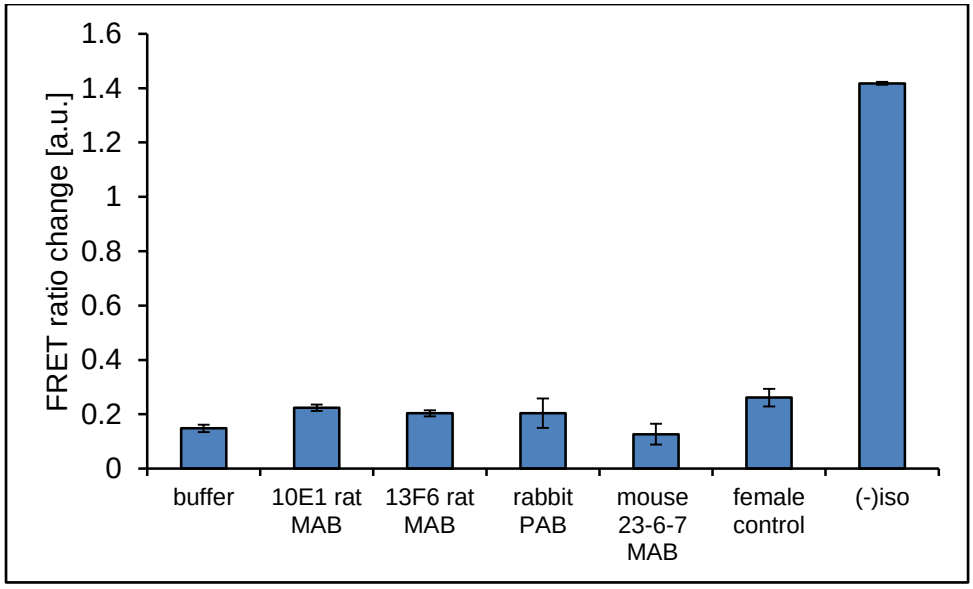

Fig. 31: Functional effects of agonist-like anti-β_1-AR and control IgG in FRET experiments with the Pathway 855 setup. *Various anti-β_1-AR ab preparations previously classified as functionally activating (rat 10E1 and 13F6 MAB, mouse 23-6-7 MAB, and rabbit PAB anti-β_1EC_{II} abs) and the ab preparation of a female control subject were tested for FRET activity with the Pathway 855 setup. Negative (buffer) and positive ((-) iso) controls are shown for comparison. Error bars indicate $\pm$ SEM, of measurements in 4 wells for each condition (~ 300 cells per well).*

3.10.4 Flow cytometry

Finally, we also employed HEKβ_1E_1 cells in order to measure FRET in an approach based on flow cytometry (Fig. 31). (-) iso treatment shifted the read-out of the treated cell population to the right indicating an increased CFP-emission and downwards signifying a decreased YFP emission. Thus the YFP/CFP FRET ratio was reduced indicating an increase in intracellular cAMP induced by β_1-AR activation. If a frame gate comprising 95.7 % of the unstimulated cells is applied to a diagram depicting the emission intensities of YFP vs. CFP for each cell is superimposed on the same graph only 19.4 % of the (-) iso stimulated cells are found within the frame's boundaries. For each condition more than 5000 cells were analyzed and both populations could be clearly separated.

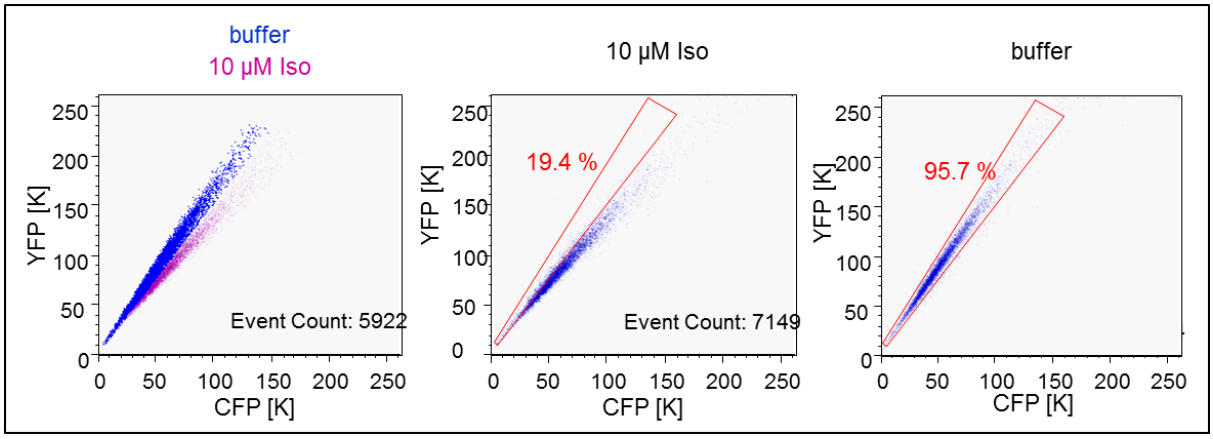

Fig. 31: FRET-analysis of unstimulated and (-) iso treated HEKβ_1E_1 cells by flow cytometry. *A population of (-) iso treated cells (purple on left panel, middle panel) could be separated from cells incubated with buffer only (blue on left panel, right panel) as indicated by gating.*

The FRET ratio change of stimulated vs. unstimulated cells amounted to approximately 16 % indicating feasibilty of the flow cytometry approach. However, previously anti-β_1-AR-ab positive judged ab preparations (mouse MAB, rabbit PAB, and human IgG preparations) did not yield results that were concordant to previous results, e.g. obtained with the iMIC setup (Tab. 7), this indicates higher variability and lower reproducibility of the flow cytometry-based detection method when attempting to differentiate stimulated from unstimulated cells, which, in addition, largely depends on the manner and thereby sensitivity of gating (Fig. 31).

Antibody	Flow cytometry FRET ratio change [% of max.]	Result	iMIC FRET ratio change [% of max.]
Female control subject	42.86	false positive	7.58
Female DCM patient	26.02		19.03
Male DCM patient	22.96		17.03
rabbit anti-β_1EC_{II} PAB	3.57	false negative	30.63
mouse anti-β_1EC_{II} MAB 26-6-7	38.27		27.25

Tab. 7: Flow cytometry vs. iMIC FRET measurements. *Relative FRET signals induced in HEKβ_1E_1 cells incubated with various ab preparations measured either by flow cytometry or by FRET microscopy (iMIC setup).*

4 Discussion

4.1 Live-cell screening for functionally active anti-β_1-AR-abs

The use of primary cardiac cells in a functional assay is one possibility to demonstrate the principle for the detection of stimulating agents and/or antibodies. We did not make use of human adult cardiac myocytes, which would have been most convincing as these cells are affected by DCM, but this approach would have required expression of a cAMP sensor in healthy human cardiomyocytes. Instead, we used adult cardiac myocytes from a mouse strain expressing Epac1-camps. The 26 AA long murine β_1EC_{II} (AA sequence: HWWRAESDEARRCYNDPKCCDFVTNR) is 100 % identical to its human counterpart (SwissProt P34971 and P08588);[27, 211] inferring that patient aabs targeting the human β_1EC_{II} would also bind to and activate the mouse β_1-AR. Cardiac myocytes stimulated with (-) iso concentrations as high as 1 µM yielded maximal FRET ratio changes of only 10 % (Fig. 4 a), which limits the detection range for functionally active anti-β_1EC_{II}-abs and lowers the signal-to-noise ratio. One general critical aspect of experiments with cardiac myocytes is to circumvent spontaneous contractions during the FRET measurements, because this results in significant artifacts. However, although BDM was used during the preparation of the cardiac myocytes and reagent plates were pre-coated with laminin, some cells started to contract after (-) iso application in the FRET assay.

In theory, the same experiments could also be performed with neonatal cardiac myocytes from Epac1-camps transgenic mice. Furthermore in spontaneously beating cardiomyocytes additional physiological parameters like beating frequency or cell shortening could be measured in parallel to the FRET response. However, this approach would be possible only in a setup triggering FRET acquisition either in the contracted or the relaxed state of the cardiomyocytes to rule out artifacts, which to date has not yet been implemented from a technical point of view.

With primary (adult murine) cardiac cells we were able to differentiate between ab-preparations from a healthy control subject (no effect on cellular cAMP) and a DCM patient, whose IgG increased cellular cAMP production (Fig. 4 b). Nevertheless, the preparation and use of primary cardiac cells is not only rather expensive and time consuming, but – in addition – a great number of animals would have to be sacrificed for larger screening efforts. Thus, for diagnostic purposes it appeared to be more appropriate to develop a stable cell line allowing for large-scale culture, yielding a clonal cell line either transiently transfected with or stably expressing both the β_1-AR and Epac1-camps. The maximal FRET signals

obtained by (-) iso stimulation did not differ significantly between both approaches (p = 0.18, Fig. 5). However, a major advantage of HEKβ_1E_1 compared with transiently transfected cells is its ease of handling, making transfections unnecessary, and a higher reproducibility as demonstrated by the lower SD of the respective FRET measurements, which can be explained by a more stable ratio of β_1AR to Epac1-camps expression. In addition, analysis of the stable cell line HEKβ_1E_1 by transmitted light and fluorescent microscopy revealed that the Epac1-camps sensor was expressed in the cytosol (as physiologically required) and not in the nucleus (Fig. 6), and the rough cell morphology of HEKβ_1E_1 did not differ from that of wild type cells.

To define our experimental system, we determined the amount and subtype distribution of β-ARs in our HEKβ_1E_1 cells by radioligand binding. The overall concentration of membrane-bound β-AR was determined by the non-selective receptor antagonist [^{125}I]-CYP. The proportion of β_1- and β_2-AR subtypes was determined by competing [^{125}I]-CYP-binding with unlabled subtype-selective receptor antagonists (ICI for the β_2- and bisoprolol for the β_1-AR, respectively). HEKβ_1E_1 cell expressed ~ 0.4 pmol β_1-AR/mg of membrane protein (Tab. 3), which is 6- to 8-fold higher compared to isolated cardiac myocytes, and fits well to the expression levels previously found in transiently Epac1-camps transfected stable HEKβ_1 cells.[144] Endogenous expression of 0.14 pmol β_2-AR/mg membrane protein was noted in HEKβ_1E_1 cells, which corresponds to values reported in the literature.[144] Radioligand-competition experiments resulted in biphasic displacement curves inferring existence of two binding sides, one with high and one with low affinity. The relative proportions of these curves were comparable with either of the unlabled antagonists (ICI/bisoprolol) and yielded a β_1:β_2 AR ratio of approximatly 65:35 %, assuming that only a negligible amount of β_3-AR is constitutively expressed in HEK cells.[212] A further increase in the expression of β_1-AR did not improve the specific signal in our assay. Possible interferences with the β_2-AR in the FRET assay were blocked by the addition of a saturating dose of the β_2-selective antagonist ICI to the experiments. We could show that the (-) iso signal achieved in HEKβ_1E_1 cells was fully reversible with an appropriate concentration of the β_1-selective antagonist bisoprolol (Fig. 9), indicating that under the aforementioned experimental conditions the (-) iso signal is indeed almost exclusively mediated through β_1-AR. In HEKβ_1E_1 the K_I for bisoprolol was 4.3 nM (Tab. 3) corresponding to a small leftward shift when compared with previous findings (22.4 nM).[213] This might be explained by differences between the cell types and expression systems employed.

The EC_{50} for (-) iso was 28.9 pM in HEKβ_1E_1 cells as determined by FRET measurements using the iMIC setup (Fig. 8), which is in good agreement with the values

obtained for transiently Epac1-camps-transfected HEKβ_1 cells[144] and the results obtained by radioligand binding in CHO cells.[213]

4.2 Purification of functionally active anti-β_1-AR-abs

For functional assays ab purification is strongly recommended because potentially prevalent catecholamines and – in case of FRET measurements the yellowish serum color – could compromise the results obtained. A broad application of a purification method to a large number serum samples requires: (a) only few sample processing steps, (b) good IgG recovery, (c) cost efficiency, and (d) a "single use" application. From three different major principles of sample processing caprylic acid precipitation (CAP) has the advantage that the IgG fraction remains in supernatant whilst most confounding proteins within the serum sample are precipitated. CAP is easy to perform and after purification and subsequent dialysis of the IgG fraction against FRET buffer, the functional effects of several mono- and polyclonal abs as well as aabs from DCM-patients were not altered in the FRET assay. In contrast to CAP, ammonium sulphate precipitation (ASP) is a method that precipitates the immunoglobulin fraction, whereas all other serum proteins remain in the supernatant. This method has the advantage of concentrating immunoglobulins during the preparation process. However, precipitation of IgG poses the potential risk of improper pellet reconstitution and structural changes in the ab that might damage the epitope recognizing hypervariable Fab parts. ASP preceding or following CAP, but not ASP alone, slightly improved sample purity (Fig. 11). Samples treated with CAP and ASP had similar immunologic and functional properties to ab preparations treated with CAP alone (Fig. 12). However, as ASP plus CAP introduces more handling steps together with an increased risk of IgG degradation and/or contamination, this procedure is not recommended.

Thiophilic agarose adsorption (TAA) yielded ab preparations suitable for the functional FRET assay. However, the protocols require a either (alkaline) pH 9 to elute the abs (which might alter their functional properties) or a shift in ionic strength for ab elution (which might better preserve functional ab properties).[197] Nevertheless, in our hands, IgG prepared by TAA caused artifacts in the FRET assay, even after excessive dialysis (Fig. 14) and IgG purity was inferior to CAP (Fig. 13) precluding the use of TAA in clinical routine.

Other purification methods would include adsorption of IgGs by their Fc part to a protein G column and subsequent elution of bound IgG by extreme pH conditions (varying between 2.0 and 9.0, which is expected to alter functional ab properties) or ionic strength shift.[112]

Instead of protein G, also linear or cyclic peptides mimicking β_1EC_{II} might be coupled to columns in order to selectively immunopurify the desired IgG fraction. However, this affinity chromatography method also causes a number of problems related to extreme elution conditions, loss of functional activity of conformational antibodies, and loss of human biomaterials. Most importantly, abs with a high affinity for the β_1EC_{II} – which would be most interesting to test in the live-cell FRET assay – might remain attached to the column and despite elusion with standard conditions.

4.3 Functionally active anti-β_1-AR-aabs in patients with heart disease

The functional FRET assay compared to conventional tests (such as ELISA, Western blotting, surface plasmon resonance or immunofluorescence) has the advantage of providing a physiological readout.[144] The assay allows to assess receptor-mediated signaling, which is potentially disease-relevant, rather than merely ab binding.

By employing the FRET method to screen for functionally active anti-β_1-abs, we were able to differentiate heart disease patients from healthy controls (Tab. 5). IgG preparations of healthy individuals yielded FRET signals of 5.6 ± 2.37 % SD (controls). Thus, abs inducing FRET signals higher than a cut-off value of 10.3 % (mean control values + 2 SD) were judged functionally activating. In our pilot study, the mean values of the HHD, ICM, and DCM patient collectives did not differ significantly from each other (Tab. 5, Fig. 15). However, particularly the HHD and ICM collectives are by far too small to draw any meaningful conclusions regarding these disease entities.

The LVEF, a parameter that reflects left ventricular (systolic) pump function, was significantly reduced in DCM patients. In DCM patients judged aab-positive a significant inverse correlation between LVEF and the magnitude of the FRET signal could be observed for DCM patients with a slope of -0.21 and a coefficient of determination (R^2) of 0.11 (Fig. 15). This suggests that worsening of cardiac function significantly coincides with the stimulating potential of β_1-AR-aabs ($p < 0.002$).

However, the inverse correlation in this pilot study (with blood samples drawn at one single time point) is not very strong and was only found in the case of DCM patients because some of the HHD and ICM patients analyzed exhibited high FRET activation despite preserved pump function and vice versa. This may be explained by immunization experiments in animals and by results from clinical observations indicating that anti-β_1-AR-aab production may precede development of heart failure.[214] Other reports suggest that

abs might also vanish in the course of the disease, e.g. in advanced (final) stages of CHF.[120] Therefore, longitudinal prospective studies are warranted in order to assess the respective aab status of patients at their first cardiac "event" and, subsequently, a tight follow up of such patients with close monitoring of cardiac remodeling and pump function parallel to aab testing. Such a study has recently been initiated and, hopefully, will further elucidate the genesis and course of β_1-receptor-aab production after cardiac injury.[215] The prospective part of the ETiCS study aims to elucidate the etiology, titer course and survival of heart failure patients developing functionally active anti-β_1-AR-aabs within one year after their first cardiac event (acute myocarditis or acute transmural myocardial infarction) including clinical impact of several other cardiac aabs.[215]

4.4 Amino acid residues involved in receptor recognition and binding by conformational anti-β_1EC_{II}-abs

The fact that the cyclic 18C/C/S β_1EC_{II} peptide was able to circumvent ab binding to and subsequent activation of native membrane-presented human β_1-AR implies that this particular CP sufficiently mimics the β_1EC_{II} to compete with it for ab binding. In contrast, 18C/S/C forming a "wrong" disulfide bridge does not mimick the target correctly and, thus, was not able to circumvent β_1-AR activation. The EC_{II} of GPCRs is thought to play a crucial role for receptor-ligand interactions by closing the binding pocket for small molecular ligands like catecholamines as a lid structure or by allosteric rearrangement of transmembrane receptor domains.[216] Antibody binding to the EC_{II} is, therefore, very likely to affect receptor conformation and activity. Another potential mechanism for the functional effect of anti-β_1EC_{II} antibodies lies in their bifunctional nature. It could be imagined that one antibody binds two receptors (one on each Fab domain) and thus initiates or facilitates receptor dimerization. This stabilization of physiologically (transient!) occurring β_1-AR dimer complexes by conformational abs might contribute equally to the activating aab-effect[38].

Only CPs containing the C/C/S motif were able to efficiently prevent both the immunoreactivity of the anti-β_1EC_{II} abs in ELISA experiments and the activation of the β1-AR expressed at the cell surface. Thus, we concluded that the cysteine bridge between the first and second cysteine residues (C209 and C215) of our CPs is essential to mimick the conformation of β_1EC_{II}. This seems to be relevant not only with respect to β_1-AR structure and function,[216] but also with respect to antibody binding (Fig. 32). A correct disulfide bridge might also allow for the binding of sodium at the negativly charged end of the α-helix thereby stabilizing its conformation.[22] Just as receptor-specificity of ortho- and allosterically

binding ligands is influenced by EC_{II} in the muscarinic receptor type 2,[217] the C5a,[218] and the dopamine type 2 receptor,[219] we suppose ab binding to the β_1-AR to depend on the three dimensional arrangement of this extracellularly exposed loop.

Because the CPs employed in this study have not yet been subjected to nuclear magnetic resonance (NMR) analysis, we can only speculate on their true 3D-conformation in solution. It could be the case that exchange of a certain residue to alanine might widely influence the overall CP structure. However, the peptides' ability to block ab binding and ab-mediated receptor activation if certain AA residues are preserved, suggest that the generated CPs resemble rather well the native β_1EC_{II} structure.

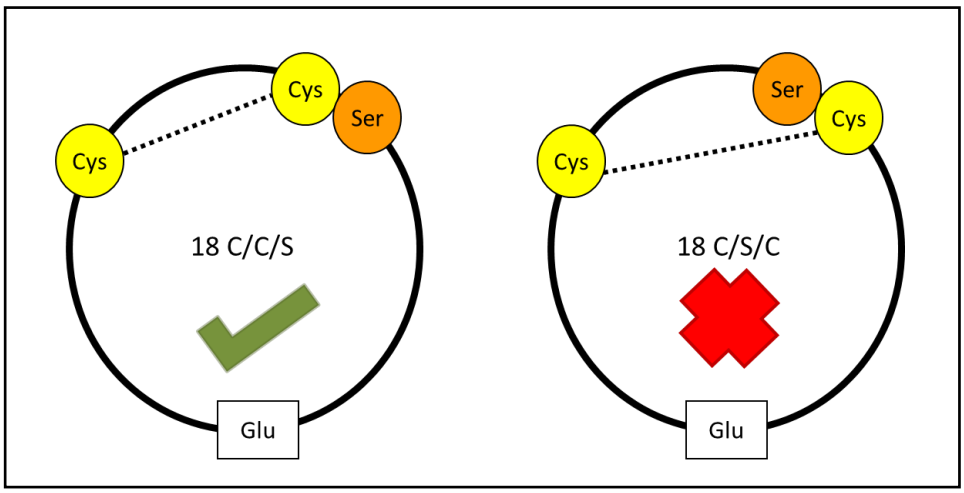

Fig. 32: CPs with correct and incorrect disulfide bridge. *Schematic representation of the cyclic 18C/C/S peptide mimicking the β_1EC_{II} able to block binding to and activation of β_1-AR by anti-β_1EC_{II}-abs (left) and the inefficient 18C/S/C cyclic peptide (right).*

In our aim to map the epitope recognized by conformational anti-β_1EC_{II}-abs responsible for receptor activation, both polyclonal and monoclonal anti-β_1-AR abs as well as aabs from DCM patients were further analyzed by fine mapping experiments with CPs and single AA ala mutations thereof. IgG preparations were assayed both for binding (ELISA) and functional activation potential (FRET assay, Fig. 20). With the ala-scan approach we checked each individual AA residue differing between the β_1- and the β_2-EC_{II} protein sequence for its potential relevance for the formation of the bound ab epitope without major changes of the overall CP structure.

The results of our ala-scan experiments suggest that not all residues in the β_1EC_{II} are equally important for the recognition and binding by anti-β_1EC_{II} abs. Ab preparations from immunized rats and rabbits indicate a relevance of a (so-called) "NDPK motif" for ab

recognition and binding to β_1EC_{II}, whereas PK alone seems to play a crucial role for the functional activity of the same abs (Fig. 20).

Besides the region between the intraloop disulfide bridge also the conformation of the bridge itself seems to be important for ab binding and activation. The region where β_1-AR-abs are supposed to bind is situated at the carboxyterminal end of the predicted backward-oriented α-helix constituting EC_{II} (if a 3D receptor structure homologous to the turkey β_1-AR is assumed). The NDPK motif is embedded (a) in a structurally unique position neighboring the disulfide bridge between EC_{II} and the transmembrane region adjacent to EC_I, and (b) in a constrained region between the cysteine residues that form the intraloop bridge. The NDPK motif consists of AAs with different chemical characteristics with e.g. the asparagine residue being polar (potentially forming H-bonds with AAs of the ab variable region) and the aspartic acid residue negatively charged with our assay conditions (enabling interactions with positively charged residues of the ab). The aspartic acid residue within this motif has also been recognized as a AA, which is relevant for β_1-AR activation, because its exchange to asparagine caused unexpected receptor activation upon binding of the antagonistic ligands broxaterol and terbutaline.[220] The nonpolar proline residue is unique among the proteinogenic AAs. Under normal conditions AA-side chains would project out of a α-helix secondary protein structure and therefore not interfere with helix orientation. In proline the side chain is tethered to the main-chain nitrogen atom and forms a ring structure which interfers with H-bond formation of neighboring helix residues. Proline is regularly found in the first turn of α-helixes but it may also form a bend.[221] We expect this specific property to be crucial for the conformation of this particular receptor region and the production of conformational abs against it. Last not least, the lysine residue of the motif is positively charged at our assay conditions and might interact with negatively charged AA residues within the Fab region of the anti-β_1-abs. This diverse assembly of particular AA residues and the receptor structure in this specific region apparently contribute to form a conformational epitope for antibodies making this target unique among GPCR receptors.

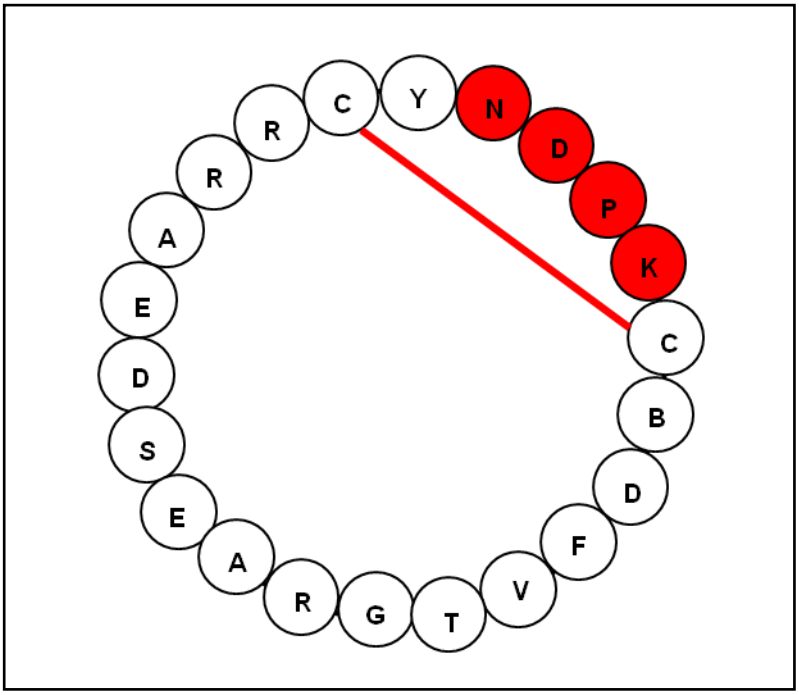

Fig. 33: Schematic representation of a 22AA-CP mimicking β_1EC_{II}. *Residues involved in forming the epitope recognized by anti-β_1EC_{II} abs are highlighted in red. Also, the intraloop disulfide bridge, required for ab recognition and ab-mediated functional effects mediated by those conformational abs is depicted in red.*

For aab preparations of DCM-patients analyzed by the ala-scan approach (Fig. 25, Fig. 26) in one case the residues RNDPK, in the other the NDPK motif together with the residue aspartic acid 204 seemed to be involved in receptor activation. These small differences in the bound epitopes indicate that – although the key binding site around the proline residue (NDPK) seems to be conserved between human IgG preparations – additional residues (like in the present case the arginine) might also contribute to determine the functional activity of a specific aab. In the future it would be interesting to fine-map anti-β_1EC_{II} aabs of a large number of DCM patients in order to gain more insight into the EC_{II} residues relevant for allosterically switching on or off the β_1-receptor.

Previously, it has been suggested that certain human anti-β_1-AR-aabs might be directed against EC_I.[144] Our experiments do not rule out that for some aabs the recognized epitope is situated more towards EC_I, which is in close spatial distance to the motif described here. To address this hypothesis in the future, probing of human aabs with β_1EC_{II} ala-scan mutants would be required.

Previously, other research groups have also performed some epitope mapping studies using IgG prepared from patients with DCM or Chagas' cardiomyopathy. The sera were screened for aabs against β_1-AR, but also other GPCRs. These studies were carried

out with short overlapping linear peptides derived from the receptor primary structure and lead to different assumptions concerning the respective epitopes recognized and bound by the aabs analyzed (Tab. 8). In the present work, the ala-scan approach with CP in which only one single AA was mutated per peptide, represents an important refinement of the methodology because (a) cyclic (3D-folded) peptides are by far closer to the native epitope than linear peptides, and (b) the mutation of a single AA per CP allowed to functionally identify single AAs that constitute the epitope targeted by activating aabs.

Disease	Receptor	Epitope	Reference
Chagas' CM	β_1-AR, M_2	AESDE	[222]
Preeclampsia, renal allograft rejection, malignant hypertension, vasculopathy	AT1	AFHYESQ ENTNIT	[223, 224]·[225]
malignant secondary hypertension	α_1-AR		[226]

Tab. 8: Previously suggested target epitopes for aabs against the EC_{II} of GPCRs *(M_2 = muscarinic acetylcholine receptor type 2, AT1 = angiotensin II type 1 receptor).*

4.5 Detection and neutralization of poly- and monoclonal functionally active rodent anti-β_1EC_{II}-abs

In order to block the functional effects of activating anti-β_1-AR-abs, the respective IgG fractions were pre-incubated with peptides mimicking the β_1EC_{II} sequence prior to the functional FRET assay.

Linear peptides mimicking β_1EC_{II} exhibited less *in vitro* blocking efficacy than their cyclic counterparts when used to neutralize the stimulating effects of polyclonal rabbit anti-β_1EC_{II}-abs (Fig. 16). We could demonstrate that linear peptides are more prone to degradation by endo- and exopeptidases than the cyclic variants (Boivin *et al.* in preparation). However, because blocking was performed at 4 °C to reduce peptidase activity degradation of the peptides did probably not significantly account for the differences in the short-term blockade (12 – 24 h) observed. It is more likely that CPs are restricted in their conformation when incubated in liquids (in a manner comparable with the EC_{II} in the native receptor, where the EC_{II} loop is restrained in between two transmembrane regions). Therefore, the more flexible linear peptide might escape ab binding more easily, also facilitated by an assumed lower affinity to the Fab fragments of conformational antibodies.

Ab preparations of immunized DCM-rats induced significant FRET-signals using both the iMIC (Fig. 22 a) and the Zeiss Axiovert 200 setup (Fig. 21), whereas IgG from control

animals had no receptor-stimulating effects. The increase in cellular cAMP induced by functionally active rat anti-β_1-AR-abs was only partially reverted by adding the β_1-AR specific antagonist bisoprolol (Fig. 21). Cyclic and (to a lesser extent) linear peptides mimicking the β_1EC_{II} were more efficient in neutralizing the cAMP increasing effects of rat anti- β_1EC_{II}-abs compared to bisoprolol *in vitro*.

This reduction in the activating potential of anti-β_1EC_{II} abs could also be detected *in vivo* by analyzing blood samples from immunized rats drawn 24 h after injection of cyclic peptides. One or both Fab regions of conformational β_1-aabs seem to be blocked by CP, thereby competing with binding of the ab to the receptor. This preliminary finding indicates that ab neutralization might also be possible in human patients and – in the future – also be monitored by the functional FRET assay.

It remains, however, to be re-evaluated to which extent the FRET activity relates to parameters of cardiac function. In a first step such analyses could be performed in cyclic peptide treated cardiomyopathic animals. Monthly injection of β_1EC_{II}-mimicking cyclic peptides reduced the β_1-AR activating potential of abs from immunized rats almost to control levels suggesting that cyclic peptides remain intact and, thus, seem capable of ab scavenging in the circulation over days or even weeks. A more detailed analysis of the pharmacokinetics of the presented β_1EC_{II}-mimicking cyclic peptides and their effect on cardiac function in immunized antibody positive rats is currently under way.

4.6 Detection and neutralization of human anti-β_1EC_{II}-aabs

Interestingly, aabs from two DCM patients yielding similar cAMP responses in the functional FRET assay were differentially neutralized by the β_1EC_{II}-mimicking 22AA CP (Fig. 24). It might be the case that the patient aabs requiring a 40-fold molar excess of CP might exhibit a greater avidity for the β_1-receptor. Another possibility would be that the specific epitope of this particular patient aab does not exactly fit with the epitope covered and presented by the CP. In a previous study with peptides mimicking β_1EC_I it was found that aabs from some DCM patients could also be neutralized by this particular peptide. However, anti-β_1EC_I-aabs produced generally lower FRET signals than those patients having anti-β_1EC_{II}-aabs[144].

4.7 Clinical implications for the use of cyclic peptides mimicking β_1EC_{II}

The presence of agonist-like anti-β_1-AR abs is associated with increased morbidity and mortality in DCM patients.[134, 227, 228] A wide range of assays have been reported in order to identify patients with stimulating aabs. The here described cell-based FRET assay represents a major step forward in this attempt. A useful strategy would be to test a given serum ab sample for the presence of activating anti-β_1-AR-aabs and, subsequently, to neutralize these aabs *in vitro* with a "CP mimicking β_1EC_{II} test". Patients with blockable aabs should be considered as anti-β_1EC_{II}-aab positive and cardiac function in such patients should be monitored closely. These patients might profit from immunoadsorption and intensified pharmaceutical therapy or – in the future – perhaps from individually tailored scavenger CPs as those described in the present work.

CPs mimicking β_1EC_{II} are currently evaluated in clinical phase I and IIa trials. In the light of these trials it is important to gain more information on the mode of action of CP. Our data suggest that the residues NDPK and the intraloop disulfide bridge between C209 and C215 are crucial for the aab-neutralizing capacity of β_1EC_{II}-mimicking CP. Therefore, these residues should not be touched when designing novel modified Cps as personalized drugs. In addition, prior to treatment individual patients could be tested *in vitro* for aab blockade of their proper anti-β_1EC_{II}-aabs by different variants of the β_1EC_{II}-mimicking CP, and the CP with the best blocking efficiency could be chosen for *in vivo* peptide treatment.

To assess functional activity of anti-β_1EC_{II}-aabs and the neutralizing efficacy of β_1EC_{II}-mimicking CPs only few FRET based diagnostic assays are suitable and, so far, non of them is used in clinical routine. In order to screen larger patient populations (and sample numbers) it is necessary to adopt a large-scale technology and to automate experimental procedures and data acquisition. The live-cell FRET assay presented in this work is theoretically promising for large-scale screening either with the iMIC or the Pathway 855 setup. However, both settings need further improvement. Perhaps additional assay modifications such as ab pre-incubation and subsequent measurement of the (-) iso response only, or optimization of the programmed measurement sequences might be tested in the future. In addition, in the futurecell-based FRET-assays could also be modified to detect aabs in other autoimmune diseases such as anti-TSH-aabs in Grave's disease or anti-AT_1-aabs in vascular rejection.[229, 230]

5 References

1. Gudermann, T., T. Schoneberg, and G. Schultz, *Functional and structural complexity of signal transduction via G-protein-coupled receptors.* Annu Rev Neurosci, 1997. **20**: p. 399-427.
2. Fredriksson, R. and H.B. Schioth, *The repertoire of G-protein-coupled receptors in fully sequenced genomes.* Mol Pharmacol, 2005. **67**(5): p. 1414-25.
3. Bohm, M. and C. Maack, *Treatment of heart failure with beta-blockers. Mechanisms and results.* Basic Res Cardiol, 2000. **95 Suppl 1**: p. I15-24.
4. Hanania, N.A., B.F. Dickey, and R.A. Bond, *Clinical implications of the intrinsic efficacy of beta-adrenoceptor drugs in asthma: full, partial and inverse agonism.* Curr Opin Pulm Med, 2010. **16**(1): p. 1-5.
5. Marinissen, M.J. and J.S. Gutkind, *G-protein-coupled receptors and signaling networks: emerging paradigms.* Trends Pharmacol Sci, 2001. **22**(7): p. 368-76.
6. Liu, G., et al., *Leydig-cell tumors caused by an activating mutation of the gene encoding the luteinizing hormone receptor.* N Engl J Med, 1999. **341**(23): p. 1731-6.
7. Xie, J., et al., *Activating Smoothened mutations in sporadic basal-cell carcinoma.* Nature, 1998. **391**(6662): p. 90-2.
8. Rosenthal, W., et al., *Molecular identification of the gene responsible for congenital nephrogenic diabetes insipidus.* Nature, 1992. **359**(6392): p. 233-5.
9. Smyth, D.J., et al., *Shared and distinct genetic variants in type 1 diabetes and celiac disease.* N Engl J Med, 2008. **359**(26): p. 2767-77.
10. Glatt, S.J. and E.G. Jonsson, *The Cys allele of the DRD2 Ser311Cys polymorphism has a dominant effect on risk for schizophrenia: evidence from fixed- and random-effects meta-analyses.* Am J Med Genet B Neuropsychiatr Genet, 2006. **141B**(2): p. 149-54.
11. Dean, B., et al., *Decreased muscarinic1 receptors in the dorsolateral prefrontal cortex of subjects with schizophrenia.* Mol Psychiatry, 2002. **7**(10): p. 1083-91.
12. Meyer-Lindenberg, A., et al., *Genetic variants in AVPR1A linked to autism predict amygdala activation and personality traits in healthy humans.* Mol Psychiatry, 2009. **14**(10): p. 968-75.
13. Jeanneteau, F. and M.V. Chao, *Promoting neurotrophic effects by GPCR ligands.* Novartis Found Symp, 2006. **276**: p. 181-9; discussion 189-92, 233-7, 275-81.
14. Lundstrom, K., *An overview on GPCRs and drug discovery: structure-based drug design and structural biology on GPCRs.* Methods Mol Biol, 2009. **552**: p. 51-66.
15. Palczewski, K., et al., *Crystal structure of rhodopsin: a G-protein coupled receptor.* Science, 2000. **289**: p. 739-745.
16. Salom, D., et al., *Crystal structure of a photoactivated deprotonated intermediate of rhodopsin.* Proc Natl Acad Sci U S A, 2006. **103**(44): p. 16123-8.
17. Standfuss, J., et al., *Crystal structure of a thermally stable rhodopsin mutant.* J Mol Biol, 2007. **372**(5): p. 1179-88.
18. Murakami, M. and T. Kouyama, *Crystal structure of squid rhodopsin.* Nature, 2008. **453**(7193): p. 363-7.
19. Shimamura, T., et al., *Crystal structure of squid rhodopsin with intracellularly extended cytoplasmic region.* J Biol Chem, 2008. **283**(26): p. 17753-6.
20. Jaakola, V.P., et al., *The 2.6 angstrom crystal structure of a human A2A adenosine receptor bound to an antagonist.* Science, 2008. **322**(5905): p. 1211-7.
21. Rasmussen, S.G., et al., *Crystal structure of the human beta2 adrenergic G-protein-coupled receptor.* Nature, 2007. **450**(7168): p. 383-7.
22. Warne, T., et al., *Structure of a beta1-adrenergic G-protein-coupled receptor.* Nature, 2008. **454**(7203): p. 486-91.
23. Wu, B., et al., *Structures of the CXCR4 Chemokine GPCR with Small-Molecule and Cyclic Peptide Antagonists.* Science, 2010.

24. Shimamura, T., et al., *Structure of the human histamine H(1) receptor complex with doxepin.* Nature, 2011. **475**(7354): p. 65-70.
25. Worth, C.L., G. Kleinau, and G. Krause, *Comparative sequence and structural analyses of g-protein-coupled receptor crystal structures and implications for molecular models.* PLoS ONE, 2009. **4**(9): p. e7011.
26. Jahns, R., V. Boivin, and M.J. Lohse, *Beta 1-adrenergic receptor-directed autoimmunity as a cause of dilated cardiomyopathy in rats.* Int J Cardiol, 2006. **112**(1): p. 7-14.
27. Frielle, T., et al., *Cloning of the cDNA for the human beta1-adrenergic receptor.* Proc. Natl. Acad. Sci. USA, 1987. **84**(22): p. 7920-7924.
28. Golan, D.E., et al., eds. *Principles of pharmacology: The pathophysiologic basis of drug therapy*. 2007, Lippincott Williams & Wilkins.
29. Vilardaga, J.P., et al., *MINIREVIEW: GPCR and G proteins: drug efficacy and activation in live cells.* Mol Endocrinol, 2009.
30. Bunemann, M., et al., *Activation and deactivation kinetics of alpha 2A- and alpha 2C-adrenergic receptor-activated G protein-activated inwardly rectifying K+ channel currents.* J Biol Chem, 2001. **276**(50): p. 47512-7.
31. Roka, F., et al., *Tight association of the human Mel(1a)-melatonin receptor and G(i): precoupling and constitutive activity.* Mol Pharmacol, 1999. **56**(5): p. 1014-24.
32. Neves, S.R., P.T. Ram, and R. Iyengar, *G protein pathways.* Science, 2002. **296**(5573): p. 1636-9.
33. Palczewski, K., *GTP-binding-protein-coupled receptor kinases--two mechanistic models.* Eur J Biochem, 1997. **248**(2): p. 261-9.
34. Lohse, M.J., et al., *Beta-Arrestin: a protein that regulates beta-adrenergic receptor function.* Science, 1990. **248**(4962): p. 1547-1550.
35. Benovic, J.L., et al., *Regulation of adenylyl cyclase-coupled b-adrenergic receptors.* Annu Rev Cell Biol, 1988. **4**(1): p. 405-28.
36. Scott, M.G., et al., *Recruitment of activated G protein-coupled receptors to pre-existing clathrin-coated pits in living cells.* J Biol Chem, 2002. **277**(5): p. 3552-9.
37. Hall, R.A. and R.J. Lefkowitz, *Regulation of G protein-coupled receptor signaling by scaffold proteins.* Circ Res, 2002. **91**(8): p. 672-80.
38. Dorsch, S., et al., *Analysis of receptor oligomerization by FRAP microscopy.* Nat Methods, 2009. **6**(3): p. 225-30.
39. Lands, A., et al., *Differentiation of receptor systems by sympathomimetic amines.* Nature, 1967. **241**: p. 597-598.
40. Ablad, B., et al., *Cardiac effects of beta-adrenergic receptor antagonists.* Adv Cardiol, 1974. **12**(0): p. 290-302.
41. Ahlquist, R.P., *Study of adrenotropic receptors.* Am.J.Physiol., 1948. **153**: p. 586-600.
42. Bylund, D.B., et al., *International Union of Pharmacology nomenclature of adrenoceptors.* Pharmacol Rev, 1994. **46**(2): p. 121-36.
43. García-Sáinz, J.A., et al., *Role of alpha 1 adrenoceptors in the turnover of phosphatidylinositol and of alpha 2 adrenoceptors in the regulation of cyclic AMP accumulation in hamster adipocytes.* Life Sci, 1980. **27**(11): p. 953-61.
44. Hein, L. and B.K. Kobilka, *Adrenergic receptor signal transduction and regulation.* Neuropharmacology, 1995. **34**(4): p. 357-66.
45. Lefkowitz, R.J., *Editorial: Selectivity in beta-adrenergic responses: clinical implications.* Circulation, 1974. **49**(5): p. 783-6.
46. Hamilton, B. and H. Doods, *Identification of potent agonists acting at an endogenous atypical β3-adrenoceptor state that modulate lipolysis in rodent fat cells.* European Journal of Pharmacology, 2008. **580**(1-2): p. 55-62.
47. Evans, B.A., et al., *Ligand-directed signalling at beta-adrenoceptors.* Br J Pharmacol, 2010.

48. Reiner, S., et al., *Differential Signaling of the Endogenous Agonists at the 2-Adrenergic Receptor.* Journal of Biological Chemistry, 2010. **285**(46): p. 36188-36198.
49. Wallukat, G., *The beta-adrenergic receptors.* Herz, 2002. **27**(7): p. 683-90.
50. Brodde, O.E., *β1- and β2-adrenoceptors in the human heart: properties, function, and alterations in chronic heart failure.* Pharmacol. Rev., 1991. **43**: p. 203-242.
51. Kobilka, B. and G.F. Schertler, *New G-protein-coupled receptor crystal structures: insights and limitations.* Trends Pharmacol Sci, 2008. **29**(2): p. 79-83.
52. Libby, P., et al., *Braunwald's Heart Disease*. 8 ed. 2007: Saunders Elsevier.
53. Jahns, R., et al., *Targeting receptor antibodies in immune cardiomyopathy.* Semin Thromb Hemost, 2010. **36**(2): p. 212-8.
54. Jahns, R., V. Boivin, and M.J. Lohse, *beta(1)-Adrenergic receptor function, autoimmunity, and pathogenesis of dilated cardiomyopathy.* Trends Cardiovasc Med, 2006. **16**(1): p. 20-4.
55. Ungerer, M., et al., *Altered expression of beta-adrenergic receptor kinase and beta 1-adrenergic receptors in the failing human heart.* Circulation, 1993. **87**(2): p. 454-63.
56. Bristow, M.R., et al., *Decreased catecholamine sensitivity and β-adrenergic receptor density in failing human hearts.* N. Engl. J. Med., 1982. **307**: p. 205-211.
57. Bristow, M.R., et al., *β1- and β2-adrenergic receptor subpopulations in nonfailing and failing human ventricular myocardium: coupling of both receptor subtypes to muscle contraction and selective β1-receptor down-regulation in heart failure.* Circ. Res., 1986. **59**: p. 297-309.
58. Xiao, R.P., *beta-Adrenergic Signaling in the Heart: Dual Coupling of the beta2-Adrenergic Receptor to Gs and Gi Proteins.* Science's STKE, 2001. **2001**(104): p. 15re-15.
59. Xiao, R.P., X. Ji, and E.G. Lakatta, *Functional coupling of the β2-adrenoceptor to a pertussis toxin-sensitive G protein in cardiac myocytes.* Mol. Pharmacol., 1995. **47**: p. 322-329.
60. Xiao, R.P., et al., *Coupling of β2-adrenoceptor to Gi proteins and its physiological relevance in murine cardiac myocytes.* Circ. Res., 1999. **84**: p. 43-52.
61. Jones, E.S., et al., *AT2 receptors: functional relevance in cardiovascular disease.* Pharmacol Ther, 2008. **120**(3): p. 292-316.
62. Bettencourt, P.M., *Clinical usefulness of B-type natriuretic peptide measurement: present and future perspectives.* Heart, 2005. **91**(11): p. 1489-94.
63. *Effect of metoprolol CR/XL in chronic heart failure: Metoprolol CR/XL Randomised Intervention Trial in Congestive Heart Failure (MERIT-HF).* Lancet, 1999. **353**(9169): p. 2001-7.
64. *The Cardiac Insufficiency Bisoprolol Study II (CIBIS-II): a randomised trial.* Lancet, 1999. **353**(9146): p. 9-13.
65. Joglar, J.A., et al., *Effect of carvedilol on survival and hemodynamics in patients with atrial fibrillation and left ventricular dysfunction: retrospective analysis of the US Carvedilol Heart Failure Trials Program.* Am Heart J, 2001. **142**(3): p. 498-501.
66. Flesch, M., et al., *Differential effects of carvedilol and metoprolol on isoprenaline-induced changes in beta-adrenoceptor density and systolic function in rat cardiac myocytes.* Cardiovasc Res, 2001. **49**(2): p. 371-80.
67. Ahmet, I., et al., *Therapeutic Efficacy of a Combination of a {beta}1 AR Blocker and {beta}2 AR Agonist in a Rat Model of Post-Myocardial Infarction Dilated Heart Failure Exceeds that of a {beta}1 AR Blocker plus ACE Inhibitor.* J Pharmacol Exp Ther, 2009.
68. Ehrlich, P., *On immunity with special reference to cell life.* Proc R Soc Lond 1900. **66**: p. 424-448.
69. Rose, N.R. and I.R. MacKay, eds. *The Autoimmune Diseases*. 4 ed. 2006, Elsevier Academic Press.
70. Janeway, C.A., P. Travers, and M. Walport, *Immunobiology*. 6 ed. 2005: Garland Science Publishing.
71. Goodnow, C.C., *Balancing immunity and tolerance: deleting and tuning lymphocyte repertoires.* Proc Natl Acad Sci U S A, 1996. **93**(6): p. 2264-71.

72. Janeway, C.A., Jr., *The immune system evolved to discriminate infectious nonself from noninfectious self.* Immunol Today, 1992. **13**(1): p. 11-6.
73. Bretscher, P. and M. Cohn, *A theory of self-nonself discrimination.* Science, 1970. **169**(950): p. 1042-9.
74. Miller, J.F. and W.R. Heath, *Self-ignorance in the peripheral T-cell pool.* Immunol Rev, 1993. **133**: p. 131-50.
75. Schwartz, R.H., *T cell anergy.* Annu Rev Immunol, 2003. **21**: p. 305-34.
76. Nemazee, D. and K.A. Hogquist, *Antigen receptor selection by editing or downregulation of V(D)J recombination.* Curr Opin Immunol, 2003. **15**(2): p. 182-9.
77. Goodnow, C.C., et al., *Cellular and genetic mechanisms of self tolerance and autoimmunity.* Nature, 2005. **435**(7042): p. 590-7.
78. Sakaguchi, S., *Regulatory T cells: key controllers of immunologic self-tolerance.* Cell, 2000. **101**(5): p. 455-8.
79. Blank, M. and Y. Shoenfeld, *B cell targeted therapy in autoimmunity.* J Autoimmun, 2007. **28**(2-3): p. 62-8.
80. King, C. and N. Sarvetnick, *Organ-specific autoimmunity.* Curr Opin Immunol, 1997. **9**(6): p. 863-71.
81. Kurts, C., et al., *CD8 T cell ignorance or tolerance to islet antigens depends on antigen dose.* Proc Natl Acad Sci U S A, 1999. **96**(22): p. 12703-7.
82. Yoshida, S. and M.E. Gershwin, *Autoimmunity and selected environmental factors of disease induction.* Semin Arthritis Rheum, 1993. **22**(6): p. 399-419.
83. Eisenberg, R.A., et al., *Stochastic control of anti-Sm autoantibodies in MRL/Mp-lpr/lpr mice.* J Clin Invest, 1987. **80**(3): p. 691-7.
84. Vyse, T.J. and J.A. Todd, *Genetic analysis of autoimmune disease.* Cell, 1996. **85**(3): p. 311-8.
85. McDevitt, H.O., *Discovering the role of the major histocompatibility complex in the immune response.* Annu Rev Immunol, 2000. **18**: p. 1-17.
86. Whitacre, C.C., S.C. Reingold, and P.A. O'Looney, *A gender gap in autoimmunity.* Science, 1999. **283**(5406): p. 1277-8.
87. Liao, Y.H. and X. Cheng, *Autoimmunity in myocardial infarction.* Int J Cardiol, 2006. **112**(1): p. 21-6.
88. Rose, N.R., *Infection, mimics, and autoimmune disease.* J Clin Invest, 2001. **107**(8): p. 943-4.
89. Kaplan, D., et al., *Antibodies to ribosomal P proteins of Trypanosoma cruzi in Chagas disease possess functional autoreactivity with heart tissue and differ from anti-P autoantibodies in lupus.* Proc Natl Acad Sci U S A, 1997. **94**(19): p. 10301-6.
90. Clynes, R. and J.V. Ravetch, *Cytotoxic antibodies trigger inflammation through Fc receptors.* Immunity, 1995. **3**(1): p. 21-6.
91. Lytton, S.D., et al., *A Novel Thyroid Stimulating Immunoglobulin Bioassay Is a Functional Indicator of Activity and Severity of Graves' Orbitopathy.* J Clin Endocrinol Metab, 2010.
92. Suzuki, S., et al., *Autoimmune Targets of Heart and Skeletal Muscles in Myasthenia Gravis.* Arch Neurol, 2009.
93. Witebsky, E., et al., *Chronic thyreoiditis and autoimmunization.* J. Am. Med. Assoc., 1957. **164**: p. 1439-1447.
94. Rose, N.R. and C. Bona, *Defining criteria for autoimmune diseases (Witebsky's postulates revisited).* Immunol Today, 1993. **14**(9): p. 426-30.
95. Jahns, R., et al., *Direct evidence for a beta 1-adrenergic receptor-directed autoimmune attack as a cause of idiopathic dilated cardiomyopathy.* J Clin Invest, 2004. **113**(10): p. 1419-29.
96. Maron, B.J., *Contemporary Definitions and Classification of the Cardiomyopathies: An American Heart Association Scientific Statement From the Council on Clinical Cardiology, Heart Failure and Transplantation Committee; Quality of Care and Outcomes Research and Functional Genomics and Translational Biology Interdisciplinary Working Groups; and Council on Epidemiology and Prevention.* Circulation, 2006. **113**(14): p. 1807-1816.

97. Lloyd-Jones, D., et al., *Heart Disease and Stroke Statistics--2009 Update: A Report From the American Heart Association Statistics Committee and Stroke Statistics Subcommittee.* Circulation, 2009. **119**(3): p. 480-486.
98. Andersson, B., K. Caidahl, and F. Waagstein, *Idiopathic dilated cardiomyopathy among Swedish patients with congestive heart failure.* Eur Heart J, 1995. **16**(1): p. 53-60.
99. Graham, R.M. and W.A. Owens, *Pathogenesis of inherited forms of dilated cardiomyopathy.* N. Engl. J. Med., 1999. **341**(23): p. 1759-62.
100. Seidman, J.G. and C. Seidman, *The genetic basis for cardiomyopathy: from mutation identification to mechanistic paradigms.* Cell, 2001. **104**: p. 557-567.
101. Caforio, A.L., N.J. Mahon, and W.J. McKenna, *Cardiac autoantibodies to myosin and other heart-specific autoantigens in myocarditis and dilated cardiomyopathy.* Autoimmunity, 2001. **34**(3): p. 199-204.
102. Goldman, J.H., et al., *Autoimmunity to alpha myosin in a subset of patients with idiopathic dilated cardiomyopathy.* Br Heart J, 1995. **74**(6): p. 598-603.
103. Baba, A., T. Yoshikawa, and S. Ogawa, *Autoantibodies produced against sarcolemmal Na-K-ATPase: possible upstream targets of arrhythmias and sudden death in patients with dilated cardiomyopathy.* J Am Coll Cardiol, 2002. **40**(6): p. 1153-9.
104. Baba, A., et al., *Antigen-specific effects of autoantibodies against sarcolemmal Na-K-ATPase pump in immunized cardiomyopathic rabbits.* Int J Cardiol, 2006. **112**(1): p. 15-20.
105. Göser, S., et al., *Cardiac troponin I but not cardiac troponin T induces severe autoimmune inflammation in the myocardium.* Circulation, 2006. **114**: p. 1693-1702.
106. Konstadoulakis, M.M., et al., *Clinical significance of antibodies against tropomyosin, actin and myosin in patients with dilated cardiomyopathy.* J Clin Lab Immunol, 1993. **40**(2): p. 61-7.
107. Schultheiss, H.P., *Disturbance of the myocardial energy metabolism in dilated cardiomyopathy due to autoimmunological mechanisms.* Circulation, 1993. **87**(5 Suppl): p. IV43-8.
108. Wang, Z., et al., *Analysis of IgG subclass antibodies and expression of T-Cell receptor signaling molecules in anti-CD4 monoclonal antibody treated mice with autoimmune cardiomyopathy.* Autoimmunity, 2006. **39**(6): p. 455-60.
109. Zhao, P., A.C. Sharma, and J. Ren, *Pathogenesis and therapy of autoimmunity-induced dilated cardiomyopathy.* Front Biosci, 2009. **14**: p. 1708-15.
110. Staudt, A., et al., *Potential role of humoral immunity in cardiac dysfunction of patients suffering from dilated cardiomyopathy.* J. Am. Coll. Cardiol., 2004. **44**: p. 829-836.
111. Fu, M.L., *Characterization of anti-heart M2 muscarinic receptor antibodies--a combined clinical and experimental study.* Mol Cell Biochem, 1996. **163-164**: p. 343-7.
112. Jahns, R., et al., *Modulation of beta1-adrenoceptor activity by domain-specific antibodies and heart failure-associated autoantibodies.* J Am Coll Cardiol, 2000. **36**(4): p. 1280-7.
113. Wallukat, G., et al., *Agonist-like beta-adrenoceptor antibodies in heart failure.* Am J Cardiol, 1999. **83**(12A): p. 75H-79H.
114. Eriksson, U., et al., *Activation of dendritic cells through the interleukin 1 receptor 1 is critical for the induction of autoimmune myocarditis.* J Exp Med, 2003. **197**(3): p. 323-31.
115. Rose, N.R., *Autoimmunity in coxsackievirus infection.* Curr Top Microbiol Immunol, 2008. **323**: p. 293-314.
116. Limas, C.J., I.F. Goldenberg, and C. Limas, *Soluble interleukin-2 receptor levels in patients with dilated cardiomyopathy. Correlation with disease severity and cardiac autoantibodies.* Circulation, 1995. **91**(3): p. 631-4.
117. Lindberg, E., et al., *Lower levels of the host protective IL-10 in DCM--a feature of autoimmune pathogenesis?* Autoimmunity, 2008. **41**(6): p. 478-83.
118. Yi, A., et al., *The prevalence of Th17 cells in patients with dilated cardiomyopathy.* Clin Invest Med, 2009. **32**(2): p. E144-50.

119. Li, J., et al., *The Treg/Th17 imbalance in patients with idiopathic dilated cardiomyopathy.* Scand J Immunol, 2010. **71**(4): p. 298-303.
120. de Leeuw, N., et al., *Autoimmune markers are undetectable in end stage idiopathic dilated cardiomyopathy.* J Clin Pathol, 1999. **52**(10): p. 739-43.
121. Francis, S.E., et al., *Interleukin-1 in myocardium and coronary arteries of patients with dilated cardiomyopathy.* J Mol Cell Cardiol, 1998. **30**(2): p. 215-23.
122. Bulut, D., et al., *Effect of protein A immunoadsorption on T cell activation in patients with inflammatory dilated cardiomyopathy.* Clin Res Cardiol, 2010.
123. Caforio, A.L., et al., *Idiopathic dilated cardiomyopathy: lack of association between circulating organ-specific cardiac antibodies and HLA-DR antigens.* Tissue Antigens, 1992. **39**(5): p. 236-40.
124. Liu, W., et al., *Association of HLA class II DRB1, DPA1 and DPB1 polymorphism with genetic susceptibility to idiopathic dilated cardiomyopathy in Chinese Han nationality.* Autoimmunity, 2006. **39**(6): p. 461-7.
125. Popovici, M., L. Groppa, and L. Kalinina, *Immunogenetic risk factors of dilated cardiomyopathy.* Blood Press Suppl, 1996. **3**: p. 49-52.
126. Portig, I., et al., *HLA-DQB1* polymorphism and associations with dilated cardiomyopathy, inflammatory dilated cardiomyopathy and myocarditis.* Autoimmunity, 2009. **42**(1): p. 33-40.
127. Buvall, L., et al., *Antibodies against the beta1-adrenergic receptor induce progressive development of cardiomyopathy.* J Mol Cell Cardiol, 2007. **42**(5): p. 1001-7.
128. Chen, J., et al., *Effects of autoantibodies removed by immunoadsorption from patients with dilated cardiomyopathy on neonatal rat cardiomyocytes.* Eur J Heart Fail, 2006. **8**(5): p. 460-7.
129. Jahns, R., et al., *Autoantibodies activating human beta1-adrenergic receptors are associated with reduced cardiac function in chronic heart failure.* Circulation, 1999. **99**(5): p. 649-54.
130. Aso, S., et al., *Anti-beta 1-adrenoreceptor autoantibodies and myocardial sympathetic nerve activity in chronic heart failure.* Int J Cardiol, 2009. **131**(2): p. 240-5.
131. Chiale, P.A., et al., *Differential profile and biochemical effects of antiautonomic membrane receptor antibodies in ventricular arrhythmias and sinus node dysfunction.* Circulation, 2001. **103**: p. 1765-1771.
132. Störk, S., et al., *Stimulating autoantibodies directed against the cardiac beta1-adrenergic receptor predict increased mortality in idiopathic cardiomyopathy.* Am. Heart J., 2006. **152**: p. 697-704.
133. Engvall, E. and P. Perlmann, *Enzyme-linked immunosorbent assay (ELISA). Quantitative assay of immunoglobulin G.* Immunochemistry, 1971. **8**(9): p. 871-4.
134. Störk, S., et al., *Stimulating autoantibodies targeting the cardiac beta1-adrenergic receptor predict increased mortality in dilated but not in ischemic cardiomyopathy.* Eur. Heart J., 2004. **25, abst. suppl.**: p. 6 (131).
135. Mobini, R., et al., *Probing the immunological properties of the extracellular domains of the human beta(1)-adrenoceptor.* J Autoimmun, 1999. **13**(2): p. 179-86.
136. Magnusson, Y., et al., *Antigenic analysis of the second extracellular loop of the human beta-adrenergic receptors.* Clin. Exp. Immunol., 1989. **78**(1): p. 42-48.
137. Tate, K., et al., *Epitope-analysis of T- and B-cell response against the human beta 1-adrenoceptor.* Biochimie, 1994. **76**: p. 159-164.
138. Caforio, A.L., et al., *Organ-specific cardiac antibodies: serological markers for systemic hypertension in autoimmune polyendocrinopathy.* Lancet, 1991. **337**(8750): p. 1111-5.
139. Caforio, A.L., et al., *Circulating cardiac autoantibodies in dilated cardiomyopathy and myocarditis: pathogenetic and clinical significance.* Eur J Heart Fail, 2002. **4**(4): p. 411-7.
140. Baba, A., *Autoantigen estimation and simple screening assay against cardiodepressant autoantibodies in patients with dilated cardiomyopathy.* Ther Apher Dial, 2008. **12**(2): p. 109-16.

141. Magnusson, Y., et al., *Autoimmunity in idiopathic dilated cardiomyopathy. Characterization of antibodies against the beta 1-adrenoceptor with positive chronotropic effect.* Circulation, 1994. **89**(6): p. 2760-7.
142. Wallukat, G. and A. Wollenberger, *Effects of the serum gamma globulin fraction of patients with allergic asthma and dilated cardiomyopathy on chronotropic beta-adrenoceptor function in cultured neonatal rat heart myocytes.* Biomed. Biochim. Acta, 1987. **46**(8-9): p. S634-9.
143. Nikolaev, V.O., Lohse, M.J., *Visualisierung von cAMP in lebenden Zellen.* BIOspektrum, 2005. **06/05**: p. 724-726.
144. Nikolaev, V.O., et al., *A novel fluorescence method for the rapid detection of functional beta1-adrenergic receptor autoantibodies in heart failure.* J Am Coll Cardiol, 2007. **50**(5): p. 423-31.
145. Nikolaev, V.O., et al., *Novel fluorescent method for the reliable detection of functional (auto-)antibodies activating the human beta1-adrenergic receptor.* Eur. Heart J., 2006. **23, suppl.1**: p. 489 (4393).
146. Nikolaev, V.O., et al., *Novel single chain cAMP sensors for receptor-induced signal propagation.* J Biol Chem, 2004. **279**(36): p. 37215-8.
147. Tsien, R.Y., *The green fluorescent protein.* Annu Rev Biochem, 1998. **67**: p. 509-44.
148. March, J.C., G. Rao, and W.E. Bentley, *Biotechnological applications of green fluorescent protein.* Appl Microbiol Biotechnol, 2003. **62**(4): p. 303-15.
149. Alieva, N.O., et al., *Diversity and evolution of coral fluorescent proteins.* PLoS ONE, 2008. **3**(7): p. e2680.
150. Shaner, N.C., G.H. Patterson, and M.W. Davidson, *Advances in fluorescent protein technology.* J Cell Sci, 2007. **120**(Pt 24): p. 4247-60.
151. Veith, D., Veith, M., *Ein Regenbogen aus dem Ozean: Biologie fluoreszierender Proteine.* Biologie in unserer Zeit, 2005. **6**: p. 11.
152. Chalfie, M., et al., *Green fluorescent protein as a marker for gene expression.* Science, 1994. **263**(5148): p. 802-5.
153. Wang, Y., J.Y. Shyy, and S. Chien, *Fluorescence Proteins, Live-Cell Imaging, and Mechanobiology: Seeing Is Believing.* Annu Rev Biomed Eng, 2008. **10**: p. 1-38.
154. Nguyen, Q.T., et al., *Surgery with molecular fluorescence imaging using activatable cell-penetrating peptides decreases residual cancer and improves survival.* Proc Natl Acad Sci U S A, 2010. **107**(9): p. 4317-22.
155. Förster, T., *Zwischenmolekulare Energiewanderung und Fluoreszenz.* Ann Physik, 1948. **2**: p. 55-75.
156. Jares-Erijman, E.A. and T.M. Jovin, *FRET imaging.* Nat Biotechnol, 2003. **21**(11): p. 1387-95.
157. Xia, Z. and Y. Liu, *Reliable and global measurement of fluorescence resonance energy transfer using fluorescence microscopes.* Biophys J, 2001. **81**(4): p. 2395-402.
158. Royant, A. and M. Noirclerc-Savoye, *Stabilizing role of glutamic acid 222 in the structure of Enhanced Green Fluorescent Protein.* J Struct Biol, 2011. **174**(2): p. 385-90.
159. Campbell, R.E., *Fluorescent-Protein-Based Biosensors: Modulation of Energy Transfer as a Design Principle.* Analytical Chemistry, 2009. **81**(15): p. 5972-5979.
160. Dickstein, K., et al., *ESC guidelines for the diagnosis and treatment of acute and chronic heart failure 2008.* European Heart Journal, 2008. **29**: p. 2388-2442.
161. Boumpas, D.T., et al., *Glucocorticoid therapy for immune-mediated diseases: basic and clinical correlates.* Ann Intern Med, 1993. **119**(12): p. 1198-208.
162. Casetta, I., G. Iuliano, and G. Filippini, *Azathioprine for multiple sclerosis.* J Neurol Neurosurg Psychiatry, 2009. **80**(2): p. 131-2; discussion 132.
163. Zhu, L.P., et al., *Selective effects of cyclophosphamide therapy on activation, proliferation, and differentiation of human B cells.* J Clin Invest, 1987. **79**(4): p. 1082-90.

164. Majithia, V. and V. Harisdangkul, *Mycophenolate mofetil (CellCept): an alternative therapy for autoimmune inflammatory myopathy.* Rheumatology (Oxford), 2005. **44**(3): p. 386-9.
165. Griffiths, B. and P. Emery, *The treatment of lupus with cyclosporin A.* Lupus, 2001. **10**(3): p. 165-70.
166. Brazelton, T.R. and R.E. Morris, *Molecular mechanisms of action of new xenobiotic immunosuppressive drugs: tacrolimus (FK506), sirolimus (rapamycin), mycophenolate mofetil and leflunomide.* Curr Opin Immunol, 1996. **8**(5): p. 710-20.
167. Hyde, C., et al., *Infliximab for the treatment of ulcerative colitis.* Health Technol Assess, 2009. **13 Suppl 3**: p. 7-11.
168. Prodanovich, S., et al., *Etanercept: an evolving role in psoriasis and psoriatic arthritis.* Am J Clin Dermatol, 2010. **11 Suppl 1**: p. 3-9.
169. Mertens, M. and J.A. Singh, *Anakinra for rheumatoid arthritis: a systematic review.* J Rheumatol, 2009. **36**(6): p. 1118-25.
170. Comi, G., *Natalizumab: state of the art and open questions.* Neurol Sci, 2010.
171. Fox, E.J., *Alemtuzumab in the treatment of relapsing-remitting multiple sclerosis.* Expert Rev Neurother, 2010. **10**(12): p. 1789-97.
172. Covelli, M., et al., *Safety of rituximab in rheumatoid arthritis.* Reumatismo, 2010. **62**(2): p. 101-6.
173. Landells, I., et al., *Efficacy outcomes in patients using alefacept in the AWARE study.* J Cutan Med Surg, 2009. **13 Suppl 3**: p. S122-30.
174. Liu, W., et al., *Effects of atorvastatin on the Th1/Th2 polarization of ongoing experimental autoimmune myocarditis in Lewis rats.* J Autoimmun, 2005. **25**(4): p. 258-63.
175. Roncarolo, M.G., et al., *Type 1 T regulatory cells.* Immunol Rev, 2001. **182**: p. 68-79.
176. Couzin-Frankel, J., *Immunology. Replacing an immune system gone haywire.* Science, 2010. **327**(5967): p. 772-4.
177. Felix, S.B., *Immunoadsorption in dilated cardiomyopathy.* Ernst Schering Res Found Workshop, 2006(55): p. 353-61.
178. Doerffel, W.V., et al., *Short-term hemodynamic effects of immunoadsorption in dilated cardiomyopathy.* Circulation, 1997. **95**: p. 1994-1997.
179. Felix, S.B. and A. Staudt, *Non-specific immunoadsorption in patients with dilated cardiomyopathy: mechanisms and clinical effects.* Int J Cardiol, 2006. **112**(1): p. 30-3.
180. Herda, L.R., S.B. Felix, and A. Staudt, *Immunoadsorption in patients with dilated cardiomyopathy.* Atheroscler Suppl, 2009. **10**(5): p. 126-128.
181. Larsson, L., et al., *Beneficial effect on cardiac function by intravenous immunoglobulin treatment in patients with dilated cardiomyopathy is not due to neutralization of anti-receptor autoantibody.* Autoimmunity, 2004. **37**(6-7): p. 489-93.
182. Arnson, Y., Y. Shoenfeld, and H. Amital, *Intravenous immunoglobulin therapy for autoimmune diseases.* Autoimmunity, 2009. **42**(6): p. 553-60.
183. Anthony, R.M., et al., *Intravenous gammaglobulin suppresses inflammation through a novel T(H)2 pathway.* Nature, 2011. **475**(7354): p. 110-3.
184. La Cava, A., *Modulation of autoimmunity with artificial peptides.* Autoimmun Rev, 2010.
185. Anderton, S.M., *Peptide-based immunotherapy of autoimmunity: a path of puzzles, paradoxes and possibilities.* Immunology, 2001. **104**(4): p. 367-76.
186. Venkatesh, N., et al., *Prevention of passively transferred experimental autoimmune myasthenia gravis by a phage library-derived cyclic peptide.* Proc Natl Acad Sci U S A, 2000. **97**(2): p. 761-6.
187. Boivin, V., et al., *115 Combination-therapy with neutralizing cyclopeptides and beta-blockers decreases molecular markers of sympathetic activation and reverses cardiomyopathy in beta1-receptor antibody-induced heart failure.* European Journal of Heart Failure Supplements, 2007. **6**(1): p. 28-28.

188. Boivin, V., et al., *A novel receptor-homologous cyclic peptide prevents β_1-adrenoceptor antibody-induced progressive cardiomyopathy.* Eur. J. Heart Fail., 2005. **4, suppl.1**: p. 24 (104).
189. Jahns, R., et al., *Immuno-modulating cyclopeptides: new biomolecules to combat stimulatory beta1-receptor antibodies in heart failure.* Eur. Heart J., 2006. **26, suppl.1**: p. 452 (4083).
190. Jahns, R., et al., *A new cyclic receptor-peptide prevents development of heart dilatation and failure induced by antibodies activating cardiac beta1-adrenergic receptors.* Circulation, 2005. **112, suppl.II**: p. 5 (120).
191. Sambrook, J. and D.W. Russell, *Molecular Cloning - a Laboratory Manual.* Cold Spring Harbor Laboratory Press, 2001.
192. Börner, S., et al., *FRET measurements of intracellular cAMP concentrations and cAMP analogue permeability in intact cells.* Nature Protocols (accepted manuscript), 2010.
193. Calebiro, D., et al., *Persistent cAMP-signals triggered by internalized G-protein-coupled receptors.* PLoS Biol, 2009. **7**(8): p. e1000172.
194. Jahns, R., et al., *Probing human beta 1- and beta 2-adrenoceptors with domain-specific fusion protein antibodies.* Eur J Pharmacol, 1996. **316**(1): p. 111-21.
195. Russ, C., et al., *Purification of IgG monoclonal antibody by caprylic acid precipitation.* J. Immunol. Methods, 1983. **65**: p. 269-271.
196. Harlow, E. and D. Lane, *Antibodies a laboratory manual.* Cold Spring Harbor Laboratory, 1988.
197. Boege, F., et al., *Eine schnelle und einfache Methode zur Reinigung von γ-Globulinen aus menschlichen Seren durch thiophile Adsorptionschromatographie.* Lab.med., 1992. **16**: p. 353-356.
198. Cheng, Y. and W.H. Prusoff, *Relationship between the inhibition constant (K1) and the concentration of inhibitor which causes 50 per cent inhibition (I50) of an enzymatic reaction.* Biochem Pharmacol, 1973. **22**(23): p. 3099-108.
199. Palmer, A.E. and R.Y. Tsien, *Measuring calcium signaling using genetically targetable fluorescent indicators.* Nat Protoc, 2006. **1**(3): p. 1057-65.
200. Zhang, J.H., *A Simple Statistical Parameter for Use in Evaluation and Validation of High Throughput Screening Assays.* Journal of Biomolecular Screening, 1999. **4**(2): p. 67-73.
201. Sui, Y. and Z. Wu, *Alternative Statistical Parameter for High-Throughput Screening Assay Quality Assessment.* Journal of Biomolecular Screening, 2007. **12**(2): p. 229-234.
202. Schlipp, A., et al., *Neue Zell-Linie zur Fluoreszenz-basierten Detektion von funktionell aktiven Antikörpern und AutoAk gegen den Beta1-adrenergen Rezeptor. (Novel cell line for the fluorescence-based detection of functional antibodies and autoantibodies directed against the beta1-AR).* J.-M.-U. Wuerzburg, Editor. 2009: Germany.
203. Brodde, O.-E., *The pharmacology of bisoprolol.* Rev. Contemp. Pharmacother., 1997. **8**: p. 21-23.
204. Warraich, R.S., et al., *Immunoglobulin G3 cardiac myosin autoantibodies correlate with left ventricular dysfunction in patients with dilated cardiomyopathy: immunoglobulin G3 and clinical correlates.* Am. Heart J., 2002. **143**: p. 1076-1084.
205. Lawn, R.M., et al., *The sequence of human serum albumin cDNA and its expression in E. coli.* Nucleic Acids Res, 1981. **9**(22): p. 6103-114.
206. Peters, T., Jr., *The biosynthesis of rat serum albumin. III. Amino acid composition of rat albumin.* J Biol Chem, 1962. **237**: p. 2182-3.
207. Anderson, L. and N.G. Anderson, *High resolution two-dimensional electrophoresis of human plasma proteins.* Proc Natl Acad Sci U S A, 1977. **74**(12): p. 5421-5.
208. Bazin, H., A. Beckers, and P. Querinjean, *Three classes and four (sub)classes of rat immunoglobulins: IgM, IgA, IgE and IgG1, IgG2a, IgG2b, IgG2c.* Eur J Immunol, 1974. **4**(1): p. 44-8.

209. Hunt, S.A., et al., *ACC/AHA 2005 Guideline Update for the Diagnosis and Management of Chronic Heart Failure in the Adult: a report of the American College of Cardiology/American Heart Association Task Force on Practice Guidelines (Writing Committee to Update the 2001 Guidelines for the Evaluation and Management of Heart Failure): developed in collaboration with the American College of Chest Physicians and the International Society for Heart and Lung Transplantation: endorsed by the Heart Rhythm Society.* Circulation, 2005. **112**(12): p. e154-235.
210. Nagueh, S.F., et al., *Recommendations for the evaluation of left ventricular diastolic function by echocardiography.* J Am Soc Echocardiogr, 2009. **22**(2): p. 107-33.
211. Jasper, J.R., et al., *Primary structure of the mouse beta 1-adrenergic receptor gene.* Biochim Biophys Acta, 1993. **1178**(3): p. 307-9.
212. Michel, M.C., S.E. Harding, and R.A. Bond, *Are there functional beta(3)-adrenoceptors in the human heart?* Br J Pharmacol, 2010.
213. Hoffmann, C., et al., *Comparative pharmacology of human β-adrenergic receptor subtypes: characterization of stably transfected receptors in CHO cells.* Naunyn Schmiedebergs Arch Pharmacol., 2004. **362**(2): p. 151-159.
214. Caforio, A.L., et al., *Organ-specific cardiac autoantibodies in dilated cardiomyopathy - an update.* Eur. Heart J., 1995. **16, Suppl.O**: p. 68-70.
215. Deubner, N., et al., *Cardiac {beta}1-adrenoceptor autoantibodies in human heart disease: rationale and design of the Etiology, Titre-Course, and Survival (ETiCS) Study.* Eur J Heart Fail, 2010.
216. Peeters, M.C., et al., *Importance of the extracellular loops in G protein-coupled receptors for ligand recognition and receptor activation.* Trends Pharmacol Sci, 2010.
217. Voigtlander, U., et al., *Allosteric site on muscarinic acetylcholine receptors: identification of two amino acids in the muscarinic M2 receptor that account entirely for the M2/M5 subtype selectivities of some structurally diverse allosteric ligands in N-methylscopolamine-occupied receptors.* Mol Pharmacol, 2003. **64**(1): p. 21-31.
218. Klco, J.M., et al., *Essential role for the second extracellular loop in C5a receptor activation.* Nat Struct Mol Biol, 2005. **12**(4): p. 320-6.
219. Shi, L. and J.A. Javitch, *The second extracellular loop of the dopamine D2 receptor lines the binding-site crevice.* Proc Natl Acad Sci U S A, 2004. **101**(2): p. 440-5.
220. Behr, B., et al., *Novel mutants of the human beta1-adrenergic receptor reveal amino acids relevant for receptor activation.* J Biol Chem, 2006. **281**(26): p. 18120-5.
221. Branden, C. and J. Tooze, *Introduction to protein structure*. 2 ed. 1998, New York: Garland Publishing.
222. Mahler, E., et al., *A monoclonal antibody against the immunodominant epitope of the ribosomal P2beta protein of Trypanosoma cruzi interacts with the human beta 1-adrenergic receptor.* Eur J Immunol, 2001. **31**(7): p. 2210-6.
223. Wallukat, G., et al., *Patients with preeclampsia develop agonistic autoantibodies against the angiotensin AT1 receptor.* J Clin Invest, 1999. **103**(7): p. 945-52.
224. Wallukat, G., et al., *Agonistic autoantibodies directed against the angiotensin II AT1 receptor in patients with preeclampsia.* Can J Physiol Pharmacol, 2003. **81**(2): p. 79-83.
225. Wallukat, G., *Agonistic autoantibodies against the angiotensin II AT1 receptor*, in *Immunology of G-protein coupled receptor*. 2006. p. 41-52.
226. Fu, M.L., et al., *Functional autoimmune epitope on alpha 1-adrenergic receptors in patients with malignant hypertension.* Lancet, 1994. **344**(8938): p. 1660-3.
227. Boivin, V., et al., *Autoantibodies directed against the human beta1-adrenergic receptor are associated with increased mortality in dilated but not in ischemic cardiomyopathy.* Heart, 2004. **90 Suppl.III**: p. A16.

228. Störk, S., et al., *Activating autoantibodies against the human beta1-adrenoceptor predict increased mortality in dilated cardiomyopathy.* Circulation, 2004. **110**(17): p. abst.suppl. III, 555 (2583).
229. Eckstein, A., et al., *[Role of TSH receptor autoantibodies for the diagnosis of Graves' disease and for the prediction of the course of hyperthyroidism and ophthalmopathy. Recommendations of the Thyroid Section of the German Society of Endocrinology].* Med Klin (Munich), 2009. **104**(5): p. 343-8.
230. Dragun, D., J. Scornik, and H.U. Meier-Kriesche, *Kidney-transplant rejection and anti-MICA antibodies.* N Engl J Med, 2008. **358**(2): p. 196; author reply 196.

5.2 Own publications

Jahns R*, Schlipp A*, Boivin V, Lohse MJ. Targeting receptor antibodies in immune cardiomyopathy. Semin Thromb Hemost 2010;36:212-8.(*contributed equally)

Schlipp A, Nikolaev VO, Jahns V, Jahns R, Lohse MJ. Neue Zell-Linie zur Fluoreszenz-basierten Detektion von funktionell aktiven Antikörpern und AutoAk gegen den Beta1-adrenergen Rezeptor. (Novel cell line for the fluorescence-based detection of functional antibodies and autoantibodies directed against the beta1-AR). German patent DE 102009 019578.5. 2009.

Borner S, Schwede F, Schlipp A, Berisha F, Calebiro D, Lohse MJ, Nikolaev VO. FRET measurements of intracellular cAMP concentrations and cAMP analogue permeability in intact cells. Nat Protoc 2011;6(4):427-38.

Deubner N, Berliner D, Schlipp A, Gelbrich G, Caforio AL, Felix SB, Fu M, Katus H, Angermann CE, Lohse MJ, Ertl G, Stork S, Jahns R. Cardiac β_1-adrenoceptor autoantibodies in human heart disease: rationale and design of the Etiology, Titre-Course, and Survival (ETiCS) Study. Eur J Heart Fail 2010;12(7):753-62.

6 Appendix

A. Chemicals

Chemical	Company	Catalog No.
Acetic acid	Carl Roth (Karlsruhe)	37382
Acrylamide 40% mix 29:1	AppliChem (Darmstadt)	A0385
Agar agar	Invitrogen (Darmstadt)	30391023
Agarose	peqLAB Biotechnologie (Erlangen)	351020
N,N-Bis(2-hydroxyethyl)-2-aminoethanesulfonic acid (BES)	Sigma-Aldrich (Taufkirchen)	B6137
Ammonium peroxo sulphate (APS)	Carl Roth (Karlsruhe)	9592.1
Ammonium sulphate ($(NH_4)_2SO_4$)	Sigma-Aldrich (Taufkirchen)	A2939
Bovine serum albumine (BSA)	Sigma-Aldrich (Taufkirchen)	A8806
Bromphenol blue	Sigma-Aldrich (Taufkirchen)	B6131
2,3-Butanedione monoxime (BDM)	Sigma-Aldrich (Taufkirchen)	B0753
Calcium chloride ($CaCl_2$)	AppliChem (Darmstadt)	A4088
Caprylic acid	Sigma-Aldrich (Taufkirchen)	C2875
Coomassie brilliant blue	AppliChem (Darmstadt)	A3480
Dimethyl sulfoxide (DMSO)	Sigma-Aldrich (Taufkirchen)	D5879
Disodium hydrogen phosphate ($Na_2HPO_4 \cdot 2H_2O$)	Merck (Darmstadt)	6346
Ethanol	Pharmacy of the University Hospital of Würzburg	-
Ethidium bromide	Sigma-Aldrich (Taufkirchen)	E2515
Ethylenediaminetetraacetic acid (EDTA)	Sigma-Aldrich (Taufkirchen)	E9884
Fetal calf serum (FCS)	PAN Biotech (Aidenbach)	-
Ficoll 400®	Sigma-Aldrich (Taufkirchen)	F4375
Geneticin (G418)	Invitrogen (Darmstadt)	345810
Glucose	Merck (Darmstadt)	8337
L-Glutamine	PAN Biotech (Aidenbach)	P0480100
Glycin	AppliChem (Darmstadt)	A1377
Glycerol	Pharmacy of the University	-

	Hospital of Würzburg	
4-(2-Hydroxyethyl)-1-piperazineethanesulfonic acid (HEPES)	AppliChem (Darmstadt)	A1069
Heparin 25000	Ratiopharm (Ulm)	-
Hoechst 33345	Sigma-Aldrich (Taufkirchen)	861405
Hydrogen peroxide (H_2O_2) 30%	AppliChem (Darmstadt)	A1134
Hygromycin B	Invitrogen (Darmstadt)	10687010
ICI-118551	Sigma-Aldrich (Taufkirchen)	I127
(-) Isoproterenol ((-) iso)	Sigma-Aldrich (Taufkirchen)	I6504
Laminin	BD Biosciences	354239
Luria broth (LB)-medium powder (Lennox)	AppliChem (Darmstadt)	A6666
Magnesium chloride hexahydrate ($MgCl_2 \cdot 6H_2O$)	AppliChem (Darmstadt)	A3618
Magnesium sulfate heptahydrate ($MgSO_4 \cdot 7H_2O$)	Merck (Darmstadt)	105886
2-Mercaptoethanol	Sigma-Aldrich (Taufkirchen)	M6250
Monopotassium phosphate (KH_2PO_4)	Merck (Darmstadt)	1048730250
o-Phenylenediamine (OPD)	Sigma-Aldrich (Taufkirchen)	P9029
Orange G	Merck (Darmstadt)	6878
Penicillin 10,000 units/ml Streptomycin 10 mg/ml solution	PAN Biotech (Aidenbach)	P0607100
Peroxidase-conjugated streptavidin	Jackson ImmunoResearch Laboratories (West Grove, USA)	016-030-084
Phenolsulfonphthalein	Merck (Darmstadt)	7241
Poly-D-lysin (PDL)	Sigma-Aldrich (Taufkirchen)	P0296
Polyethylene glycol (PEG) 3000	Sigma-Aldrich (Taufkirchen)	81230
Polyethyleneimine (PEI)	Sigma-Aldrich (Taufkirchen)	P3143
Potassium acetate (KAc)	Sigma-Aldrich (Taufkirchen)	P1190
Potassium bicarbonate ($KHCO_3$)	Merck (Darmstadt)	4928
Potassium chloride (KCl)	AppliChem (Darmstadt)	A3582,1000
Puromycin	Sigma-Aldrich (Taufkirchen)	P9620
Skimmed milk powder	AppliChem (Darmstadt)	A0830
Sodium acetate (NaAc)	Sigma-Aldrich (Taufkirchen)	S2889
Sodium bicarbonate ($NaHCO_3$)	Merck (Darmstadt)	6392
Sodium carbonate (Na_2CO_3)	Merck (Darmstadt)	6392

Sodium dodecyl sulfate (SDS)	Merck (Darmstadt)	822050
Sodium hydroxide (NaOH)	Merck (Darmstadt)	6498
Sodium chloride (NaCl)	AppliChem (Darmstadt)	A1371
Sulphuric acid (H_2SO_4)	Merck (Darmstadt)	0731
Taurine	Sigma-Aldrich (Taufkirchen)	T0625
Tetramethylethylenediamine (TEMED)	Carl Roth (Darmstadt)	2367.1
Thiophilic agarose (Affi-T®)	Kem en tec (Taastrup, DK)	1340C
Tris(hydroxymethyl)aminomethane (Tris)	AppliChem (Darmstadt)	A2264
Tween 20	AppliChem (Darmstadt)	A1389

B. Enzymes

Enzyme	Company	Catalog No.
Liberase	Roche Diagnostics (Mannheim)	05401054001
Rnase A	AppliChem (Darmstadt)	A2760
Trypsin	Invitrogen (Darmstadt)	15090
Trypsin/EDTA (0.05/0.02 % in PBS, -Ca^{2+}, -Mg^{2+})	PAN Biotech (Aidenbach)	P04-36500

C. Buffers

If not otherwise indicated the following buffers are prepared with deionized water, stored at RT and handled under non-sterile conditions.

Ammonium sulphate solution I:	$(NH_4)_2SO_4$	0.75 M
	pH adjusted to 7.4.	
Ammonium sulphate solution II:	$(NH_4)_2SO_4$	1 M
	pH adjusted to 7.4.	

BBS buffer 2x:	BES	50 mM
	NaCl	280 mM
	$Na_2HPO_4 \cdot 2H_2O$	1.5 mM
	pH adjusted to 6.95 and sterile filtrated.	
BDM solution:	BDM	500 mM
	Sterile filtrated and stored at -20 °C.	
Blocking milk:	skimmed milk powder	3 % (w/v)
	Tween 20	0.1 % (v/v)
	Disolved in PBS buffer and stored at 4 °C.	
BSA solution:	BSA	10 % (w/v)
	Sterile filtrated and stored at -20 °C.	
Calcium chloride solution I:	$CaCl_2$	100 mM
	Sterile filtrated and stored at 4 °C.	
Calcium chloride solution II:	$CaCl_2$	10 mM
	Sterile filtrated and stored at 4 °C.	
Calcium chloride solution III:	$CaCl_2$	2.5 M
	Sterile filtrated.	
Coating buffer:	sodium carbonate	15 mM
	sodium bicarbonate	35 mM
	pH adjusted to 9.6 with HCl and stored at 4 °C.	
Coomassie staining bath:	ethanol	45 % (v/v)
	acetic acid	10 % (v/v)
	Coomassie Brilliant Blue	2.5 $^0/_{00}$ (w/v)

Cracking buffer 2x:	Tris base	120 mM
	pH adjusted to 6.8.	
	SDS	70 mM
	glycerole (85 %)	23,5 % (v/v)
	bromphenol blue	3 mM
	2-mercaptoethanol	640 mM
Destaining buffer:	ethanol	10 % (v/v)
	acetic acid	10 % (v/v)
Dialysis hose buffer:	EDTA	5 mM
	$NaHCO_3$	200 mM
	Prepared freshly.	
Digestion buffer:	perfusion buffer 1x	29.4 ml
	calcium chloride solution I	3.75 µl
	trypsin solution	450 µl
	liberase solution	150 µl
	Prepared freshly, trypsin and liberase solution were added straight before use.	
DMEM (Dulbecco's Modified Eagle's Medium):	with 4.5 g glucose and 3.7 g sodium bicarbonate per liter, with sodium pyruvate, without L-glutamate, from PAN Biotech (Aidenbach), catalog no. P04-03600. Stored at 4 °C, handled under sterile conditions.	
DPBS (Dulbecco's phosphate buffered saline):	without magnesium or calcium, from PAN Biotech (Aidenbach), catalog no. P04-36560. Stored at 4 °C, handled under sterile conditions.	
Electrophoresis buffer 4x:	Tris base	100 mM
	glycin	768 mM
	pH adjusted to 8.5.	
	SDS	10 mM

FRET buffer:	HEPES	10mM
	NaCl	140 mM
	KCl	5.4 mM
	$MgCl_2 \cdot 6H_20$	1 mM
	$CaCl_2$	2 mM
	pH adjusted to 7.34.	
KCM buffer 5x:	KCl	500 mM
	$CaCl_2$	150 mM
	$MgCl_2 \cdot 6H_2O$	250 mM
L1 solution:	glucose	50 mM
	Tris HCl pH 8.0	25 mM
	EDTA pH 8.0	10 mM
	RNaseA	100 µg/ml
	RNaseA is boiled for 15 min to render it DNase-free before adding it to the solution, stored at 4 °C.	
L2 solution:	NaOH	200 µM
	SDS	1 % (w/v)
L3 solution:	KAc	3 M
	acetic acid	11.5 % (v/v)
	Stored at 4 °C.	
Laminin solution:	laminin	10 %
	DPBS	90 %
	Stored in aliquots of 1 ml at -20 °C.	
Liberase solution:	liberase	1 % (w/v)
	Prepared under sterile conditions and stored in aliquots of 150 µl (i.e. 4.2 Wünsch units) at -20 °C.	

LB agar:	agar agar	2 % (w/v)
	LB medium	98 %
	Autoclaved and stored at 4 °C, handled under sterile conditions. Antibiotics are added after the autoclave step below 50 °C under sterile conditions and constant stirring of the molten agar.	
LB medium:	LB-medium powder	2 % (w/v)
	Autoclaved and stored at 4 °C, handled under sterile conditions. Antibiotics are added after the autoclave step below 50 °C under sterile conditions.	
Loading buffer 5x:	Ficoll 400®	20 % (w/v)
	EDTA	50 mM
	bromphenol blue	1 ‰ (w/v)
	orange G	1 ‰ (w/v)
PBS (phosphate buffered saline):	NaCl	140 mM
	KCl	2.7 mM
	$Na_2HPO_4 \cdot 2H_2O$	10.1 mM
	KH_2PO_4	1.8 mM
	pH adjusted to 7.3.	
PDL solution:	1:10 diluted in DPBS	
	Stored at 4 °C and handled under sterile conditions.	

Perfusion buffer 10x:	NaCl	1.13 M
	KCl	47 mM
	KH_2PO_4	6 mM
	Na2HPO4·2H2O	6 mM
	MgSO4·7H2O	12 mM
	phenolsulfonphthalein	320 µM
	$NaHCO_3$	120 mM
	$KHCO_3$	100 mM
	HEPES	100 mM
	taurine	300 mM
	Sterile filtrated and stored at 4 °C.	
Perfusion buffer 1x:	perfusion buffer 10x	10 % (v/v)
	BDM solution	2 % (v/v)
	glucose	1 ‰ (w/v)
	Prepared freshly, sterile filtrated.	
Separating buffer 2x:	Tris base	0.75 M
	pH adjusted to 8.8 with 37 % HCl.	
	SDS	7 mM
Separating gel 12 %:	separating buffer 2x	50 % (v/v)
	dH_20	15 % (v/v)
	acrylamide/bisacrylamide (29:1)	30 % (v/v)
	APS (10 %)	5 %
	TEMED	3 $^0/_{00}$ (v/v)
Sodium acetate buffer:	NaAc	60 mM
	Prepared freshly, pH adjusted to 4.0 with acetic acid.	
Sodium chloride solution:	NaCl	0.5 M
Stocking buffer 2x:	Tris base	0.25 M
	pH adjusted to 6.8 with 37 % HCl.	
	SDS	7 mM

Stocking gel:	stocking buffer 2x	50 % (v/v)
	dH_2O	20 %
	acrylamide/bisacrylamide (29:1, 40 %)	10 % (v/v)
	APS (10 %)	5 %
	TEMED	0.1 % (v/v)
Stopping buffer I:	BSA solution	10 % (v/v)
	calcium chloride solution I	2 ‰ (v/v)
	Prepared freshly in perfusion buffer 1x.	
Stopping buffer II:	BSA solution	20 % (v/v)
	Calcium chloride solution I	2.67 ‰ (v/v)
	Prepared freshly in perfusion buffer 1x.	
Substrate buffer:	acetic acid	100 mM
	disodium hydrogen phosphate	100 mM
	pH adjusted to 4.5 with NaOH and stored at 4 °C.	
TBS buffer:	PEG 3000	10 % (w/v)
	DMSO	5 % (v/v)
	$MgCl_2 \cdot 6H_2O$	20 mM
	LB medium	85 % (v/v)
	Sterile filtrated and stored at 4 °C.	
TAE buffer:	Tris-base	4 mM
	Acetic acid	17.5 % (v/v)
	EDTA pH 8.0	1 mM
TE buffer I:	Tris HCl pH 7.4	10 mM
	EDTA pH 8.0	1 mM
TE buffer II:	Tris HCl pH 7.4	5 mM
	EDTA pH 8.0	2 mM
	pH adjusted to 7.4.	

Tris buffer I:	Tris-base pH adjusted to 9.	50 mM
Tris buffer II:	Tris HCl pH 7.4 pH adjusted to 7.4.	50 mM
Trypsin solution:	trypsin Prepared under sterile conditions and stored in aliquots of 450 µl at -20 °C.	2.5 % (v/v)

D. Summary

Dilated cardiomyopathy (DCM) represents an important subgroup of patients suffering from heart failure. The disease is supposed to be associated with autoimmune mechanisms in about one third of the cases. In the latter patients functionally active conformational autoantibodies directed against the second extracellular loop of the β_1-adrenergic receptor (AR, β_1EC_{II}-aabs) have been detected. Such antibodies chronically stimulate the β_1-AR thereby inducing the adrenergic signaling cascade in cardiomyocytes, which, in the long run, contributes to heart failure progression.

We analyzed the production of cAMP after aab-mediated β_1-AR activation *in vitro* using a fluorescence resonance energy transfer (FRET) assay. This assay is based on HEK293 cells stably expressing human β_1-AR as well as the cAMP-sensor Epac1-camps. The assay showed a concentration-dependent increase in intracellular cAMP upon stimulation with the full agonist (-) isoproterenol. This response was comparable to results obtained in isolated adult murine cardiomyocytes and was partially blockable by a selective β_1-AR antagonist. In the same assay poly- and monoclonal anti-β_1EC_{II}-abs (induced in different animals) could activate the adrenergic signaling cascade, whereas isotypic control abs had no effect on intracellular cAMP levels. Using the same method, we were able to detect functionally activating aabs in the serum of heart failure patients with ischemic and hypertensive heart disease as well as patients with DCM, but not in sera of healthy control subjects. In patients with DCM we observed an inverse correlation between the stimulatory potential of anti-β_1-aabs and left ventricular pump function.

To adopt this assay for the detection of functionally activating anti-β_1EC_{II}-aabs in clinical routine we attempted to establish an automated large-scale approach. Neither flow cytometry nor FRET detection with a fluorescence plate reader provided an acceptable signal-to-noise ratio. It was possible to detect (-) isoproterenol in a concentration-dependent manner using two different FRET multiwell microscopes. However, due to focus problems large-scale detection of activating anti-β_1EC_{II}-abs could not be implemented.

Neutralization of anti-β_1-aabs with the corresponding epitope-mimicking peptides is a possible therapeutic approach to treat aab-associated autoimmune DCM. Using our FRET assay we could demonstrate a reduction in the stimulatory potential of anti-β_1EC_{II}-abs after *in vitro* incubation with β_1EC_{II}-mimicking peptides. Cyclic (and to a lesser extent linear) peptides in 40-fold molar excess acted as efficient ab-scavengers *in vitro*. Intravenously

injected cyclic peptides in a rat model of DCM also neutralized functionally active anti-β_1EC_{II}-abs efficiently *in vivo.*

For a detailed analysis of the receptor-epitope targeted by anti-β_1EC_{II}-abs we used sequentially alanine-mutated β_1EC_{II}-mimicking cyclic peptides. Our data revealed that the disulfide bridge between the cysteine residues C209 and C215 of the human β_1-AR appears essential for the formation of the ab-epitope. Substitution of further amino acids relevant for ab-binding in the cyclic scavenger peptide by alanine reduced its affinity to the ab and the receptor-activating potential was blocked less efficiently. In contrast, the non-mutant cyclic peptide almost completely blocked ab-induced receptor activation. Using this ala-scan approach we were able to identify a “NDPK”-epitope as essential for ab binding to the β_1EC_{II}.

In summary, neutralization of conformational activating anti-β_1EC_{II}-(a)abs by cyclic peptides is a plausible therapeutic concept in heart failure that should be further exploited based on the here presented data.

E. Zusammenfassung

Dilatative Kardiomyopathie (DCM) stellt eine wichtige Subgruppe von Patienten mit Herzinsuffizienz dar und ist vermutlich in etwa einem Drittel der Fälle mit einem Autoimmunmechanismus assoziiert. In diesen Patienten konnten funktionell aktive konformationelle Autoantikörper gegen die zweite extrazelluläre Schleife des β_1-adrenergen Rezeptors (Anti-β_1EC_{II}-AAK) nachgewiesen werden. Diese AK stimulieren chronisch den β_1-AR und induzieren dadurch die adrenerge Signaltransduktionskaskade in Kardiomyozyten, was, auf lange Sicht, zur Verschlimmerung der Herzinsuffizienz beiträgt.

Mittels eines Fluoreszenz-Resonanz Energie Transfer (FRET) Assays analysierten wir die Bildung von cAMP nach aab-vermittelter β_1-AR Aktivierung *in vitro*. Dieser Assay verwendet HEK293 Zellen, die den humanen β_1-AR sowie den cAMP-Sensor Epac1-camps stabil exprimieren. Der Assay zeigte einen konzentrationsabhängigen Anstieg von cAMP bei Stimulation mit dem vollen Agonisten (-) Isoproterenol. Diese Antwort war mit den Ergebnissen an isolierten adulten murinen Kardiomyozyten vergleichbar und konnte durch einen selektiven β_1-AR Antagonist blockiert werden. In verschiedenen Tieren induzierte poly- und monoklonale Anti-β_1EC_{II}-abs konnten die adrenerge Signalkaskade in dem gleichen FRET Assay aktivieren, wogegen isotypische Kontroll-AK keine intrazellulären cAMP Änderungen herbeiführten. Mit dem gleichen Ansatz konnten wir funktionell aktivierende AAK im Serum von Herzinsuffizienzpatienten mit ischämischer und hypertensiver Herzerkrankung sowie bei Patienten mit dilatativer Kardiomyopathie nachweisen, jedoch nicht im Serum von gesunden Kontrollpersonen. Bei Patienten mit dilatativer Kardiomyopathie beobachteten wir eine inverse Korrelation zwischen dem stimulierenden Potential der Anti-β_1-AAKs und der linksventrikulären Pumpfunktion.

Um diesen Assay zur Detektion funktionell aktivierender Anti-β_1EC_{II}-aabs in der klinischen Routinediagnostik einzusetzen, versuchten wir ein automatisiertes Hochdurchsatzverfahren zu etablieren. Weder die Durchflusszytometrie noch die FRET Detektion mittels eines Fluoreszenz Plattenlesegeräts wiesen einen akzeptabelen Signal-zu-Rausch-Quotienten auf. Es gelang mit zwei verschiedenen FRET-Multiwell-Mikroskopsystemen die Aktivierung durch (-) isoproterenol konzentrationsabhängig zu detektieren, allerdings war es aufgrund von Fokusproblemen nicht möglich aktivierende Anti-β_1EC_{II}-AAKs im Hochdurchsatzverfahren zu detektieren.

Einen möglichen Therapieansatz zur Behandlung der Anti-β_1-AAK-assoziierten autoimmunen DCM stellt die Neutralisierung der AAKs mittels korrespondierender Epitop-

imitierender Peptide dar. Wir konnten im FRET Assay eine Reduktion des aktivierenden Effekts von Anti-β_1EC_{II}-AAKs nach *in vitro* Inkubation mit β_1EC_{II}-imitierenden Peptiden nachweisen. Hierbei erwiesen sich zyklische (in geringerem Maß als lineare) Peptide in 40-fachem molarem Überschuss als effektive Antikörper-„Fänger“ *in vitro*. Eine intravenöse Gabe der Zyklopeptide in einem Rattenmodell der DCM neutralisierte funktionell aktivierende Anti-β_1EC_{II}-abs ebenfalls effizient *in vivo*.

Zur genaueren Analyse des von Anti-β_1EC_{II}-AAK gebundenen Rezeptor-Epitops setzten wir sequentiell Alanin-mutierte β_1EC_{II}-imitierende Zyklopeptide ein. Unsere Daten zeigten, dass die Disulfidbrücke zwischen den Cysteinresten C209 und C215 des humanen β_1AR essentiell für die Ausbildung des AAK-Epitops zu sein scheinen. Ein Austausch weiterer AK-bindungsrelevanter Aminosäuren im zyklischen Fängerpeptid durch Alanin verminderte dessen Avidität zum AK und inhibierte dessen Rezeptor-aktivierendes Potential weniger effizient. Im Gegensatz dazu verhinderte das nicht-mutierte Zyklopeptid nahezu vollständig die AK-vermittelte Rezeptoraktivierung. Durch diesen Ala-Scan Ansatz konnten wir ein „NDPK“-Epitop identifizieren, das für die AK-Bindung an β_1EC_{II} essentiell zu sein scheint.

Zusammenfassend ist festzuhalten, dass die Neutralisation von konformationellen aktivierenden Anti-β_1EC_{II}-(A)AKs durch Zyklopeptide ein viel versprechendes Therapiekonzept bei Herzinsuffizienz darstellt, das im Hinblick auf die hier vorgestellten Daten weiter ausgebaut werden sollte.

6 Appendix

6 Appendix

Danksagung

Mein Dank gilt zu allererst Herrn Prof. Roland Jahns für die Bereitstellung des überaus interessanten Themas und der Betreuung während meiner Doktorarbeit.
Vielen Dank auch an Herrn Prof. Martin Lohse für die Betreuung am Institut für Pharmakologie und Toxikologie und Übernahme der Zweitbegutachtung.
Danke auch an Herrn Prof. Thomas Müller für die Drittbegutachtung der vorliegenden Arbeit.

Vielen Dank an alle die im wörtlichsten Sinne mit ihrem „Herzblut“ zu dieser Arbeit beigetragen haben.

Ganz herzlich möchte ich allen Mitarbeitern des Instituts für Pharmakologie für die tolle Arbeitsatmosphäre und die große Hilfsbereitschaft während meiner Doktorarbeit danken.

Vor allem die Kollegen der AG Jahns haben mir bewundernswerte Geduld und Freundschaft entgegengebracht. Dafür ein großes Dankeschön an Frau Dr. Valérie Jahns, die stets ein offenes Ohr für Diskussionen hatte. Julia, Christina, Katja, Christin, Tanja, Petra, Sonja, Priya, Mathias, Yuxiang und Dr. Vladimir Kocoski danke für die vielen Stunden Freude und Leid des Laboralltags, die wir gemeinsam durchlebt haben. Dr. Viacheslav Nikolaev und Dr. Alexander Zürn danke ich für die Einführung in die grundlegende Methodik der FRET-Mikroskopie.

Danke meinen meinen Familien in Asselheim und Theinheim für die unschätzbar große Unterstützung.

Mein größter Dank gilt Stefan, ohne den nichts möglich gewesen wäre.